PLANT SCIENCE

Evolutionary flexibility in flooding response circuitry in angiosperms

Mauricio A. Reynoso[1]*†, Kaisa Kajala[2,3,4]*, Marko Bajic[5,6]*, Donnelly A. West[2]*, Germain Pauluzzi[1]*, Andrew I. Yao[2,3], Kathryn Hatch[5], Kristina Zumstein[2], Margaret Woodhouse[2], Joel Rodriguez-Medina[2,3], Neelima Sinha[2]‡, Siobhan M. Brady[2,3]‡, Roger B. Deal[5]‡, Julia Bailey-Serres[1,4]‡

Flooding due to extreme weather threatens crops and ecosystems. To understand variation in gene regulatory networks activated by submergence, we conducted a high-resolution analysis of chromatin accessibility and gene expression at three scales of transcript control in four angiosperms, ranging from a dryland-adapted wild species to a wetland crop. The data define a cohort of conserved submergence-activated genes with signatures of overlapping cis regulation by four transcription factor families. Syntenic genes are more highly expressed than nonsyntenic genes, yet both can have the cis motifs and chromatin accessibility associated with submergence up-regulation. Whereas the flexible circuitry spans the eudicot-monocot divide, the frequency of specific cis motifs, extent of chromatin accessibility, and degree of submergence activation are more prevalent in the wetland crop and may have adaptive importance.

Climate change has increased the frequency and intensity of floods that affect agricultural productivity. Of major crops, only rice [*Oryza sativa* (*Os*)] is resilient to waterlogging of roots and submergence of aerial tissue, because of adaptation to a semiaquatic habitat. Other angiosperms experience intermittent flooding and are not adapted to these conditions. Submergence triggers signaling in plant cells as a consequence of entrapment of the gaseous hormone ethylene and depletion of available oxygen (hypoxia), leading to inefficient anaerobic metabolism and energy starvation (*1*). To understand the variation in response to submergence, we studied rice as a representative monocot and flood-resilient species, the legume *Medicago truncatula* (*Mt*), and two *Solanum* species, domesticated tomato [*Solanum lycopersicum* (*Sl*) cultivar M82] and its dryland-adapted wild relative *Solanum pennellii* (*Sp*) (Fig. 1A). Roots are the first responders to flooding, and we thus monitored the early response of seedling apical root tips to complete seedling submergence. By monitoring the sentinel response gene family *ALCOHOL DEHYDROGENASE* (*ADH*), required for anaerobic production of adenosine 5′-triphosphate (*1*) (Fig. 1B), we identified 2 hours, the midpoint of maximal up-regulation, as a physiologically relevant time to compare initiation of the submergence response across species.

To conserve energy under hypoxia, stress-induced mRNAs are preferentially translated over transcripts associated with development in the model *Arabidopsis thaliana* (*2*–*4*). We therefore considered both transcriptional and post-transcriptional regulation under submergence across the species surveyed. To do so, we deployed Isolation of Nuclei TAgged in specific Cell Types (INTACT) (*5*) and Translating Ribosome Affinity Purification (TRAP) (*6*), using constitutive promoters. INTACT was used to profile chromatin accessibility by ATAC (assay for transposase-accessible chromatin)–sequencing (ATAC-seq) (*7*) and to measure the abundance of nuclear RNA (nRNA). TRAP was used to monitor ribosome-associated polyadenylated mRNA (TRAP RNA) and to evaluate the position of individual ribosomes along transcripts (Ribo-seq) (*8*) (Fig. 1C and figs. S1 and S2). We also profiled total polyadenylated mRNA (polyA RNA). Multidimensional scaling analysis confirmed the reproducibility and distinctness of each of the RNA subpopulations and their changes after submergence (fig. S3 and data S1 and S2).

Flood-adapted rice displayed the greatest plasticity in terms of the number of differentially up- and down-regulated transcripts (Fig. 1D, fig. S4, and data S3). Cultured hairy roots (*Sl*-HRs) were used as a contrast to intact roots of tomato (*Sl*) plants and were more responsive. The clustering of modulated RNAs resolved variation in regulation in all four species (Fig. 1D and figs. S5 to S9). Rice gene regulation was coordinated across scales (except in clusters 7 and 8, in which transcripts were enriched or depleted in the nucleus). In *Mt* and tomato, regulation of gene activity was more evident in the ribosome-associated RNAs, whereas in the dryland-adapted *Sp*, regulation was evident as nRNA enrichment or depletion.

Selection likely acts on species-specific traits and adaptation to specific environments that are largely regulated by a common set of gene families. The root meristem is frequently oxygen deprived because of high metabolic activity and periodic soil inundation; therefore, its capacity to transiently up-regulate anaerobic metabolism might be expected in all species. Yet, rice may have evolved a higher proportion of gene family members that are regulated by submergence than flooding-sensitive species did. We leveraged gene families (*9*) to investigate conservation in submergence-responsive genes of the four species, focusing on the shared families (6685) plus those conserved between the two *Solanum* species (3301) (Fig. 1E and data S4). Tabulation of the submergence-responsive gene family members of each species identified families with at least one member differentially controlled in any of the RNA populations evaluated (Fig. 1F, fig. S10, and data S5). This uncovered a set of 68 submergence–up-regulated families (SURFs: 249 genes in *Os*, 121 in *Mt*, 137 in *Sl*, 181 in *Sl*-HR, and 92 in *Sp*). The 68 SURFs include 17 of the 49 ubiquitously hypoxia-responsive genes of *Arabidopsis* seedlings (*6*), demonstrating evolutionary conservation of gene families activated by submergence and hypoxia (data S5).

The 68 SURFs include 1 to 13 up-regulated genes per family, leading us to investigate whether similar proportions of these families are elevated in each species (fig. S11 and data S6). Consistent with overall numbers, rice had the highest and *Sp* had the lowest proportion of up-regulated genes per family. The restrained response of wild tomato was evident from the 412 *Solanum*-specific gene families that were up-regulated in tomato but not in *Sp*. This motivated exploration of the aerial tissue (shoot apex) response in the *Solanum* species, which uncovered more gene families and family members up-regulated in shoots of wild tomato than those of domesticated tomato (fig. S12 and data S7). The shoot response of *Sp* showed greater overlap with *Arabidopsis* shoot-specific hypoxia-responsive genes (*10*). Distinctions between the two *Solanum* species included genes involved in cell elongation and auxin signaling, which predominated in *Sp*.

We reasoned that dynamics in chromatin accessibility and transcriptional activation may be coordinated and conserved for SURF members across species. ATAC-seq exposed open chromatin regions of rice and *Mt* primarily within 1 kb upstream of the transcription start site (TSS) and downstream of the polyadenylation (pA) site of genes (Fig. 2A and data S8). By contrast, *Solanum* roots showed a majority of intergenic ATAC-seq reads (fig. S13). The rice and *Mt* transposase hypersensitive sites (THS) (*11*) uncovered a preference for opening of chromatin in response to submergence (Fig. 2B and fig. S13), with increases in 3497 and 7501 THSs, respectively. Highly submergence–up-regulated genes had elevated

[1]Center for Plant Cell Biology, Botany and Plant Sciences Department, University of California, Riverside, CA, USA. [2]Department of Plant Biology, Division of Biological Sciences, University of California, Davis, CA, USA. [3]Genome Center, University of California, Davis, CA , USA. [4]Institute of Environmental Biology, Utrecht University, 3584 CH Utrecht, Netherlands. [5]Department of Biology, Emory University, Atlanta, GA, USA. [6]Graduate Program in Genetics and Molecular Biology, Emory University, Atlanta, GA, USA.
*These authors contributed equally to this work.
†Present address: Instituto de Biotecnología y Biología Molecular, FCE-UNLP CCT-CONICET, 1900 La Plata, Argentina.
‡Corresponding author. Email: roger.deal@emory.edu (R.B.D.); nrsinha@ucdavis.edu (N.S.); sbrady@ucdavis.edu (S.M.B.); serres@ucr.edu (J.B.-S.)

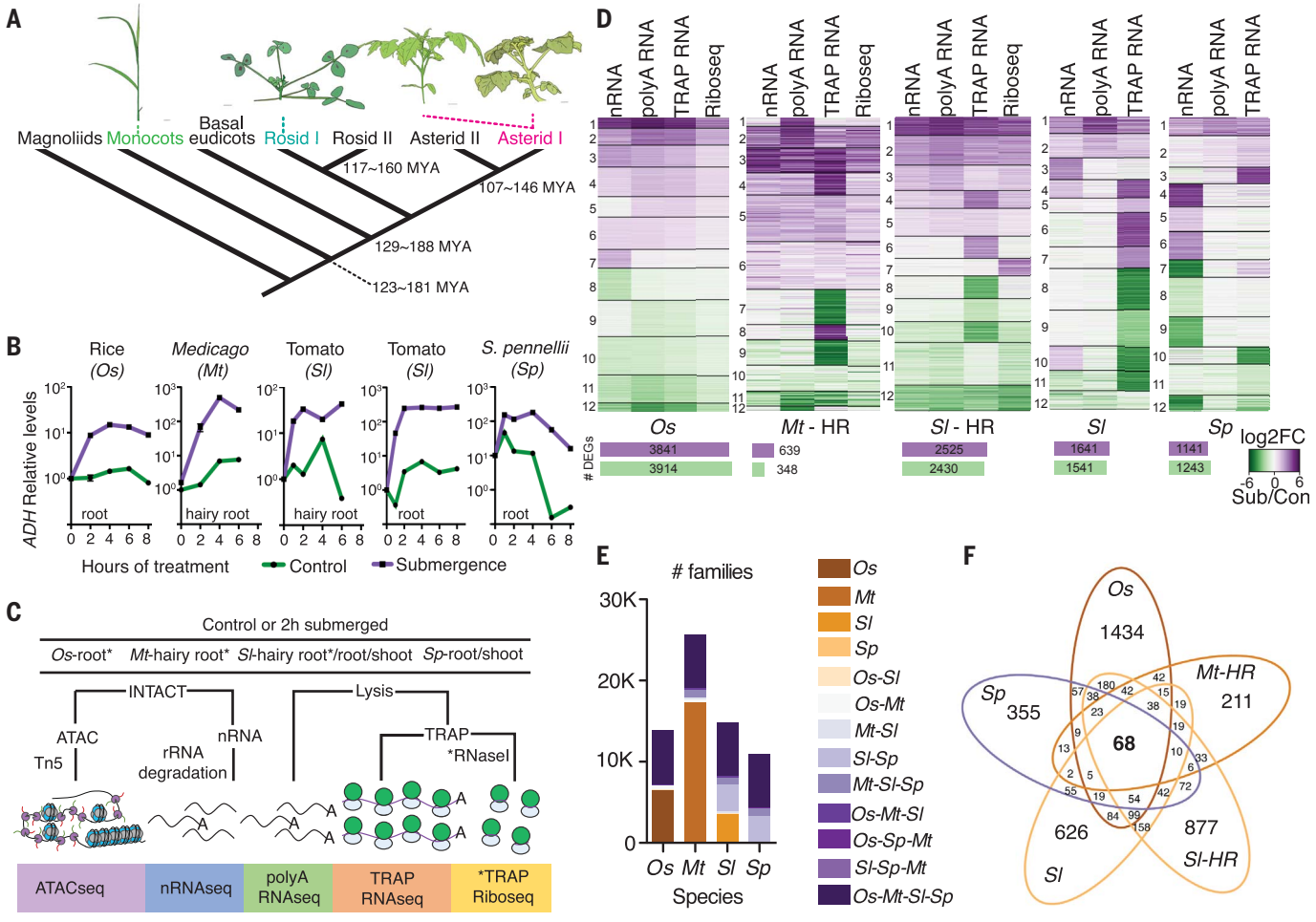

Fig. 1. Multitier evaluation of gene activity in four angiosperms identifies highly conserved submergence–up-regulated genes. (**A**) Relatedness of target species (*19*). MYA, million years ago. (**B**) *ADH* transcript levels of submerged seedlings. (**C**) Overview of experimental strategy. rRNA, ribosomal RNA. (**D**) Cluster analysis heatmap of $\log_2$ fold change [FC; submergence (Sub) versus control (Con) RNA] of differentially expressed genes [DEGs; $|\log_2 FC| > 1$ and adjusted *P* (*P*adj) < 0.01]. (Bottom) Bars indicate number of up or down DEGs after submergence $|\log_2 FC| > 1$ and *P*adj < 0.05. (**E**) Gene families per species and their overlap. (**F**) Conserved SURFs and species-specific up-regulated family numbers.

accessibility 5′ of their TSS and 3′ of their pA sites (Fig. 2C and figs. S5, S6, and S14), demonstrating that nucleosome depletion accompanies activation of transcript production under submergence. Down-regulated genes had lower chromatin accessibility overall, particularly in rice (Fig. 2C and figs. S5, S6, and S14).

We exploited the ATAC-seq data to explore conservation in gene regulatory circuitry. A pipeline was developed to identify transcription factor (TF) binding site motif enrichment in promoters and their THS regions of the up-regulated SURFs (Fig. 2D). Four significantly enriched TF motifs were identified. These included the hypoxia-responsive promoter element (HRPE), transactivated by low-oxygen–stabilized ethylene response group VII (ERFVII) TFs that up-regulate genes key to anaerobic metabolism and flooding survival in *Arabidopsis* (*12*–*14*); a basic helix-loop-helix (bHLH); a MYB; and a WRKY-type motif (Fig. 2D, figs. S15 and S16A, and data S9). At least one of the four motifs was present in >84% of the up-regulated SURF genes of rice and *Mt* and >68% of those of the *Solanum* species. HRPE and bHLH motifs predominated near the TSS in all species, with the MYB near the TSS in tomato and WRKY motifs more evenly distributed across the upstream region (fig. S16B). Differential wiring of up-regulated SURFs was evident from the HRPE enrichment in rice (55%) versus the MYB or bHLH motif enrichment in these three eudicots (fig. S16A and data S9).

Accessibility of chromatin in response to abiotic stress can be rapid and transient (*15*, *16*). We hypothesized that concordance between a TF binding site and a THS would be representative of a more static regulatory architecture, whereas discordance could reflect the transient propagation of a stress signal. Chromatin accessibility increased during submergence around HRPE and bHLH sites in rice and *Mt* (fig. S17). A more modest increase was observed for MYB and WRKY sites, potentially representing more rapid and/or transient regulatory interactions (fig. S17). The co-occurrence of an HRPE and THS corresponded with more pronounced polyA RNA up-regulation, with a similar trend observed for bHLH sites in rice and *Mt* (Fig. 2E, fig. S18, and data S10). In *Mt*, the presence of a THS alone in the proximal promoter was associated with greater elevation of polyA RNA, and co-occurrence of a MYB and THS corresponded with higher up-regulation than did the presence of the motif alone (Fig. 2F and fig. S18). Repetitive motifs of the same type in accessible regions coincided with greater up-regulation than with repetitive motifs outside THSs. The incidence of multiple HRPE or WRKY motifs corresponded with higher up-regulation in tomato, whereas only an HRPE or multiple bHLH motifs corresponded with up-regulation in *Sp*. These results establish a link between the four conserved motifs, chromatin accessibility, and transcriptional activation under submergence.

The discovery of the SURFs and four conserved cis regulatory TF binding motifs in submergence-accessible chromatin regions motivated us to evaluate whether the conservation prevails in genes maintained at syntenic chromosomal regions

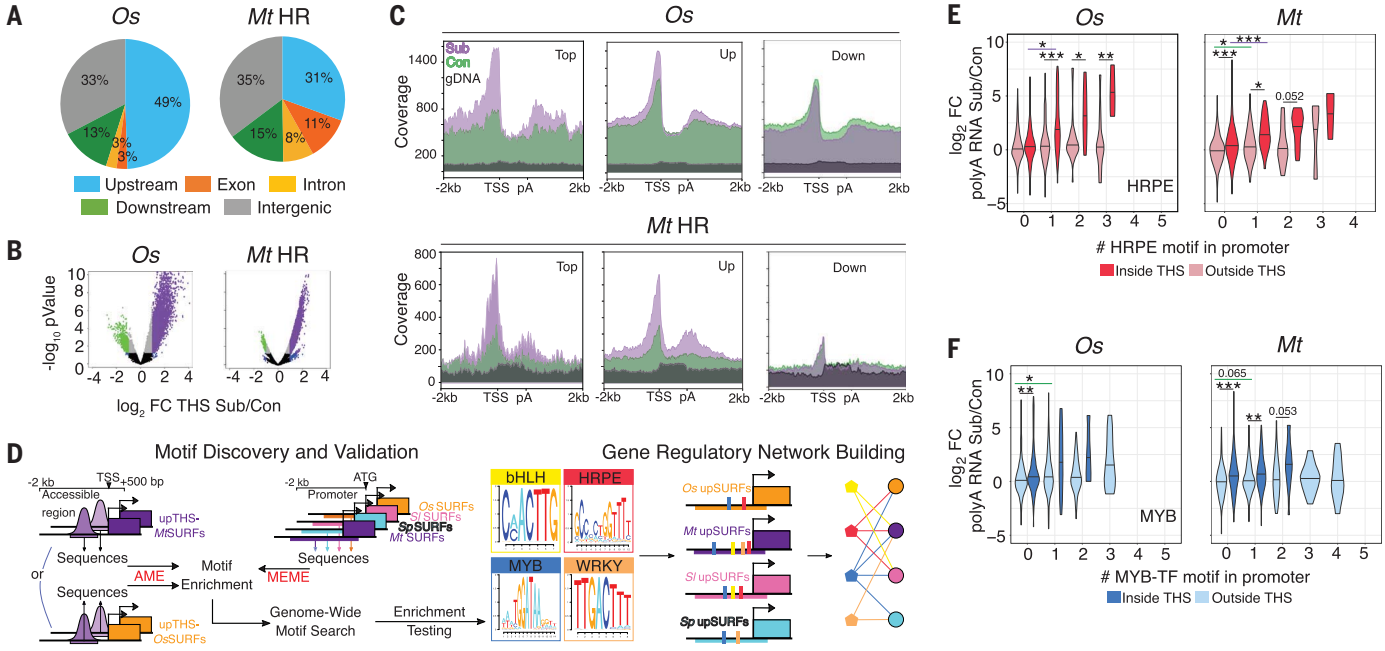

Fig. 2. Enhanced chromatin accessibility and motif enrichment in responsive genes. (**A**) Accessible chromatin regions (THSs) measured by ATAC-seq. Categories: 2 kb upstream of the TSS, exons, introns, 1 kb downstream of pA site, and intergenic. (**B**) THS change in response to submergence. (**C**) Control and submergence ATAC-seq reads on genes of up-regulated (Top; cluster 1; Up) and down-regulated (Down) clusters from Fig. 1D. Genomic DNA (gDNA) is ATAC-seq on naked DNA. (**D**) Discovery pipeline for enriched transcription factor motifs present in up-regulated THSs and SURF promoters, using unsupervised [Multiple Em for Motif Elicitation (MEME)] and supervised [Motif Comparison Tool (TOMTOM), Analysis of Motif Enrichment (AME), and Find Individual Motif Occurrences (FIMO)] methods. (**E** and **F**) Distribution of $\log_2$ FC polyA RNA submergence and control for SURFs arranged by presence and number of HRPE or MYB motif upstream of the ATG, inside or outside THSs. Student's *t* test; $*P < 0.05$, $**P < 0.01$, $***P < 0.001$; values ≤ 0.1.

Fig. 3. Syntenic genes are more highly expressed. (**A**) Median $\log_2$ FC of syntenic genes across four species for 12 up-regulated clusters. Dashed lines indicate two clusters with conserved interspecies up-regulation. (**B**) Plot of $\log_{10}$ reads per kilobase per million reads (rpkM) for all detected syntenic and non-syntenic genes under the control condition. Rice synteny was evaluated to *Brachypodium distachyon*, *Mt* to *Sl*, and between *Solanum* species. Variances between syntenic and non-syntenic genes are significant in every RNA population (*F* test). (**C**) Control (white columns) and submergence (blue columns) plots for SURF genes. Highly expressed SURF genes under submergence (>50 rpkM) with an HRPE are depicted as a red or blue dot for those located in or outside a THS, respectively. Central horizontal lines indicate median values.

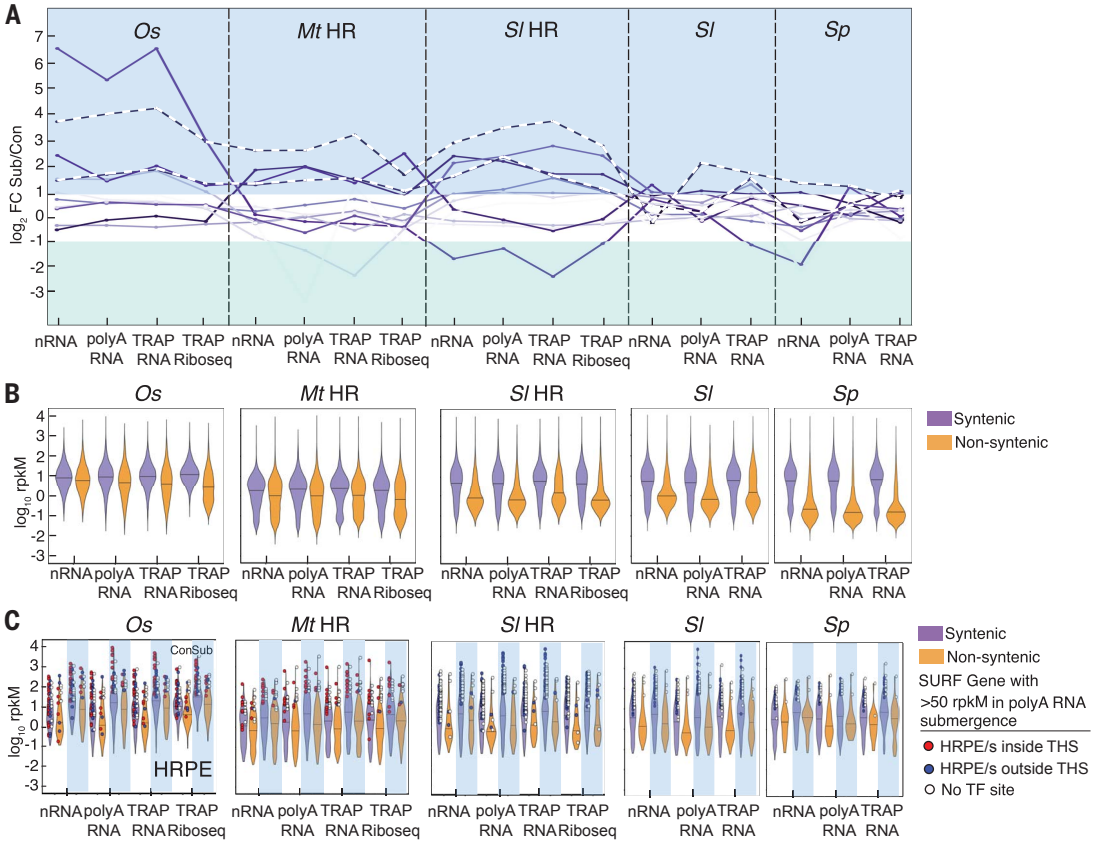

(syntelogs). To do so, the gene activity data were reclustered for the differentially regulated syntelogs across the four species (711), which included 22 of the 68 SURFs (Fig. 3A, fig. S19, and data S11). Syntelog clusters 2 and 3 had coordinated up-regulation across the scales of gene activity in all species. These comprised seven SURFs with functions in anaerobic metabolism, nutrient transport, abscisic acid (ABA) perception, and survival of extreme stress. The up-regulated syntelogs included 32 and 53 SURFs in all three eudicots and the two *Solanum* species, respectively (figs. S20 to S22 and data S11).

Next, we explored conservation of gene regulation on more recent evolutionary time scales by evaluating the activity of syntelogs of related species (Fig. 3B, fig. S23, and data S12 to S14). Syntenic genes had higher transcript abundance than nonsyntenic genes had, as reported previously (*17*). This was evident in all RNA populations under both conditions, with the most pronounced difference between syntenic and nonsyntenic genes in the *Solanum* species. Rice and *Mt* syntenic gene control regions had slightly higher chromatin accessibility than did nonsyntenic genes at the global scale (fig. S14), consistent with their higher expression. Transcript elevation was similar for syntenic and nonsyntenic SURF genes, especially for the *Solanum* species (Fig. 3C, fig. S24, and data S14), indicating that up-regulated nonsyntenic genes have maintained or acquired features enabling their stress activation. Consistent with this, most highly expressed syntenic and nonsyntenic SURF genes contained at least one of the four TF motifs recognized (80% rice, 80% *Mt*, >70% *Solanum* species) (Fig. 3C, fig. S24, and data S15). Most TF motifs were coincident with THSs in rice and *Mt*. Although the number of highly expressed but nonsyntenic SURF genes was fewer than six in the *Solanum* species, all from *Sl* contained at least one motif. The four identified TF motifs are therefore a broadly conserved feature of both syntenic and nonsyntenic submergence-responsive genes.

To appraise conservation in regulation across eudicots and monocots, we built networks that associate TF motif presence with each up-regulated SURF gene for each species (Fig. 4A, figs. S25 to S28, and data S16). The individual species networks emphasize the presence of species-specific motif biases. The combinatorial nature of target gene regulation was also evident (overlapping outer circles of network), with >70% of the genes having more than one of the four motifs. Syntenic up-regulated SURF genes across the four species (represented with black borders) expose a single conserved putative regulatory network (Fig. 4B, fig. S29, and data S16). This network illustrates conservation of TF motifs of syntelogs of responsive genes, in addition to the HRPE regulated by ERFVIIs.

As oxygen levels decline below a threshold, constitutively synthesized ERFVIIs accumulate because of attenuation of their conversion into an N-degron for active turnover (*1*). The unified SURF network uncovered HRPE conservation across eudicots-monocots in promoters of genes essential to anaerobic metabolism and hypoxia survival, including *PLANT CYSTEINE OXIDASE* (*PCO*) genes (Fig. 4C, fig. S30, and data S17), which catalyze the oxygen-promoted degradation of ERFVIIs to temper the adaptive response (*18*). The up-regulated SURF genes included *ERFVII*s in all four species, with at least one with an HRPE motif, suggesting possible autoregulation (fig. S31).

The syntelog network also identified conservation of bHLH motif enrichment in genes not well associated with submergence [i.e., *PYRABACTIN RESISTANCE 1*/*PYR1-LIKE* (*PYL*)] (Fig. 4B and fig. S32) and MYB motif enrichment in genes that contribute to hypoxia tolerance (*14*) (fig. S33 and S34). The up-regulation of these genes often coincided with a TF motif in a region of submergence-enhanced chromatin accessibility (Fig. 4, D to G, and fig. S33), supporting functionality of the regulatory sequences. As for the ERFVIIs, the up-regulated SURF genes included bHLH, MYB, and WRKY family members (fig. S31).

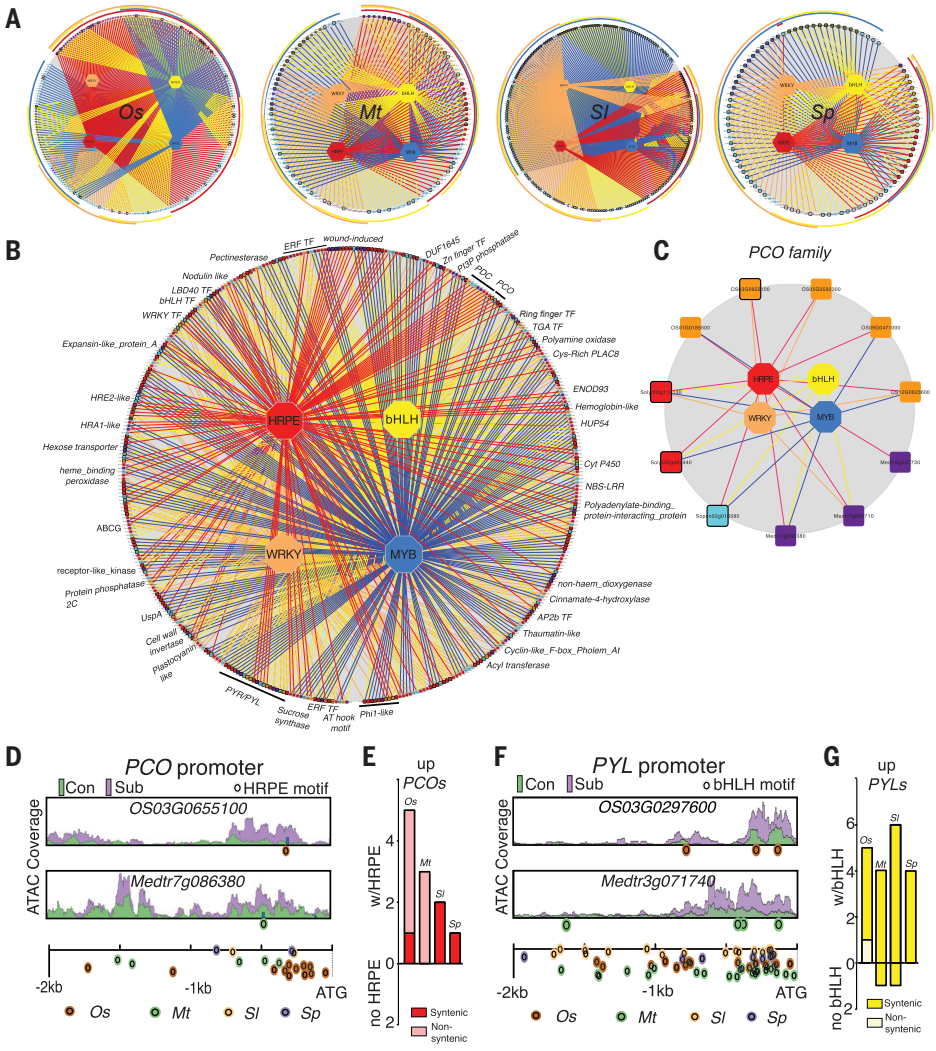

Fig. 4. Conserved transcription factor motifs in SURFs and accompanying chromatin dynamics. (**A**) Regulatory networks for up-regulated SURF genes (expanded in figs. S25 to S28). Hexagons, TFs; rectangles, genes; colored lines (edges), interactions of promoter and TF based on motif presence. Outer circles: genes grouped with shared motifs. Genes with black borders have a syntenic ortholog (rice to *Mt*; *Mt* to *Sl*; and between *Solanum* species). (**B**) Network for syntenic conserved SURF genes across species (expanded in fig. S29). Genes of alternating families have alternating gray or black borders. Families represented in three species are labeled. ABCG, ATP-binding cassette G; Cyt, cytochrome; LRR, leucine-rich repeat. (**C**) Regulatory network of *PCO* up-regulated genes. Syntenic orthologs have black borders. (**D** and **F**) Chromatin accessibility in promoters of syntenic *PCO* and *PYL*. ATAC coverage scale is the same for genes shown in each panel. (Bottom) Locations of HRPE or bHLH motifs for four species. (**E** and **G**) Number of up-regulated genes containing motifs classified by syntenic and nonsyntenic.

Information from single genes is used in breeding or modifying crops for stress tolerance. The use of multiscale gene regulatory information of gene families across flowering plant clades to infer regulatory networks demonstrates that conservation of flooding resilience mechanisms is complex and involves diverse regulatory mechanisms. Targeted manipulation of the four submergence-activated modules and seven SURF loci discovered in this study with the greatest interspecies conservation might be used to enhance flooding tolerance of susceptible crops.

REFERENCES AND NOTES

1. L. A. C. J. Voesenek, J. Bailey-Serres, *New Phytol.* **206**, 57–73 (2015).
2. C. Branco-Price, K. A. Kaiser, C. J. H. Jang, C. K. Larive, J. Bailey-Serres, *Plant J.* **56**, 743–755 (2008).
3. R. Sorenson, J. Bailey-Serres, *Proc. Natl. Acad. Sci. U.S.A.* **111**, 2373–2378 (2014).
4. P. Juntawong, T. Girke, J. Bazin, J. Bailey-Serres, *Proc. Natl. Acad. Sci. U.S.A.* **111**, E203–E212 (2014).
5. R. B. Deal, S. Henikoff, *Nat. Protoc.* **6**, 56–68 (2011).
6. A. Mustroph *et al.*, *Proc. Natl. Acad. Sci. U.S.A.* **106**, 18843–18848 (2009).
7. J. D. Buenrostro, P. G. Giresi, L. C. Zaba, H. Y. Chang, W. J. Greenleaf, *Nat. Methods* **10**, 1213–1218 (2013).
8. N. T. Ingolia, S. Ghaemmaghami, J. R. S. Newman, J. S. Weissman, *Science* **324**, 218–223 (2009).
9. D. M. Goodstein *et al.*, *Nucleic Acids Res.* **40**, D1178–D1186 (2012).
10. M. Klecker *et al.*, *Plant Physiol.* **165**, 774–790 (2014).
11. K. A. Maher *et al.*, *Plant Cell* **30**, 15–36 (2018).
12. P. Gasch *et al.*, *Plant Cell* **28**, 160–180 (2016).
13. S. C. Lee *et al.*, *New Phytol.* **190**, 457–471 (2011).
14. A. Mustroph *et al.*, *Plant Physiol.* **152**, 1484–1500 (2010).
15. B. O. R. Bargmann *et al.*, *Mol. Plant* **6**, 978–980 (2013).
16. A. Para *et al.*, *Proc. Natl. Acad. Sci. U.S.A.* **111**, 10371–10376 (2014).
17. J. W. Walley *et al.*, *Science* **353**, 814–818 (2016).
18. D. A. Weits *et al.*, *Nat. Commun.* **5**, 3425 (2014).
19. J. Barba-Montoya, M. Dos Reis, H. Schneider, P. C. J. Donoghue, Z. Yang, *New Phytol.* **218**, 819–834 (2018).

ACKNOWLEDGMENTS

We thank members of our labs, R. Mataki, S. Cabanlit, E. Viox, K. Tran, A. Addetia, S. Winte, M. Hummel, T. Lee, A. Mason, and H. Nakayama for support and discussions and J. Bazin, D. Koenig, D. Kliebenstein, T. Bailey, A. Reynoso, M. Covington, and S. Gray for guidance. **Funding:** Supported by United States National Science Foundation Plant Genome Research Program (IOS-1238243) to R.B.D., N.S., S.M.B., and J.B.-S., a Finnish Cultural Foundation fellowship to K.K., and an HHMI Faculty Scholar Fellowship to S.M.B. National Science Foundation (IOS-1558900) to N.S. **Author contributions:** M.A.R., K.K., M.B., G.P., D.A.W., N.S., S.M.B., R.B.D., and J.B.-S. conceived the study, designed experiments, and performed analysis; M.A.R., K.K., M.B., G.P., D.A.W., A.Y., K.H., K.Z., and M.W. performed experiments. M.A.R., K.K., M.B., N.S., S.M.B., R.B.D., and J.B.-S. wrote the manuscript. J.B.-S. can be contacted for rice genetic materials, R.B.D. for *Medicago* genetics materials, S.M.B. for tomato genetic materials, and N.S. for *S. pennellii* genetic materials. **Competing interests:** The authors declare no competing interests. **Data and material availability:** Sequence data are deposited in GEO (accession GSE128680); code and resources are in http://plant-plasticity.github.io/data-and-code/. All other data are in the main paper or supplementary materials.

SUPPLEMENTARY MATERIALS

science.sciencemag.org/content/365/6459/1291/suppl/DC1
Materials and Methods
Figures S1 to S34
References (*20*–*72*)
Data S1 to S18

1 May 2019; accepted 26 August 2019
10.1126/science.aax8862

science.sciencemag.org/content/365/6459/1291/suppl/DC1

Supplementary Materials for

Evolutionary flexibility in flooding response circuitry in angiosperms

Mauricio A. Reynoso*, Kaisa Kajala*, Marko Bajic*, Donnelly A. West*, Germain Pauluzzi*, Andrew I. Yao, Kathryn Hatch, Kristina Zumstein, Margaret Woodhouse, Joel Rodriguez-Medina, Neelima Sinha†, Siobhan M. Brady†, Roger B. Deal†, Julia Bailey-Serres†

*These authors contributed equally to this work.
†Corresponding author. Email: roger.deal@emory.edu (R.B.D.); nrsinha@ucdavis.edu (N.S.); sbrady@ucdavis.edu (S.M.B.); serres@ucr.edu (J.B.-S.)

Published 20 September 2019, *Science* **365**, 1291 (2019)
DOI: 10.1126/science.aax8862

This PDF file includes:

Other Supplementary Material for this manuscript includes the following:
(available at science.sciencemag.org/content/365/6459/1291/suppl/DC1)

Data S1 to S18 (.xlsx)

Materials and Methods

Plant material and transformation

Rice (*Oryza sativa japonica cv.* Nipponbare), tomato (*Solanum lycopersicum var. M82,* LA3475), *Solanum pennellii* (LA0716), and *Medicago truncatula* (ecotype Jemalong A17) were used. The previously reported stable transgenic rice lines used were *35S:OsNTF2-7* for INTACT (*20*) and *35S:His6-FLAG:OsRPL18-2* for TRAP (*21*). Production of transgenic INTACT lines was described previously for all but *S. pennellii (11, 20, 22)*. For the *Solanum* species and *M. truncatula,* the INTACT construct with the Arabidopsis WPP domain was used (*22*). These carry a constitutively expressed dicot codon-optimized *BirA* driven by the *S. lycopersicum SlACT2* promoter (*SlACT2p:mBirA*) for the *Solanum* species and *Arabidopsis thaliana AtACT2* promoter (*AtACT2p:mBirA*) for *M. truncatula*. The TRAP construct for *Solanum* species was *His_6-FLAG-GFP-AtRPL18* (*22*). For *M. truncatula,* the TRAP construct was identical to that of tomato except the *M. truncatula* 60S ribosomal protein RPL18-3 gene (*Medtr1g083460*) replaced *Arabidopsis* RPL18, and 2) the pB7WG backbone (https://gateway.psb.ugent.be/vector/show/pB7WG/search/index/), conferring phosphinothricin (BASTA) resistance, was used instead of the kanamycin resistance conferring pK7WG backbone.

Stable transgenic *Solanum* species were produced by use of *Agrobacterium tumefaciens* transformation by UC Davis Plant Transformation Facility (*11*). The specific *Solanum* lines used were tomato *35S:INNTF-1*; *35S:His6-FLAG-GFP-AtRPL18-5*, and *S. pennellii 35S:NTF-3; 35S:His6-FLAG-GFP-AtRPL18B-1*.

Hairy root cultures of *Agrobacterium rhizogenes* transformed *S. lycopersicum* roots were initiated and cultivated as described (*22*).

Hairy root composite *M. truncatula* plants were initiated by injecting the primary roots with *A. rhizogenes* K599. To do so, the day before injection, a small volume of glycerol stock of *A. rhizogenes* K599 carrying either *35S:NTF;AtACT2p:mBirA* or *35S:His6-FLAG-GFP-MtRPL18-3* plasmid was used to inoculate 5 ml of Yeast Extract Beef media (5 g/L tryptone, 1 g/L yeast extract, 5 g/L nutrient broth, 5 g/L sucrose, 0.49 g/L $MgSO_4x7H_2O$, 15 g/L agar, pH 7.2) additionally containing 100 mg/L Spectinomycin and grown overnight at 28°C at 200 rpm. When the OD_{600} was equal to 1.0, cultures were centrifuged at 5,000 rpm for 5 min. The supernatant was poured off and the pellet was resuspended in Injection Media (IM) (1X PBS, 100 uM acetosyringone, 1/10,000 (v/v) Silwet). Seedlings germinating for 2.5-days were injected by placing them in 5 mL of IM-resuspended *A. rhizogenes* poured out on a Petri dish and stabbing the root a few times with an 18G1 needle. Additionally, 1-2 mm of the primary root tip was cut off. Injected seedlings were moved to slanted Fahräeus Media (FM) plates (0.5 mM $MgSO_4$, 0.7 mM KH_2PO_4, 0.8 mM Na_2HPO_4, 50 nM FeEDTA, 0.5 mM NH_4NO_3, 1mM $CaCl_2$, 0.1 mg of $MnSO_4$, $CuSO_4$, Zn SO_4, H_3BO_3, and Na_2MoO_4, 8 g/L Phytoblend agar, pH 6.5) with no selection and were grown horizontally for 3 days, and then were moved to FM plates with 5 mg/L phosphinothricin and were grown vertically for 3 weeks before transfer to 1X MS media without vitamins (1% w/v agar, 1% w/v sucrose).

Growth conditions and submergence treatment

For rice, seeds were dehulled and surface sterilized in 50% (v/v) bleach solution for 30 min, rinsed ten times with sterile distilled water and grown on plates (100 cm^2) containing 0.5x Murashige and Skoog medium (MS), 1% (w/v) agar 1% (w/v) sucrose for 7 days (16h day / 8h night; at 28°C/25°C day/night; 110 $\mu Em^{-2}s^{-1}$). For tomato, seeds were surface sterilized in 50% (v/v) bleach solution for 5 min (*S. pennellii*) or 20 min (*S. lycopersicum*) and then rinsed three times with sterile distilled water. Growth was on vertical plates (10 cm x 10 cm) containing full-strength MS without vitamins, with 1% (w/v) agar (w/v) and 1% (w/v) sucrose. *S. lycopersicum* hairy root cultures transformed with *A. rhizogenes* were subcloned using a 2-cm hairy root segment, grown on horizontal plates (10 cm x 10 cm) containing full-strength MS with vitamins, with 1% (w/v) agar (w/v) and 3% (w/v) sucrose, 200 mg/L kanamycin and 200 mg/L cefotaxime. All tomato root cultures or germinating seeds were grown for 7 days in a growth chamber (at 25°C, 16h day/8h night; 60-65 $\mu Em^{-2}s^{-1}$).

M. truncatula seeds were surface-sterilized by incubating in concentrated sulfuric acid for 8 minutes with gentle stirring, washing 3 times with 4°C sterile, distilled water, then 4-8 minutes in 3% (w/v) hypochlorite (diluted bleach), washing 4 times with sterile, distilled water, and finally placing the seeds onto moist filter paper. Seeds were germinated without stratification on moist filter papers in inverted Petri dishes wrapped with surgical tape wrapping. These were kept in the growth room in the dark at 20°C for 2 days. The seedlings were then injected with *A. rhizogenes*, and composite plants with transformed hairy roots were obtained three weeks later. After the composite plant transformation protocol, the plants were grown vertically for one week (at 20°C, 16h day/8h night; 150 $\mu Em^{-2}s^{-1}$) before being used for the submergence experiment. The day before the experiment was performed, root tips from one plate were collected and visualized on a fluorescence stereomicroscope to check for GFP expression. Transformation efficiency was calculated as the percentage of root tips with ubiquitous GFP expression.

Four independent biological replicates were grown for each species. For whole plant submergence, plates were placed horizontally, opened and the seedlings covered with 5 cm of autoclaved distilled water at ZT 4h. Root tips (apical 1 cm including the meristem, elongation zone and early differentiation zone; all four species) and the shoot apical meristem region (*Solanum* species) were harvested at ZT 6h (2h before relative noon). Control plates were not opened, but positioned horizontally for the duration of the treatment and harvested at ZT 6h. Oxygen partial pressure was measured with the NeoFox Sport O_2 sensor and probe (Ocean Optics). The dissolved oxygen content in the water covering the plants remained above 18% (v/v) for the 2 h duration of the stress treatment.

Quantitative real-time reverse transcriptase PCR (qRT-PCR)

Three independent biological replicates of submergence and control time courses were conducted. Root tips (apical 1 cm) were harvested every two hours after submergence for qRT-PCR. For the *Solanum* species, RNA was extracted by polyA mRNA extraction (*23*), cDNA was synthesised by Superscript III (Invitrogen) and qRT-PCR was performed with SensiFast SYBR Hi-RIX kit (Bioline) with CFX384 Touch™ Real-Time PCR Detection System (Bio-Rad), all as per the manufacturer's instructions. For *M. truncatula*, RNA was extracted using the RNeasy

Plant Mini Kit (Qiagen). Genomic DNA was removed using the TURBO DNA-free Kit (Ambion) and first-strand synthesis was performed using SuperScript III on 150 ng of RNA. qRT-PCR was performed with Power SYBR Green Master Mix (Applied Biosystems) on the StepOnePlus Real-Time PCR System (Applied Biosystems). For rice, RNA was extracted using Direct-zol RNA Miniprep (Zymo Research). qRT-PCR was performed with 500 ng of RNA pre-treated with DNAse I (Thermo Scientific), reverse transcribed using Maxima reverse transcriptase (Thermo Fisher) in a total volume of 20 µl, according to the manufacturer's instructions. cDNA was diluted with 180 µl of ddH_20 and real-time (RT) PCR was performed with 5 µl of the diluted cDNA using SsoAdvanced™ Universal SYBR Green Supermix (Bio-Rad) and the CFX96 Touch Real-Time PCR Detection System (Bio-Rad) using defined primers (data S18). *ADH* mRNA abundance was compared to *UBCII* (*O. sativa*), *ACT2* (*S. lycopersicum* and *S. pennelli*) and *RPL2* (*M. truncatula*). The ΔΔCt method (*24*) was used to calculate relative in RNA abundance, using a Student's *t* test to evaluate significance using three technical and three biological replicates.

Nuclei purification by INTACT for ATAC-seq and nRNA-seq

Nuclei were purified from frozen and pulverized tissue as described previously for *A. thaliana* (*25*) with minor modifications (*20*). Tagmentation using Tn5 insertion and ATAC-seq libraries were prepared using 20,000-50,000 nuclei as previously described (*11*)(*26*), with slight modifications. For rice, minor modifications in nuclei purification include: 1) the use of a 30 µm filter to exclude 30 to 70 µm cellular debris from the crude extract and extended centrifugation times (*20*), and 2) using AMPureXP beads instead of columns to purify amplified libraries. For nRNA, samples were processed as described (*20*, *27*). In brief, nuclei captured by INTACT were processed using the RNeasy Micro kit (Qiagen), treated with Turbo DNase I (ThermoFisher Scientific) and concentrated using Agencourt RNAClean XP beads (Beckman Coulter). To remove contaminating pre-rRNA/rRNA a subtraction step using biotinylated oligos tiling pre-rRNA/rRNA and high temperature double-stranded nuclease was performed (*20*). Samples were re-treated with Turbo DNase I (ThermoFisher Scientific) and cleaned up with Agencourt RNAClean XP beads prior to use in library construction as described below.

Polysomal mRNA purification by TRAP and Total RNA isolation and RNA-seq library construction

TRAP was performed as previously described (*28, 29*) with the following modifications: α-FLAG conjugated IgG Dynabeads were used for binding; after magnetic collection and washing the polysomes were removed from the magnetic beads by the addition of Lysis and Binding Buffer (LBB) buffer for polyA mRNA isolation using biotinylated oligo-dT primers and streptavidin magnetic beads (NEB) (*23*). Total RNA was extracted from frozen tissue using polysome extraction buffer (*28*) followed by LBB polyA mRNA isolation using biotinylated oligo(dT) and streptavidin magnetic beads (*23*). Random primer-primed RNA-seq library construction for nRNA (pre-rRNA and rRNA digested), polyadenylated total RNA and polyadenylated TRAP RNA was performed as described (*23*) in at least four biological replicates for each condition and species.

Ribo-seq library construction

Ribo-seq libraries were generated as described by (*30*) but with ribosome isolation by TRAP as described by (*32*) starting with pulverized frozen root tip tissue (~1,000 1 cm root tip) thawed in 5 mL of Polysome Extraction Buffer and using α-FLAG conjugated IgG Dynabeads for binding instead of anti-FLAG M2 magnetic beads. Manipulations were as previously described by (*32*) through to the generation of ribosome footprint fragments (RFs) and on-magnetic bead digestion of 1 mL of resuspended beads with 2,000 units of RNase I (Ambion; ca. 15 U/µg RNA) by incubation for 180 min at 23-25 °C. RFs of 26-34 nt were gel purified, dephosphorylated using T4 polynucleotide kinase, ligated 500 ng preadenylylated miRNA cloning linker (IDT, miRNA cloning linker #1). The ligated-RFs were excised, recovered and resuspended in 10.0 µl of 10 mM Tris (pH 8). After this step, rRNA removal of RFs was done by use of Ribo-Zero rRNA Removal Kit (Plant; Illumina) probe solution. Library construction continued as described by (*31*) and the resultant 130 nt RF cDNAs were circularized and contaminating rRNA was subtracted by a second hybridization with custom-designed biotinylated oligos corresponding to pre-rRNA and rRNA as described (*31*). rRNA-subtracted circularized fragments were used for 12 cycles of 10s at 98°C, 10s at 60°C, and 5s at 72 °C PCR amplification including library and indexing primers. *M. truncatula* and *S. lycopersicum* libraries used indexing primers described (*23*), rice libraries used the same primers as described by Ingolia et al., 2012 (*32*). The amplified RF library (~175-180 bp) was excised and recovered from the gel, purified, analysed on Agilent BioAnalyzer DNA 1000 chip, multiplexed and sequenced.

Short read processing, quality assessment, alignment to genomes, and read coverage

For rice, *S. lycopersicum* and *S. pennellii*, nRNA, total poly(A)$^+$ and TRAP libraries and all Ribo-seq libraries, including *M. truncatula*, were sequenced on the Illumina HiSeq 3000 to obtain 50 nt single-end reads at the UC Davis DNA Technologies Core. Raw reads were filtered to remove adapter-only or polyA-pulldown primer sequences. For *M. truncatula*, nRNA, total poly(A)+ and TRAP libraries were sequenced on the Illumina NextSeq 500 at the Georgia Genomics and Bioinformatics Core at UGA to obtain 75 nt single-end reads for nRNA libraries and 36 nt paired-end reads for total poly(A)$^+$ and TRAP libraries.

Rice and *M. truncatula* data analysis steps were performed on the University of California, Riverside Institute for Integrative Genome Biology high performance bioinformatics cluster (http://www.bioinformatics.ucr.edu/), supported by NSF MRI DBI 1429826 and NIH S10-OD016290. R packages from Bioconductor including systemPipeR (*33*) were used. Quality reports of raw reads were generated with the FastQC package (http://www.bioinformatics.babraham.ac.uk/projects/fastqc/). Adaptors were removed from Ribo-seq reads and RNA raw reads were mapped with the splice junction aware short read alignment suite Bowtie2/Tophat2 to the IGRSP1.0-30 genome for rice (http://plants.ensembl.org/Oryza_sativa/Info/Index) and Mt4.0 genome for *M. truncatula*, allowing unique alignments with ≤2 nt mismatches. nRNA, polyadenylated total RNA and polyadenylated TRAP RNA was filtered by mapping first to the mitochondrial and chloroplast genomes before mapping to the nuclear genome. Expression analyses were performed by

generating read count data for features of exons-by-genes using the summarizeOverlaps function from the GenomicRanges package(*4*).

For the *Solanum* samples, mapping was executed in the CyVerse Discovery Environment. STAR v2.4.0.1 was used to align nRNA-seq reads to organelle sequences to filter out reads that map to organelles (*S. lycopersicum* AFYB01.1 mitochondrial sequence, *S. lycopersicum* NC_007898.3 chloroplast sequence, and *S. pennellii* HG74452 chloroplast sequence, all downloaded from NCBI); alignment parameters were set to include unmapped reads as the output (--outSAMunmapped Within, --outReadsUnmapped Fastx). For all RNA-seq libraries, reads were then mapped to either *S. lycopersicum* ITAG3.10 or *S. pennellii* cDNA (exonic) sequences (downloaded from SolGenomics). For both *Solanum* species the 90 gene models identified to potentially encode for rRNA were masked. STAR GenerateGenomeIndex was set to --limitGenomeGenerateRAM 36000000000 to account for the large number of cDNA inputs) using the STAR v2.4.0.1 aligner (default parameters, SAM output). Estimated count (est_counts) abundances were calculated using eXpress v1.5.1, default parameters. For visualization of read mapping, the reads were also mapped to either the *S. lycopersicum* ITAG3.10 or the *S. pennellii* genome using STAR v2.4.0.1, default parameters.

For all species, reads were converted from SAM to sorted BAM files using Samtools 1.0.9 and the BAM files were converted to bigwig files using BedTools 2.26 genomeCoverageBed followed by UCSC bedGraphtoBigWig 332--0, default parameters.

Ribo-seq reads periodicity analysis was performed using Ribotaper (*34*). Modified GTF files for each species to select protein-coding annotated genes and TRAP RNA expressed genes were used to create annotation files (create_ annotation_files.bash). Merged bam files were used to generate periodicity plots with the script create_metaplots.bash.

RNA-seq differential expression

Statistical analysis of differentially expressed genes was carried out using limma-voom (*35*) Bioconductor package in R. Raw RNA-seq read counts were normalized with voom using the *quantile* method. The functions lmfit, contrasts.fit, and ebayes were used to calculate differential gene expression for different contrasts, including $\log_2$ Fold Change (FC) values and adjusted P values (adj.P.Val). The *fdr* method was used for controlling the false discovery rate (FDR). Multidimensional scaling (MDS) plots were generated using Glimma Bioconductor package in R (*36*) using genes with more than 0.5 count per million in at least 3 replicates. Following normalization, count data were used to calculate reads per kilobase per million reads (rpkM). Enrichment analysis of Gene Ontology (GO) terms was performed with systemPipeR (*33*) using the GO definitions from the BioMart database for rice and *M. truncatula*, and with goseq R package (*37*) using the category list specifically built for *S. lycopersicum* (*38*) for the *Solanum* species.

Transcript read (average) coverage plots were calculated and produced over selected groups of genes with the functions computeMatrix and plotHeatmap from deepTools (http://deeptools.readthedocs.io/en/latest/index.html) using bigwig files. For each group of genes the 5% most highly and 5% lowly expressed genes were removed from the coverage plots, as

highly covered regions can bias the mean. Log_2 FC values for genes identified as differentially expressed were clustered using the Partitioning Around Medoids (PAM) method with k = 12 to 24 clusters. The method of clustering and the k values were optimum for resolution of correlated genes based on the evaluation of results with multiple k values. Clustering and heatmaps plotting the mean log_2 FC values were created using the following R packages: gplots, cluster, e1071, and RColorBrewer installed from https://cran.r-project.org.

Identification of genes families and syntenic orthologous genes (syntelogs) across species

Predicted angiosperm gene families were extracted from Phytozome v11 including *O. sativa*, *M. truncatula* and *S. lycopersicum* (*11*). These families were established by Phytozome using InParanoid, which uses BLAST alignment between two related protomes to identify orthology groups, defined by the developers as homologs from a speciation event (*39*). Gene families shared between *S. lycopersicum* ITAG3.10 and *S. pennellii* were independently generated in three ways: 1) using the synteny aligner CoGe SynMap, megablast, with an e-value of 0.001; 2) a two-directional syntenic alignment using CoGe SynFind, default parameters, both with ITAG3.10 as the query and *S. pennellii* as the query; and 3) the best blastn hit, default parameters, between the cDNAs of ITAG3.10 and *S. pennellii*. The gene identifier (ID) obtained was used to associate the gene to a gene family. As the Phytozome list used the ITAG 2.4 annotation, for the genes annotated in ITAG3.10, which do not have an assigned gene ID in ITAG2.4, we performed a blastp (-max_target_seqs 1) search between the cDNAs to find the closest related gene in *A. thaliana.* The resultant gene ID was used to associate the *Solanum* gene to a gene family. To identify conserved responses across species, the overlaps in families containing differentially expressed genes were produced with the function overLapper from systemPipeR. Venn diagrams were plotted with the function vennPlot.

Syntenic orthologs (syntelogs) were identified using a combination of CoGe SynFind (https://genomevolution.org/CoGe/SynFind.pl) with default parameters, and CoGe SynMap (https://genomevolution.org/coge/SynMap.pl) with the QuotaAlign feature selected and a minimum of six aligned pairs required (*40*, *41*). Rice and *Brachypodium distachyon,* or *Zea mays* syntelogs were obtained from ensembl plants (http://plants.ensembl.org/compara_analyses.html). To identify corregulated syntelogs, each gene which had a syntelog in the comparison species and was differentially expressed was clustered by the PAM method as described. To simplify the visualization the median of the cluster was calculated and plotted using the functions geom_line and geom_point from the R package ggplots2.

To evaluate the differences in transcript (nRNA, polyA RNA or TRAP RNA) levels between syntenic and non syntenic genes, the mean of normalized rpkM values were plotted for genes with transcript abundance > 0.5 rpM using the function geom_violin. Significant differences of means were evaluated using the Student's t test, comparing a single population of transcripts under one condition (*i.e.*, nRNA in control samples) for syntenic and non-syntenic genes. An F-test was used to evaluate the difference in the variances of the two populations using the R function var.test (data S13).

Enrichment for regulated genes in gene families in each species

For each upregulated gene family in any species and comparison, the number of upregulated and non-regulated genes were quantified to generate a contingency table including the overall number of regulated genes. A linear model was generated to test for the enrichment in a gene family in a species compared to others (mod=glm(formula = family ~ species + degs,data=my.data, family = binomial(logit), weights=Freq)).

Mapping of chromatin accessibility, identification of Transposase Hypersensitive Sites, and evaluation of accessibility changes between conditions

Rice libraries were sequenced on the HiSeq 3000 at the UC Davis DNA Technologies Core to obtain 50 nt single-end reads. *M. truncatula* ATAC-seq libraries were sequenced on the NextSeq 500 at the UGA Georgia Genomics and Bioinformatics Core to obtain 36 nt paired-end reads. *S. lycopersicum*, *S. pennellii*, and a few rice ATAC-seq libraries were sequenced on the NextSeq 500 at the UC Davis DNA Technologies Core to obtain 36 nt paired-end reads. Genomic DNA ATAC-seq libraries from root tips for each species were sequenced on the NextSeq 500 at the UGA Georgia Genomics and Bioinformatics Core to obtain 36 nt paired-end reads. Sequencing reads were mapped using Bowtie2 software (*42*) with default parameters to each species' corresponding genome build; rice was mapped to IGRSP1.0-30, *M. truncatula* was mapped to Mt4.0, *S. lycopersicum* was mapped to ITAG3.10, and *S. pennellii* was mapped to the genome assembly of Bloger et al. (2014) (*43*). Mapped reads were processed as previously described (*44*), which included converting to *.bam* format using Samtools 0.1.19 (*45*), sorting and filtering to retain only reads that had a mapping quality score of 2 or higher, and filtering to retain only the reads that mapped to nuclear chromosomes and scaffolds.

Peak calling was done using the "*Findpeaks*" function of the HOMER package (*46*) with the parameters "*-minDist 150*" "*-region*" and "*-regionRes 1*". Peaks called between replicates were kept if they replicated at least once between replicates given the condition that they overlap by at least 50%. This was done using the Bedtools software (*47*) and the "*intersect*" function. Reproducible peaks that overlapped by 150 bp, half the size of the mean peak sizes called in each species, were merged together using the Bedtools "*merge*" function to give the final list of reproducible, non-redundant chromatin accessible regions identified in each species. These regions are referred to as Transposase Hypersensitive Sites (THSs).

Read alignments, referred to as counts, present in the coordinates of identified THSs were quantified in each species for control and submergence samples using HTSeq's *htseq-count* script (*48*). At least two replicates of each condition were counted and the counts were statistically evaluated using DESeq2 (*49*). THSs that had a log fold change value of 1 or more, or -1 or less, and a p-value $\leq$ 0.05 were identified as THSs that are either upregulated, or downregulated, during submergence stress. Upregulated THSs refer to chromatin regions where chromatin was more accessible during submergence stress, compared to control conditions.

For visualization of chromatin accessibility data, *.bam* files were converted to bigiwg files using the deeptools 2.0 (*50*) "*bamCoverage*" script, using the bin size of 1 bp and RPKM normalization parameters, and UCSC's "*bigWigMerge*" and "*bedGraphToBigWig*" programs. Replicates for a specific condition were processed such that each replicate had the same number

of mapped reads before merging. This was done using the Samtools "*view -c*" command to count the number of aligned reads within the replicate and the Samtools "*view -S*" command to scale down globally the number of reads for that replicate. Heatmap and metaplots of chromatin accessibility data were generated using the deepTools "*computeMatrix*" "*plotHeatmap*" and "*plotProfile*" functions.

Annotation of Transposase Hypersensitive Sites

For each THS, distance to and identity of the nearest gene was assigned using the "*TSS*" function of the PeakAnnotator 1.4 program (*51*). Each THS was assigned to a genomic feature (upstream, exon, intron, downstream, or intergenic) using HOMER's "*annotatePeaks.pl*" program. Genomic features were defined using published annotation files for the genomes used for alignment, as well as HOMER's "*parseGTF.pl*" and "*assignGenomeAnnotation*" programs. The "upstream" regions were defined as the 2,000 bp upstream of the transcription start site, and "downstream" regions were defined as the 1,000 bp downstream of the transcription end site.

Identification of enriched regulatory motifs

Two methods of cis-element enrichment were used. (Method 1) *De novo* discovery: To identify motifs enriched in promoter regions of SURFs, the 2 kb upstream region of the ATG for all the upregulated genes in a family were evaluated for sequence enrichment using MEME (*52*). Motifs significantly enriched (E-value<0.01) were compared to databases of known transcription factors, including DAP-seq (*53*) and CIS-BP (*54*), by using TOMTOM (*55*) on the MEME output. As a control, genes not regulated from each family were processed in the same way to detect putative regulatory elements in control conditions that are non-submergence specific. Detected motifs were screened in all annotated genes using RSAT and the enrichment of SURFs were evaluated using a Fisher's exact test using the fisher.test() function in R. (Method 2) *De novo* discovery in promoter-bound accessible regions of SURFs: To identify motifs enriched in accessible sites found in promoter regions of SURFs, THS sequences found in the 2 kb upstream and +500 bp region of the TSS, highest density of THS localization for rice and *M. truncatula*, for all upregulated genes in a family were evaluated for sequence enrichment using AME (*56*). This enrichment analysis was done using both DAP-seq and CIS-BP databases to match enriched motifs to known transcription factors. Motifs with an E-value<0.01 were considered as significantly enriched motifs found in SURF promoter-bound THSs.

Motif mapping and validation of SURF-regulated enrichment

The FIMO program (*57*) was used to map motifs throughout repeat-masked genome sequences of rice (IGRSP1.0-30), *M. truncatula* (Mt4.0), *S. lycopersicum* (ITAG3.10), and *S. pennellii* genome assembly of Bloger et al. (2014) (*43*). The default parameters for FIMO mapping were adjusted to account for memory considerations and p-value scoring bias for smaller, more precise positional weight matrices. This was done by using the "*--max-stored-scores 100000000*" option and the "*--thresh*" option. The p-value threshold was set manually by choosing a low significance value, such as "*--thresh 0.005*" and then visually examining the results to determine at which cutoff there was more than 1 base pair mismatch between the identified motif and the

sequence reported in the positional weight matrix. The only p-value cutoff changed for the main motifs described in this work was bHLH, which was set to 0.0002 instead of the default value of 0.0001 to account for the smaller size of the motif.

A total of 23 motifs were identified as potential regulators of increased SURF expression. To remove false-positive motifs that are found in high abundance within all gene promoters we used the Fisher's exact test to compare the percentage of SURF promoters of a given species that had a motif versus the percentage of all other genes' promoters that had a motif within that species. Through this validation process, bHLH, HRPE, and MYB were found to be significantly enriched in SURF promoters of all four species. WRKY was significantly enriched in SURF promoters of rice, *M. truncatula*, and *S. lycopersicum*, but not *S. pennellii*.

Network analyses

The Cytoscape software (*58*) was used to build gene regulatory networks between the four TF-binding sequence motifs (bHLH, HRPE, MYB, and WRKY) and the SURF genes of each species. The TF-binding sequence motif must be located within the -2 kb upstream and +500 bp downstream region of the TSS of the SURF gene being regulated in order for the TF-gene connection to be made.

Phylogenetic analyses

Gene family conservation was inferred by using a Maximum Likelihood method based on the JTT matrix-based model in the software MEGA 7 (*59*). The consensus tree is generated from 1000 bootstrap replicates. Branches corresponding to partitions reproduced in less than 50% bootstrap replicates are collapsed. Initial tree(s) for the heuristic search were obtained automatically by applying Neighbor-Join and BioNJ algorithms to a matrix of pairwise distances estimated using a JTT model, and then selecting the topology with superior log likelihood value. All positions with less than 95% site coverage were eliminated. That is, fewer than 5% alignment gaps, missing data, and ambiguous bases were allowed at any position.

Accessible datasets

The data reported are accessible from Gene Expression Omnibus (GEO) database, www.ncbi.nlm.nih.gov/geo (accession no. GSE128680). The scripts used are available at: http://plant-plasticity.github.io/data-and-code/

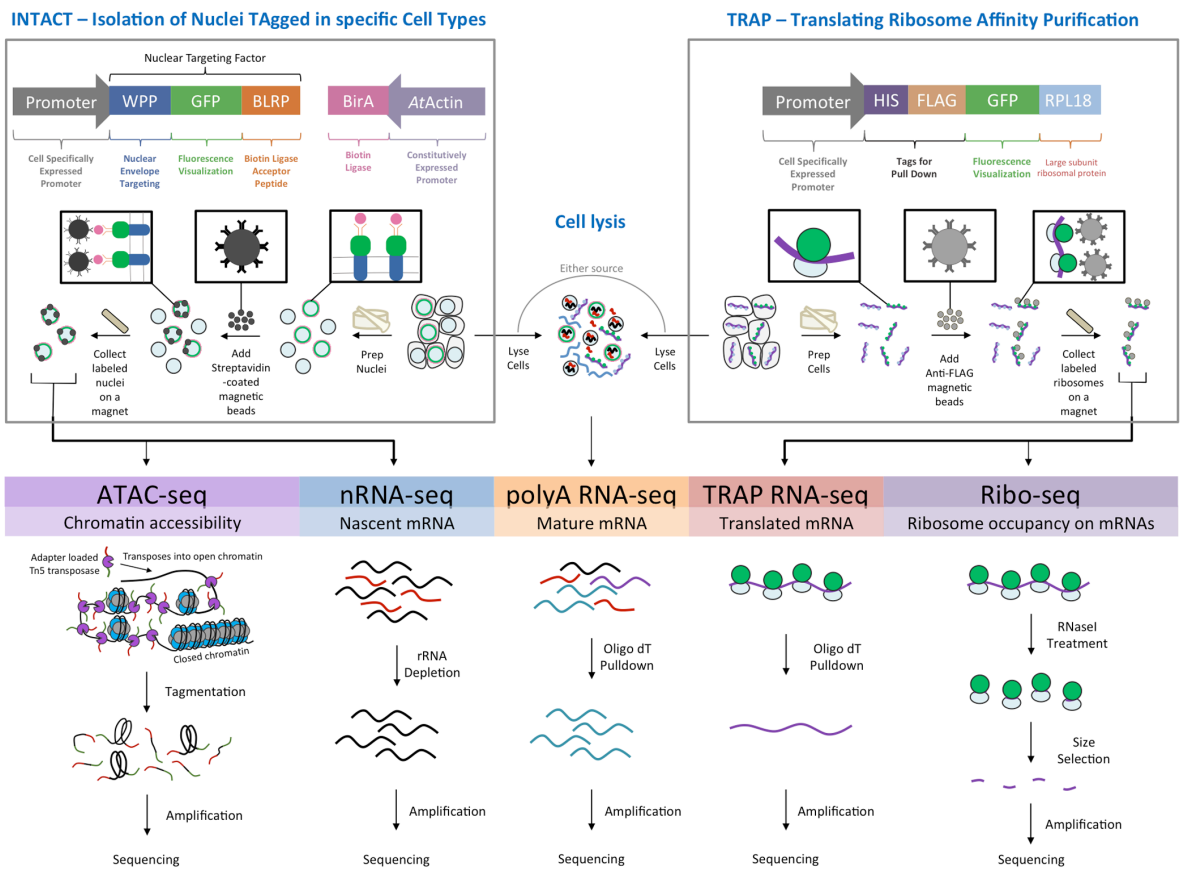

Fig. S1. Experimental scheme for the evaluation of nuclear and cytoplasmic gene regulatory activity in four species. Nuclei were isolated by Isolation of Nuclei TAgged in specific Cell Types (INTACT), which utilizes plants expressing a chimeric biotinylated Nuclear Targeting Factor that interacts with the nucleus (*Solanum* ssp. and *M. truncatula*) (*11*, *25*) or that is an integral part of the nuclear envelope (rice) (*20*). Nuclei were used to evaluate chromatin accessibility by Assay for Transposase-Accessible Chromatin (ATAC-seq). Gene transcripts present in the nucleus (nRNA) were isolated following INTACT and subtraction of rRNA. These were used for library construction without the selection of polyadenylated RNA. Total cellular polyadenylated mRNA (polyA RNA) was obtained by use of biotinylated oligo-dT hybridization and streptavidin magnetic bead purification. Ribosomes and associated mRNA were purified from cell extracts by Translating Ribosome Affinity Purification (TRAP), which takes advantage of plants expressing a FLAG-epitope tagged RPL18 (*Solanum* ssp., *AtRPL18B (22); Medicago MtRPL18B (60)*; rice *OsRPL18A* (*21*)). Polyadenylated mRNAs associated with ribosomes (TRAP RNA) was obtained by TRAP followed by biotinylated oligo-dT hybridization and streptavidin magnetic bead purification. Ribosome footprint profiling (Ribo-seq) was used to evaluate the position of individual ribosomes on mRNA. Non-directional RNA-sequencing libraries were prepared for nRNA, polyA RNA and TRAP RNA.

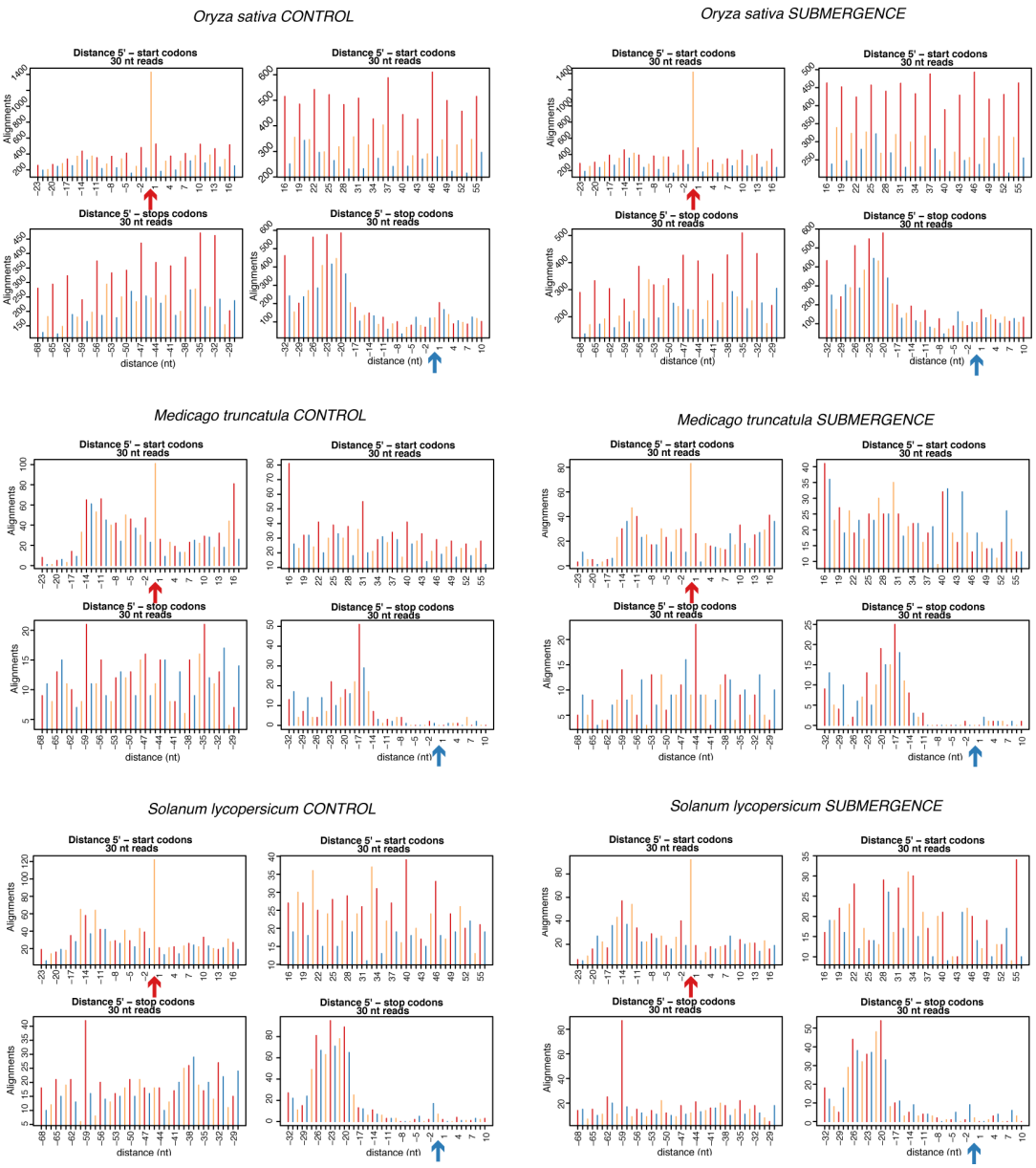

Fig S2. Mapped ribosome footprints demonstrate coding sequence coverage. Ribosome footprint fragments (RFs) were generated by RNAse digestion, isolated by TRAP, sequenced and mapped to each genome. Plots show coverage values [reads per million reads (rpM)] of the first nucleotide of 30-nt ribosome footprints in the start and stop codon regions of expressed protein-coding genes. Values represent three replicates each for control and submergence. Each group of four plots are (i) 5' untranslated region (UTR) and the coding sequence, centered on the initiation (start) codon (position 0, red arrow) and extending to codon 5; (ii) codons 6-19; (iii) the region of the coding sequence just prior to stop codon; and (iv) region around the stop codon (blue arrow) and extending into the first part of the 3'UTR. Each bar represents a nucleotide. To visualize codon-by-codon periodicity, colors of bars correspond to the first (red), second (blue) and third (orange) position of each codon. The 3 nt periodicity characteristic of translation is most evident for rice (*O. sativa*) and tomato (*S. lycopersicum*) and then *M. truncatula.* All of the species show a rapid decline in RFs on the 3'UTR indicative of translation termination.

Fig. S3. Multidimensional scaling analysis of nuclear and cytoplasmic responses to submergence in multiple plant species. Comparison of complete RNA-seq datasets obtained for nuclear RNA (nRNA), polyadenylated RNA (polyA), ribosome-associated RNA (TRAP) and ribosome footprint fragments (Ribo-seq) after mapping to the corresponding genome and normalized (filtered to remove very low expression genes) for the two conditions (control and submergence). Each column corresponds to a species (*Os*, *O. sativa*/rice; *Mt*, *M. truncatula*; *Sl*, *S. lycopersicum*/tomato; *Sp, S. pennellii*). Each row corresponds to two different dimensions determining the variation in the data. Each dot in the graph corresponds to a sample library. Vertically oriented pairs of graphs are labeled by either the type of library or the condition. For *S. lycopersicum*, the types of samples assayed are also compared (root tips, shoot apexes and tips of hairy roots). Distinction between samples was driven by RNA readout and condition. Data presented in data S2.

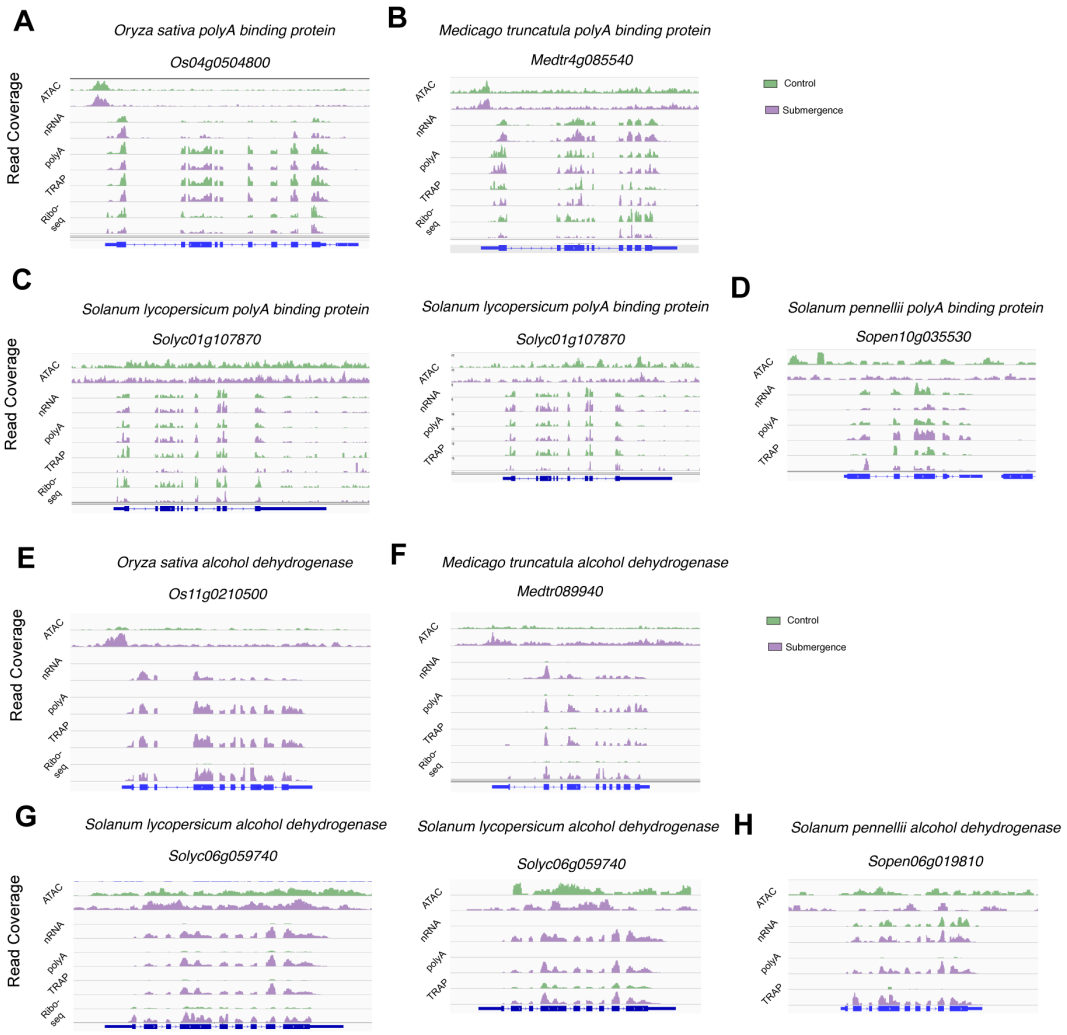

Fig. S4. Visualization of multiple tiers of regulation. (**A-D**). Tracks for ATAC-seq, nRNA, polyA RNA, TRAP RNA and Ribo-seq for a constitutively expressed gene in each species under control and submergence. (**E-H**). Tracks showing accumulation of *ADH* under submergence. Data represent merged Bigwigs files of at least two biological replicates; scales are the same for each pair of tracks for the same gene activity readout. Transcription direction for all genes is from left to right.

Fig. S5. Comparison of chromatin accessibility, nRNA, polyadenylated RNA, translated RNA and ribosome footprints on differentially regulated genes of rice. Coverage of ATAC and nRNA, polyA RNA (TOT), TRAP RNA and Ribo-seq for root-regulated genes. Regions upstream of the transcription start site (TSS) and downstream of the polyadenylation site (pA) are shown for ATAC coverage. Heatmap of gene clusters from Figure 1D.

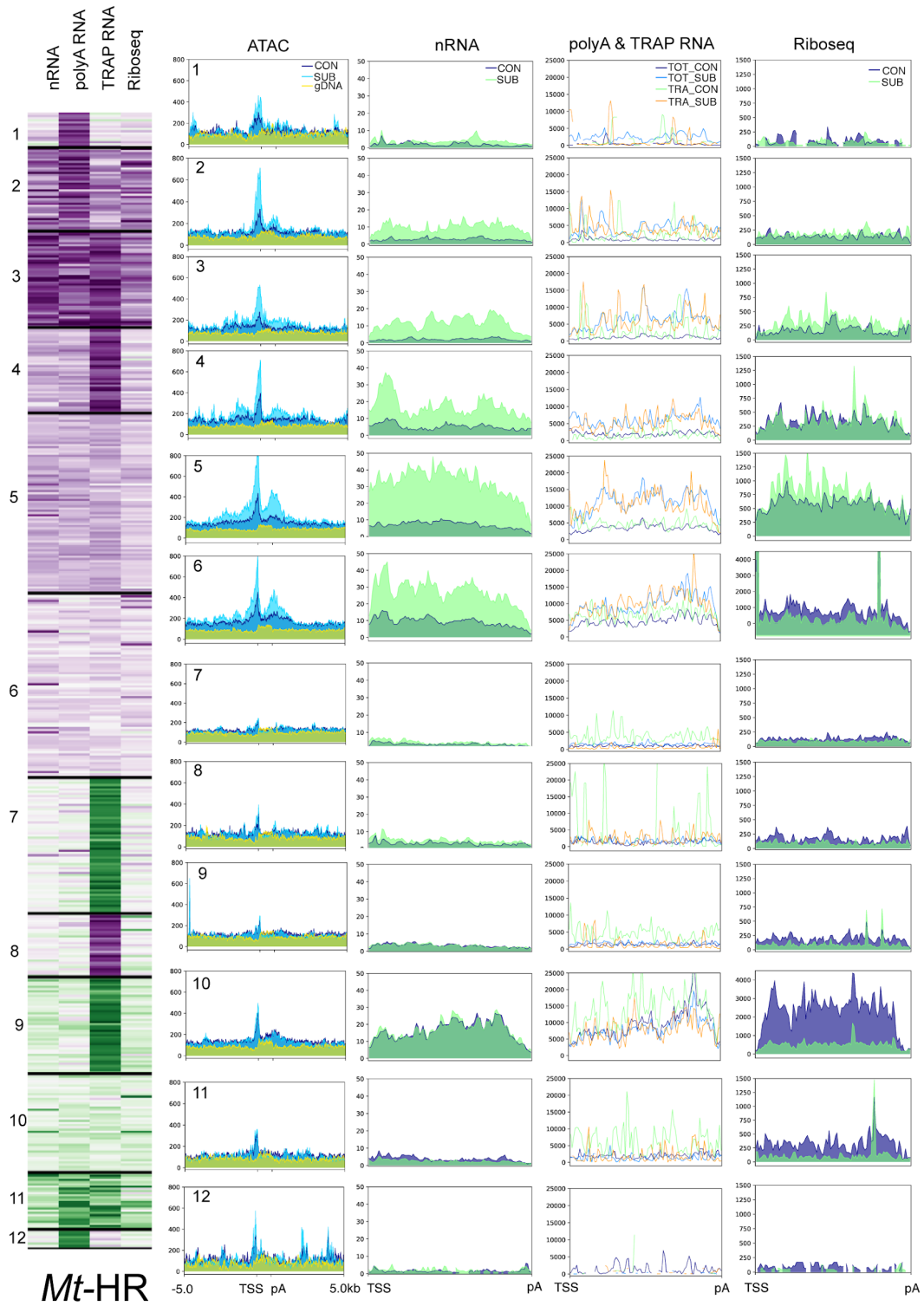

Fig. S6. Comparison of chromatin accessibility, nRNA, polyadenylated RNA, translated RNA and ribosome footprints on differentially regulated genes in hairy roots of *M. truncatula*. At left, heatmap of gene clusters from Figure 1D. Coverage of ATAC and nRNA, polyA RNA (TOT), TRAP RNA and Ribo-seq for hairy root-regulated genes. Regions upstream of the transcription start site (TSS) and downstream of the polyadenylation site (pA) are shown for ATAC coverage.

Fig. S7. Comparison of chromatin accessibility, nRNA, polyadenylated RNA, translated RNA and ribosome footprints on differentially regulated genes in *S. lycopersicum* hairy roots. At left, heatmap of gene clusters from Figure 1D. Coverage of ATAC and nRNA, polyA RNA (TOT), TRAP RNA and Ribo-seq in hairy root-regulated genes. Regions upstream of the transcription start site (TSS) and downstream of the polyadenylation site (pA) are shown for ATAC coverage.

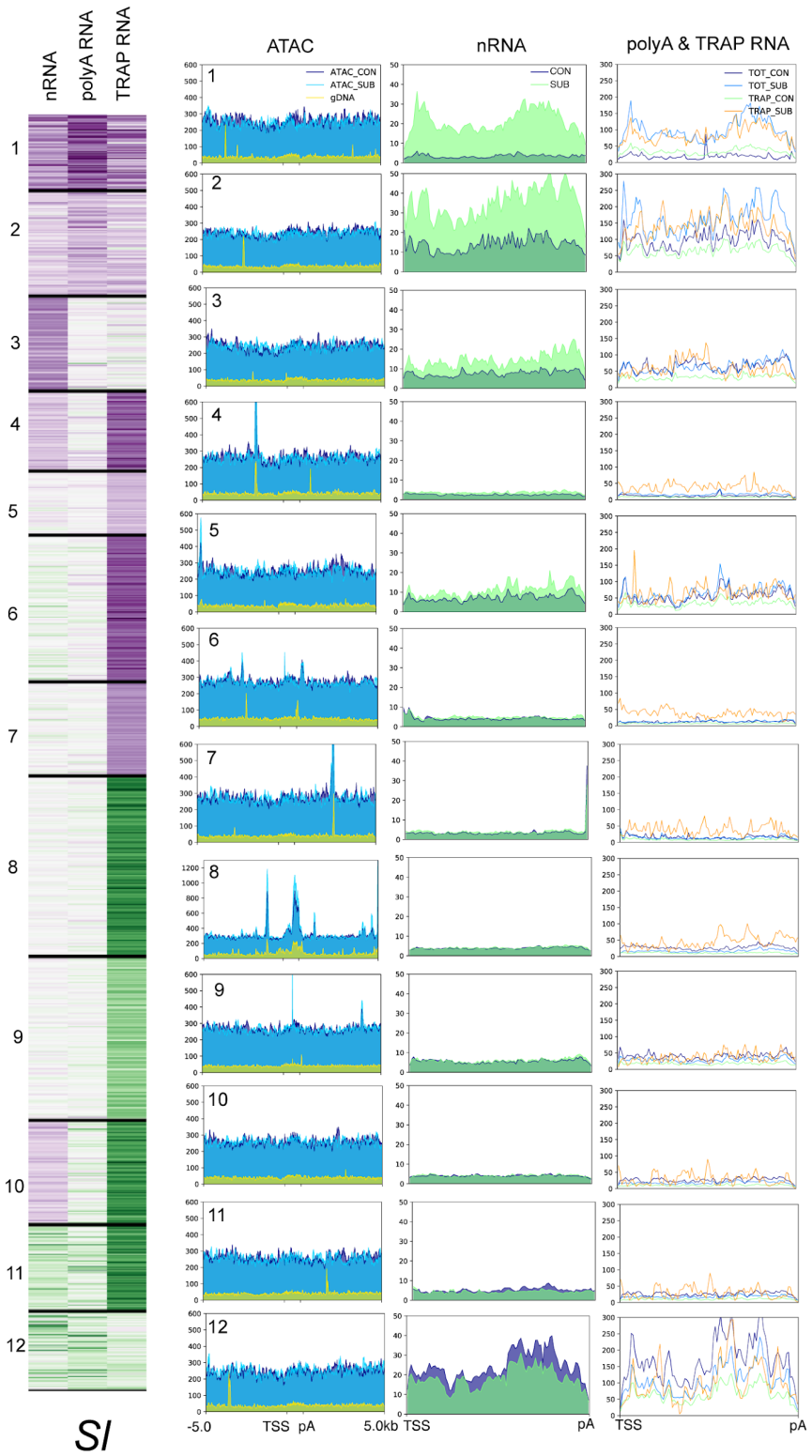

Fig. S8. Comparison of chromatin accessibility, nRNA, polyadenylated RNA, translated RNA and ribosome footprints on differentially regulated genes in *S. lycopersicum*. At left, heatmap of gene clusters from Figure 1D. Coverage of ATAC, and polyA RNA (TOT) and TRAP RNA for root-regulated genes. Regions upstream of the transcription start site (TSS) and downstream of the polyadenylation site (pA) are shown for ATAC coverage.

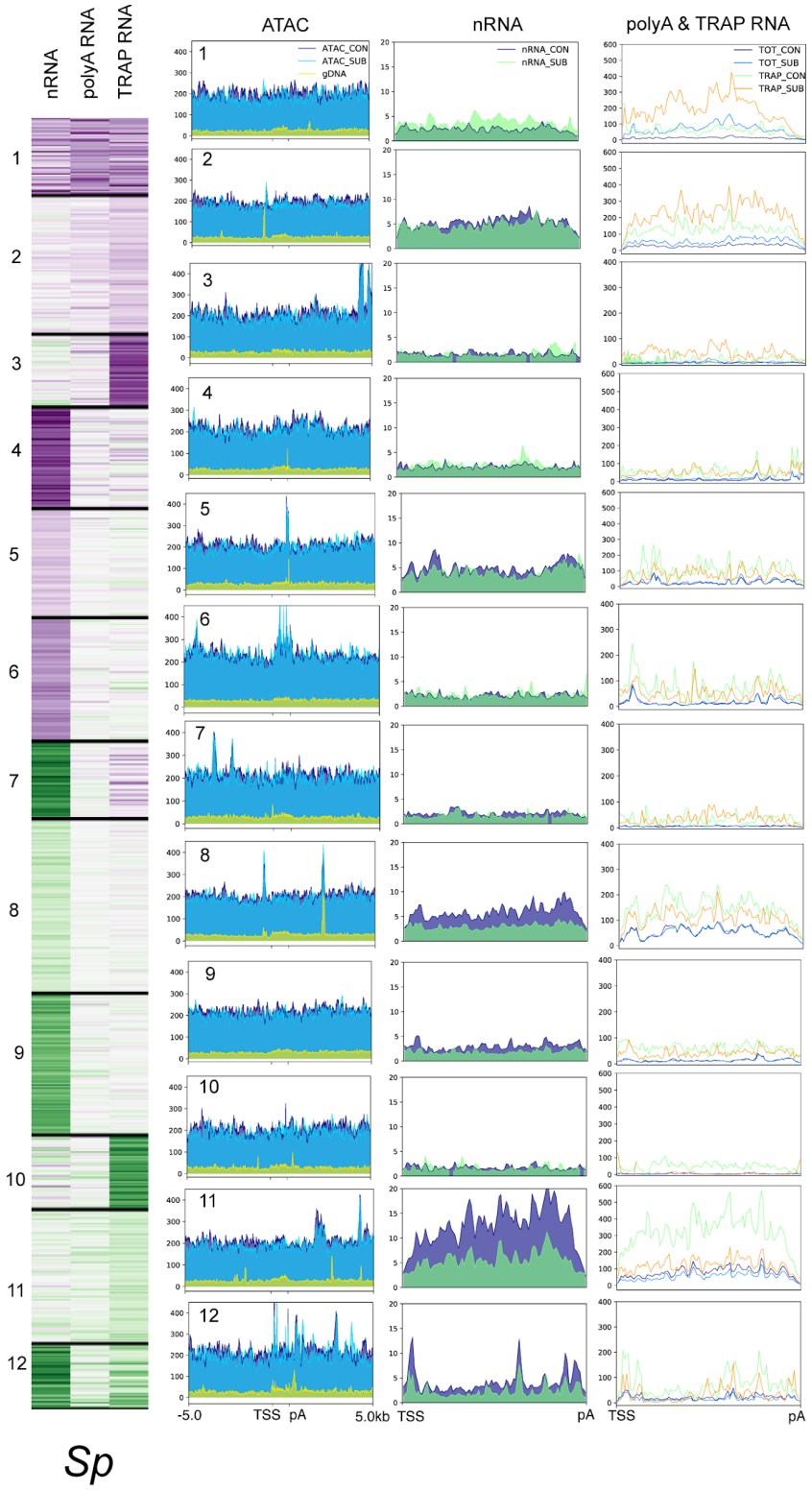

Fig. S9. Comparison of chromatin accessibility, nRNA, polyadenylated RNA, translated RNA and ribosome footprints on differentially regulated genes of *S.pennellii*. At left, heatmap of gene clusters from Figure 1D. Coverage of ATAC and nRNA, polyA RNA (TOT) and TRAP RNA for root-regulated genes. Regions upstream of the transcription start site (TSS) and downstream of the polyadenylation site (pA) are shown for ATAC coverage.

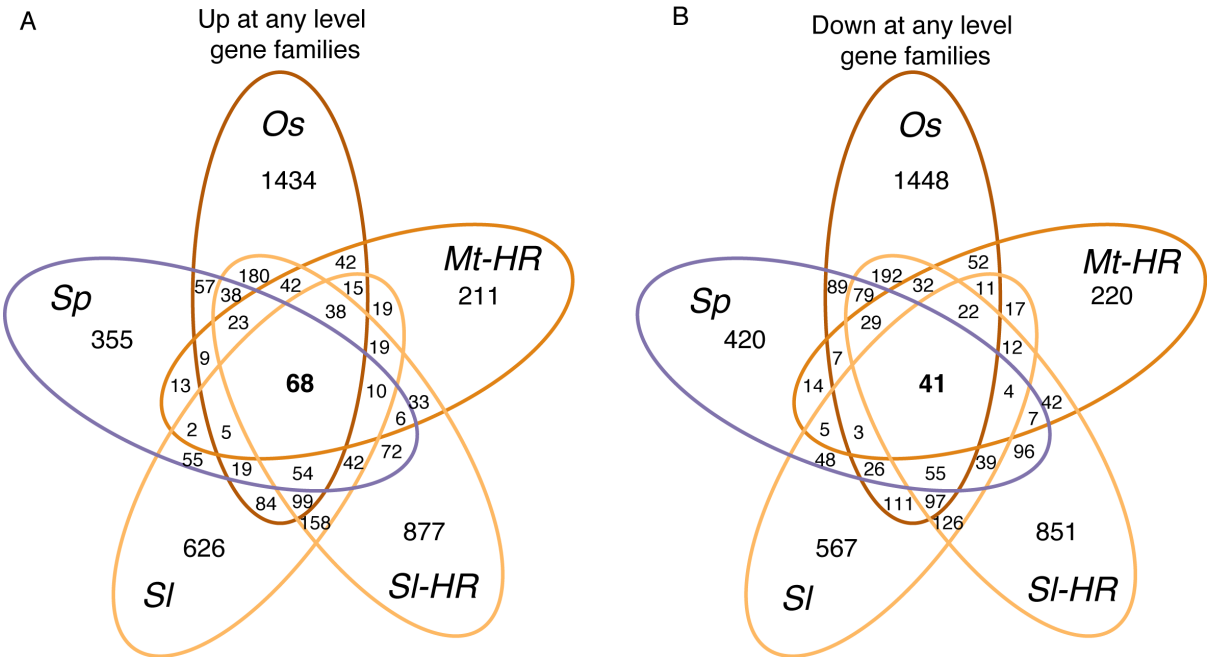

Fig. S10. Identification of conserved submergence-responsive gene family members across the four species. Related to Figure 1F. Tabulation of gene family members conserved across the four species that were differentially regulated ($|\log_2 FC|>1$ and padj<0.05) in at least one RNA population. This analysis identified the 68 submergence-upregulated families (SURFs) across the four species (**A**) and 41 submergence downregulated gene families across the four species (**B**). Of the conserved down-regulated genes, only three were among the genes reduced by hypoxia in multiple cell types of Arabidopsis (*6*). Data presented in data S5.

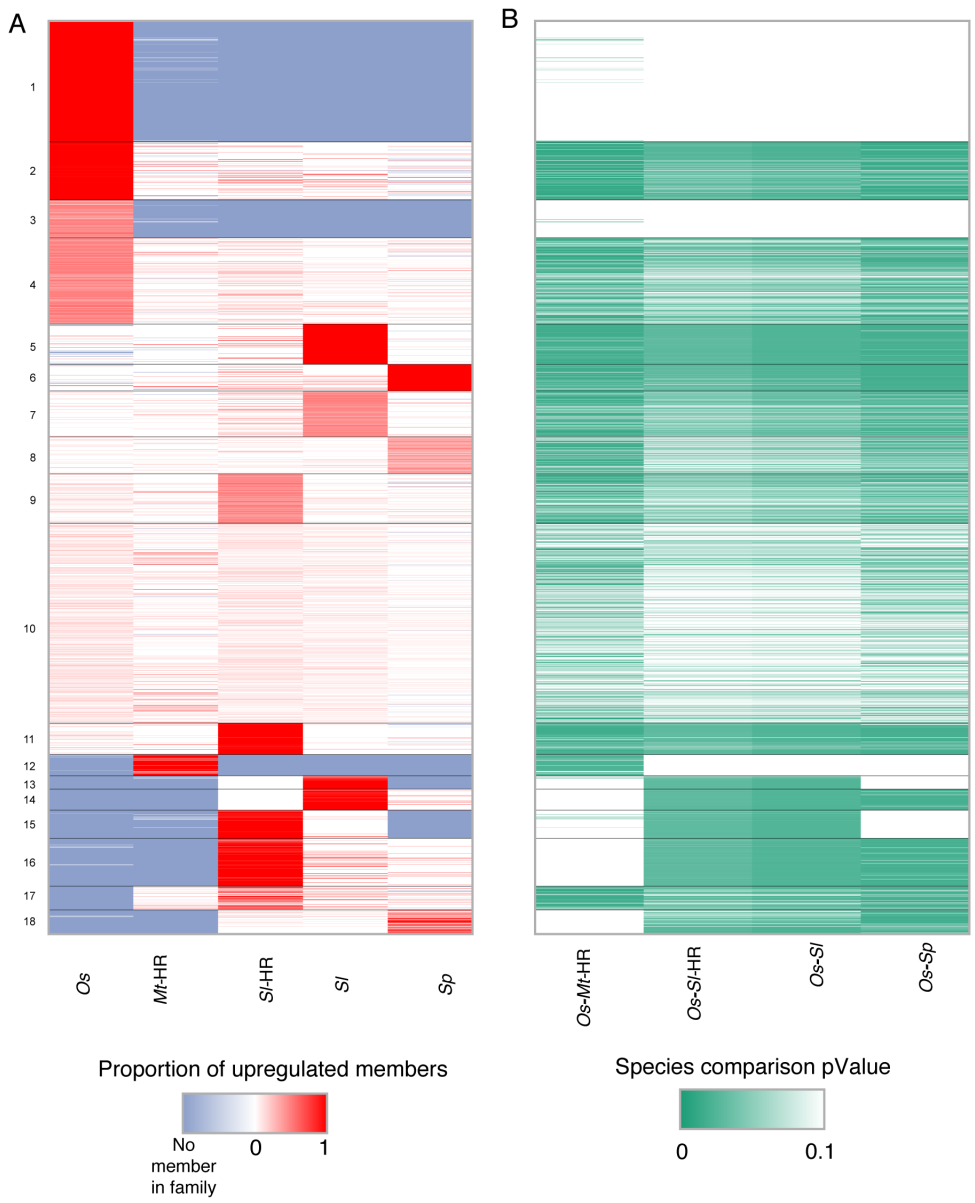

Fig. S11. SURFs show varied enrichment in the four angiosperms surveyed. (**A**) Heatmap showing the proportion of submergence upregulated gene members per gene family at any RNA population in root tips. Each row shows this proportion for a different gene family. Absence of gene family members in a species is indicated in grey. Clusters were generated by Partition around the mediod method. (**B**) Heatmap of pValues of the differential enrichment of each family in panel A for the four species compared to rice. The analysis illustrates species-specific distinctions in the enrichment of SURFs active in root tips in response to submergence. Some upregulated SURFs genes predominate in rice (clusters 1-4) and others in the other species. Distinctions are evident for the two *Solanums*. Data presented in data S6.

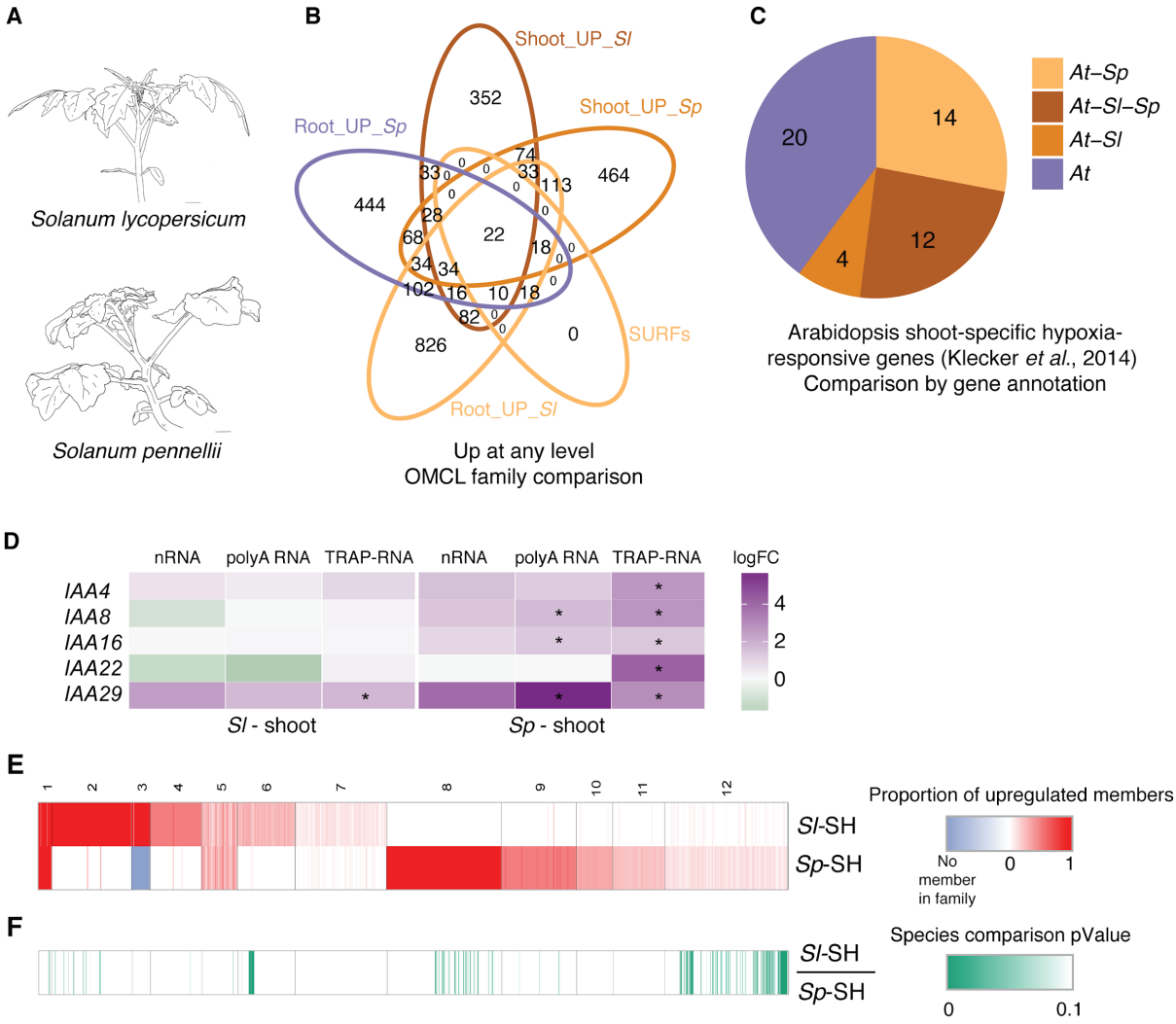

Fig. S12 (A-D). Comparison of submergence upregulated genes in root tip and shoot apex regions of *Solanum* species. (**A**) Cartoon of mature *S. lycopersicum* (*Sl*) and *Solanum pennellii* (*Sp*) shoots. (**B**) Gene family comparison of upregulated transcripts at any level (nRNA, polyA RNA, TRAP RNA) in *Sl* and *Sp* shoot and root apex regions shows that both species and tissues have many of uniquely regulated transcripts. Half of the conserved SURFs are represented in genes upregulated in shoot (32 of 68 in *Sl*, 40 of 68 in *Sp*). Twenty-two of the conserved SURFs are upregulated in both organs of *Sl* and *Sp*. The upregulated gene families in shoots are more specific to each species: 139 shared, 493 *Sl*-specific, 697 *Sp*-specific. (**C**) Comparison of *Solanum* shoot-specific submergence response to *Arabidopsis* shoot-specific hypoxia response from (*6*). (**D**) Expression patterns of submergence-responsive *IAA* genes in the shoot apex (data S7). (**E**) Heatmap of the proportion of submergence-upregulated gene family members per gene family, similar to S11, in shoots of *Sl*, and *Sp*. Each column shows this proportion for a different gene family. Absence of gene family members is indicated in grey. (**F**) Heatmap for pValues of the differential enrichment between the two species. Analysis illustrates species-specific distinctions in the enrichment of SURFs elevated by submergence. Some upregulated SURF genes predominate in *Sl* (clusters 2-4,6) and others in the *Sp* (8-12) (data S6).

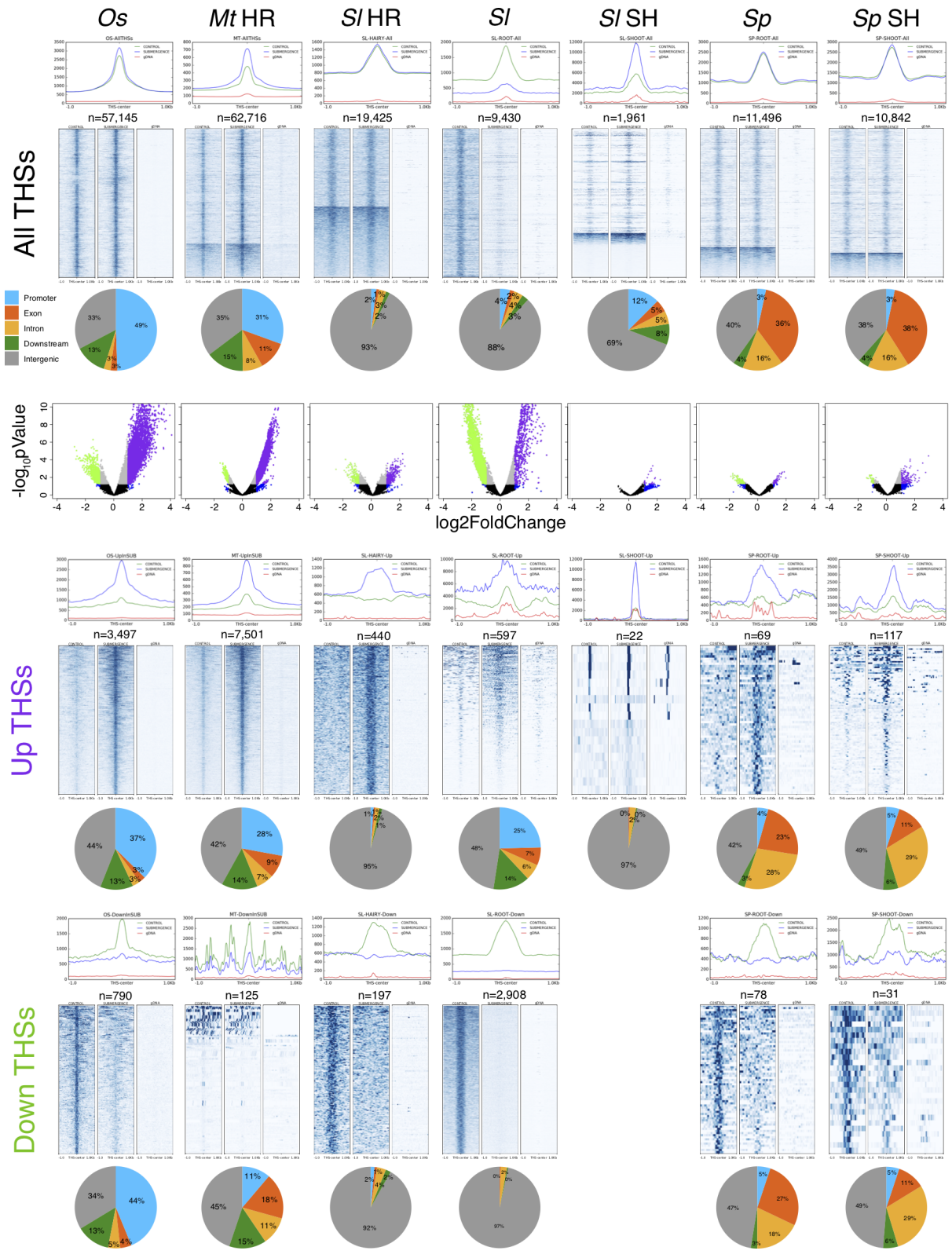

Fig. S13. Identification of Transposase Hypersensitive Sites that are enriched or depleted during submergence stress. Chromatin accessibility visualization, evaluation, and annotation in *Oryza sativa* roots (*Os*), *M. truncatula* composite plant hairy roots (*Mt* HR), *Solanum*

lycopersicum hairy roots (*Sl* HR), *S. lycopersicum* roots (*Sl*), *S. lycopersicum* shoot apex (*Sl* SH), *S. pennellii* roots (*Sp*), and *S. pennellii* shoot apex (*Sl* SH). The different sample types are organized into columns. For each column, information for all the Transposon Hypersensitive Sites (THSs) identified within that sample is described at the top. This information includes a metaplot of all the THSs, the number of THSs, and heatmaps of all THSs in control, submergence, and genomic ATAC-seq datasets. Pie charts describe the proportions of THSs found in different genomic features. Volcano plots depict the distribution of THSs that are upregulated (Up THSs, purple dots) or downregulated (Down THSs, green dots) during submergence. Metaplots, numbers, heatmaps, and genomic distribution for upregulated THSs (Up THSs) and downregulated THSs (Down THSs) is shown in the middle and the bottom, respectively. Data presented in data S8.

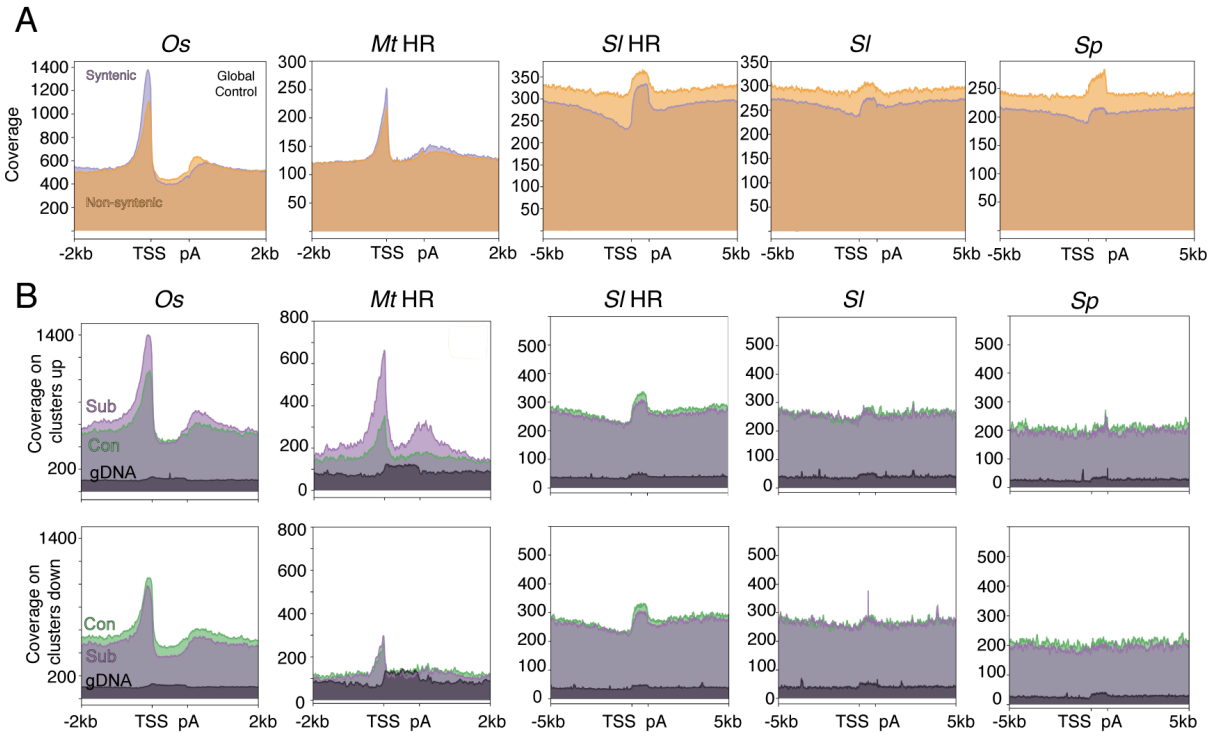

Fig. S14. Chromatin accessibility over detected genes and regulation by submergence in different species. (**A**) Coverage plots for chromatin accessibility for all detected genes classified in syntenic and non-syntenic under control condition (related to Fig. 3B). Rice genes were evaluated for synteny to *Brachypodium distachyon* genes, *M. truncatula* genes to *Solanum lycopersicum* and *S. lycopersicum* to *S. pennellii* and *vice versa*. (**B**) Profiles of chromatin accessibility measured via ATAC-seq under control and submergence for the genes included in predominantly up or down regulated clusters shown in Fig 1D and their corresponding upstream and downstream regions. gDNA indicates readout from purified genomic DNA.

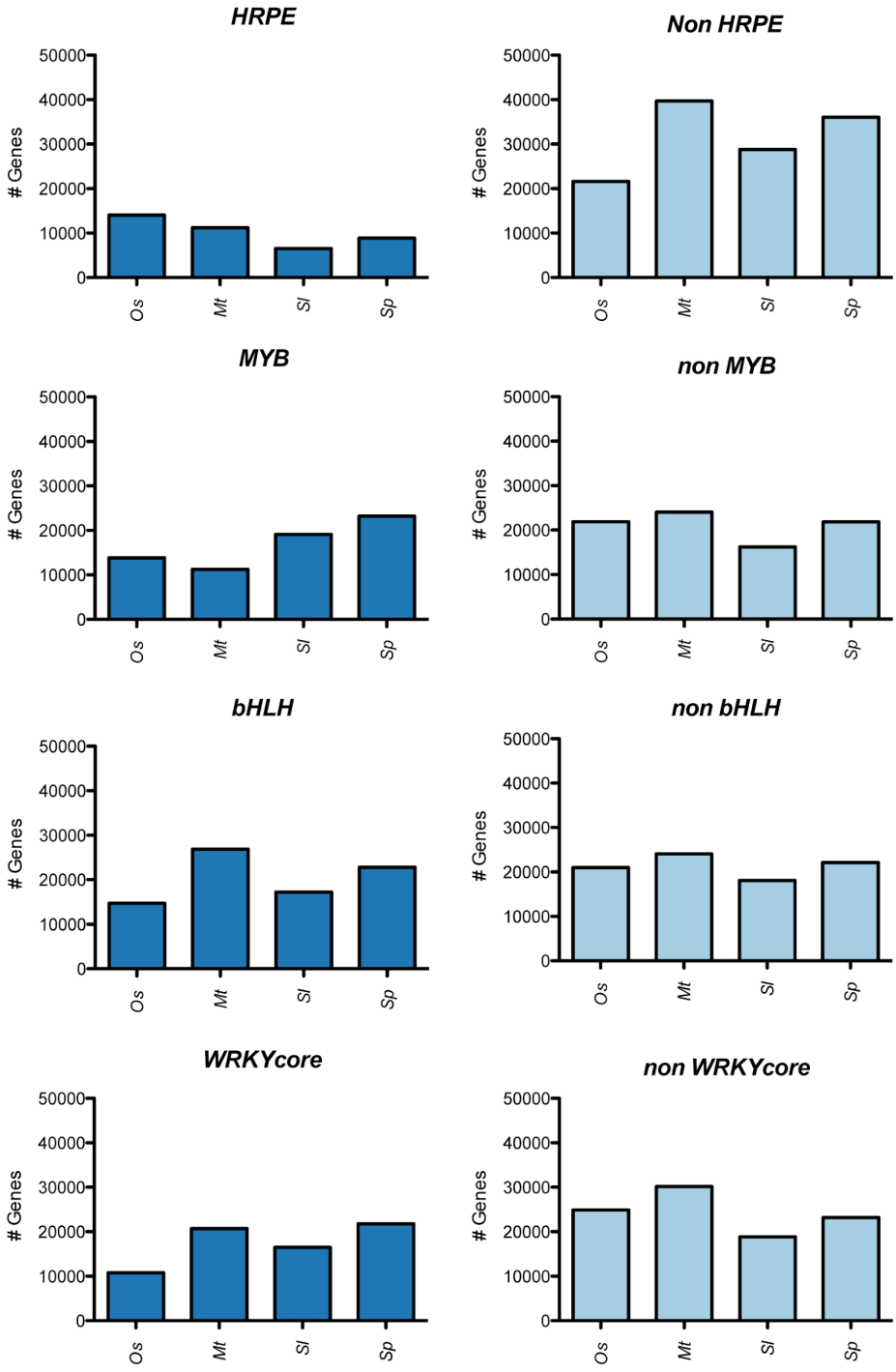

Fig. S15. Overall presence of HRPE, MYB, bHLH, WRKY TF motifs in promoter regions of genes. Number of genes that possess (left) or lack (right) an HRPE, MYB, bHLH, WRKY binding motif in the region 2 kb upstream and 500 bp downstream of the TSS. Data presented in data S9.

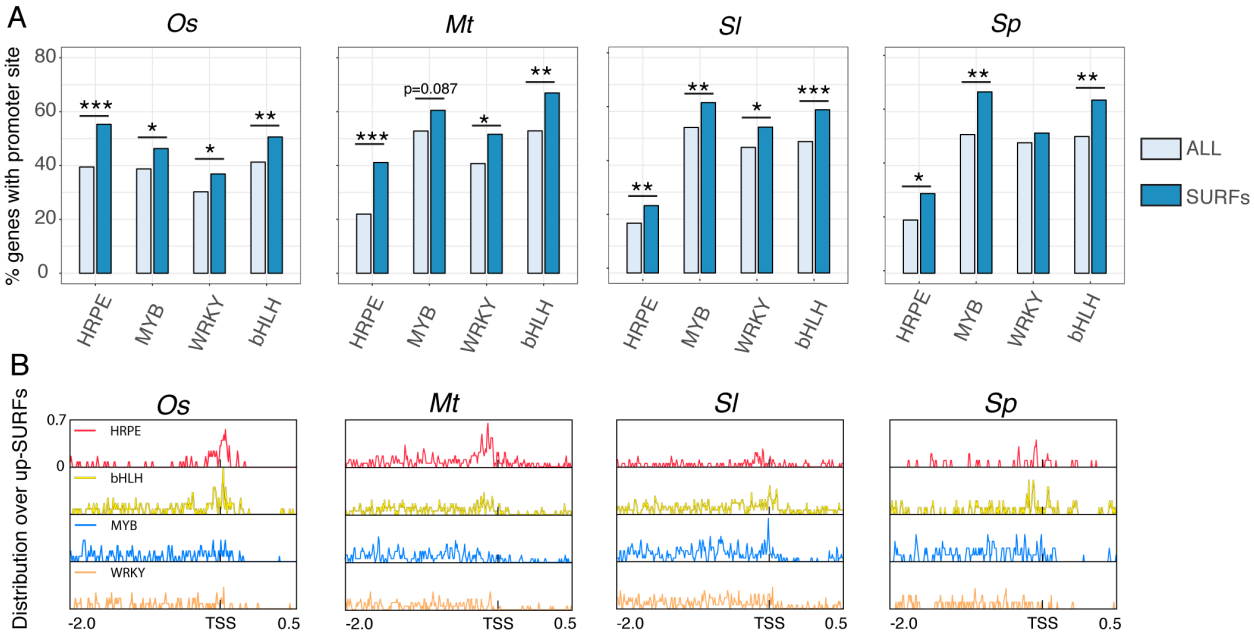

Fig S16. TF motifs enrichment in conserved SURF promoters across species. (**A**) Percentage of HRPE, MYB, WRKY and bHLH site containing promoters (-2000 to +500 bp relative to the TSS) of all genes in the genome and genes in the conserved SURF distributed in two groups containing upregulated and non-upregulated gene family members, respectively. pValues lower than 0.1 in a Fisher's exact test are indicated (* $p<0.05$; ** $p<0.01$; *** $p<0.001$). Data presented in data S9. (**B**) Distribution of enriched TF motifs in upregulated SURF genes. HRPE and bHLH motifs predominated near the TSS in all four species whereas the position of MYB and WRKY was more varied and species specific.

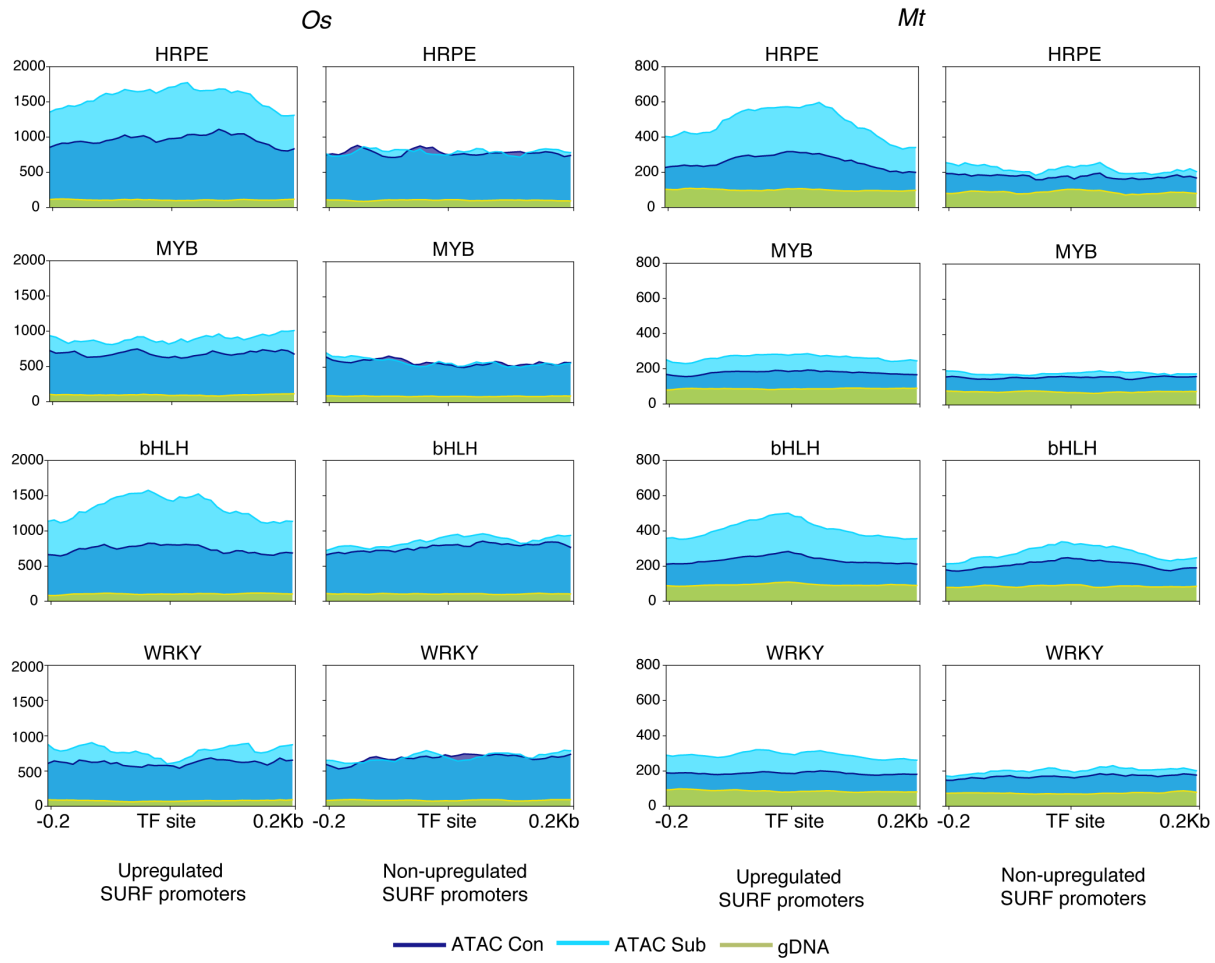

Fig. S17. Chromatin accessibility over regions nearby submergence TF binding sites in conserved SURF gene members. ATAC coverage was evaluated in HRPE, MYB, bHLH and WRKY binding sites present on SURF promoters of the members of the family classified in upregulated or non-upregulated. Tracks include control (Con), submergence (Sub) and genomic DNA (gDNA).

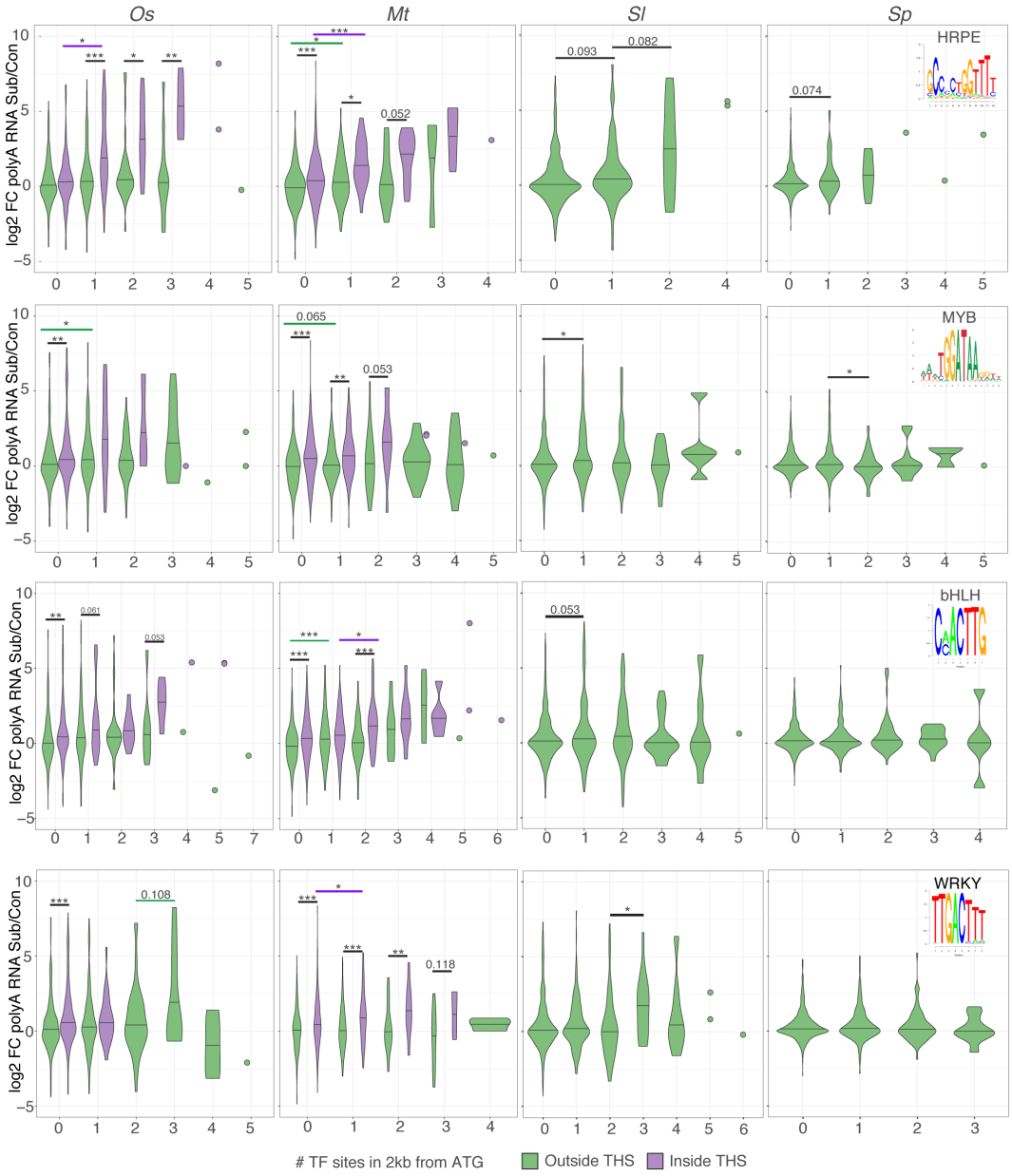

Fig. S18. Co-occurrence of regions of open chromatin, regulatory sites in promoter and up regulation of genes downstream for conserved upregulated families. Violin plots depicting $\log_2$ FC polyA RNA Sub/Con for all genes in SURFs arranged by presence of HRPE, MYB, bHLH or WRKY motifs in 2 kb upstream of the ATG, inside or outside regions of accessible chromatin Transposase Hypersensitive Site (THS). Asterisks indicate significant differences of the mean in t.tests comparing means of $\log_2$ FC polyA RNA Sub/Con (* = p<0.05, ** = p<0.01, *** =p<0.001, values smaller than 0.12 are indicated). Black lines indicate comparison for genes containing n regulatory sites inside or outside THSs, green and violet lines indicate comparisons between groups of genes having n and n-1 sites outside and inside THS respectively. Data presented in data S10.

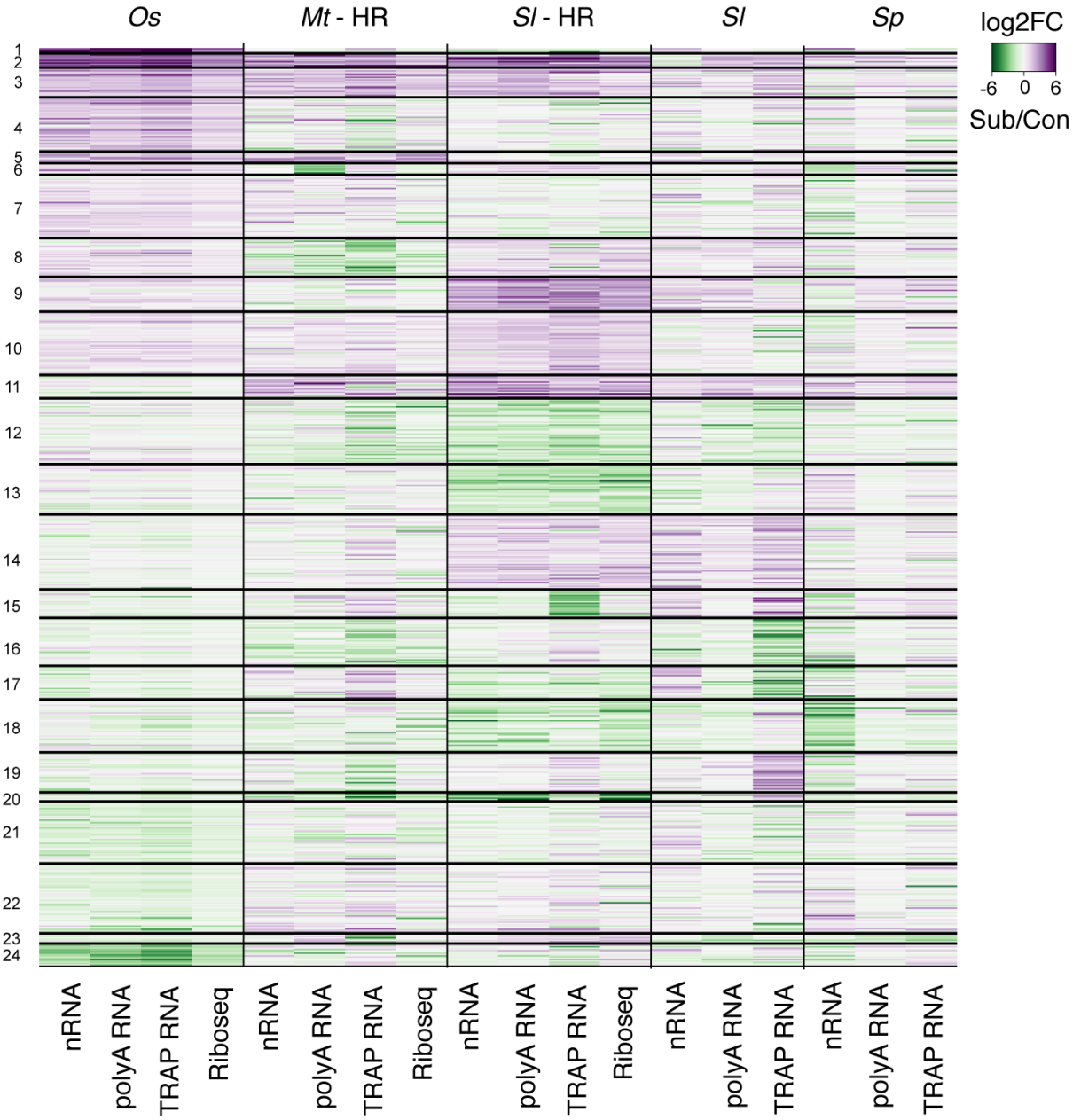

Fig. S19. Stress regulation of syntenic genes is not coordinated across four angiosperm species. Related to Fig 3A, this heatmap presents the $\log_2$ FC submergence vs. control of syntenic genes recognized across the four species which are regulated in at least one RNA population across all the species analyzed. Data for clusters 1-11 and 14 are plotted in Fig. 3A. Data for downregulated clusters are plotted as a line in fig. S22A. Data presented in data S11.

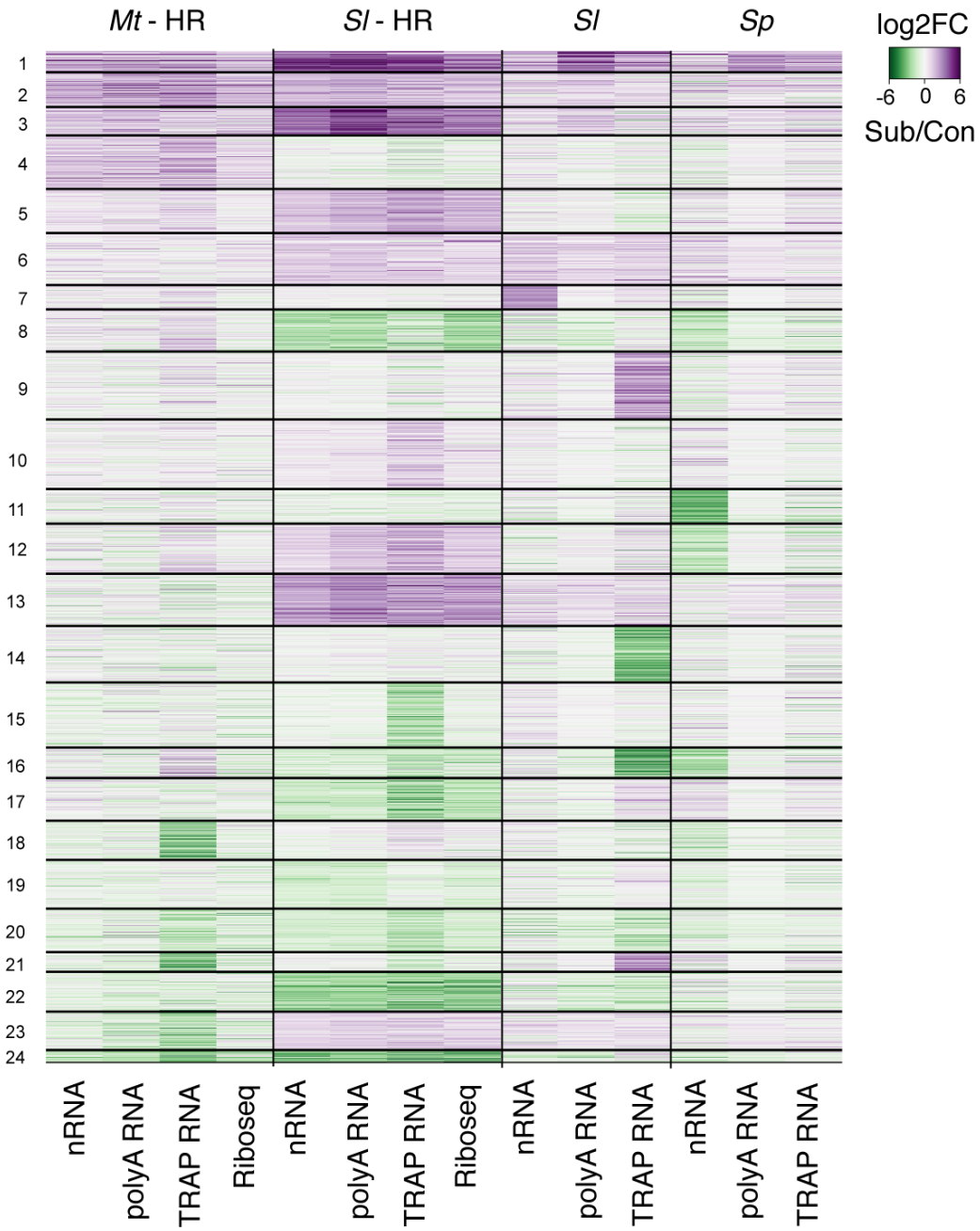

Fig. S20. Stress regulation of syntenic genes coordination across three eudicots. This heatmap represents the $\log_2$ FC of syntenic genes recognized across *Medicago* and *Solanum* species that are regulated in at least one RNA population. Plotted as a line in fig. S22B. Data presented in data S11.

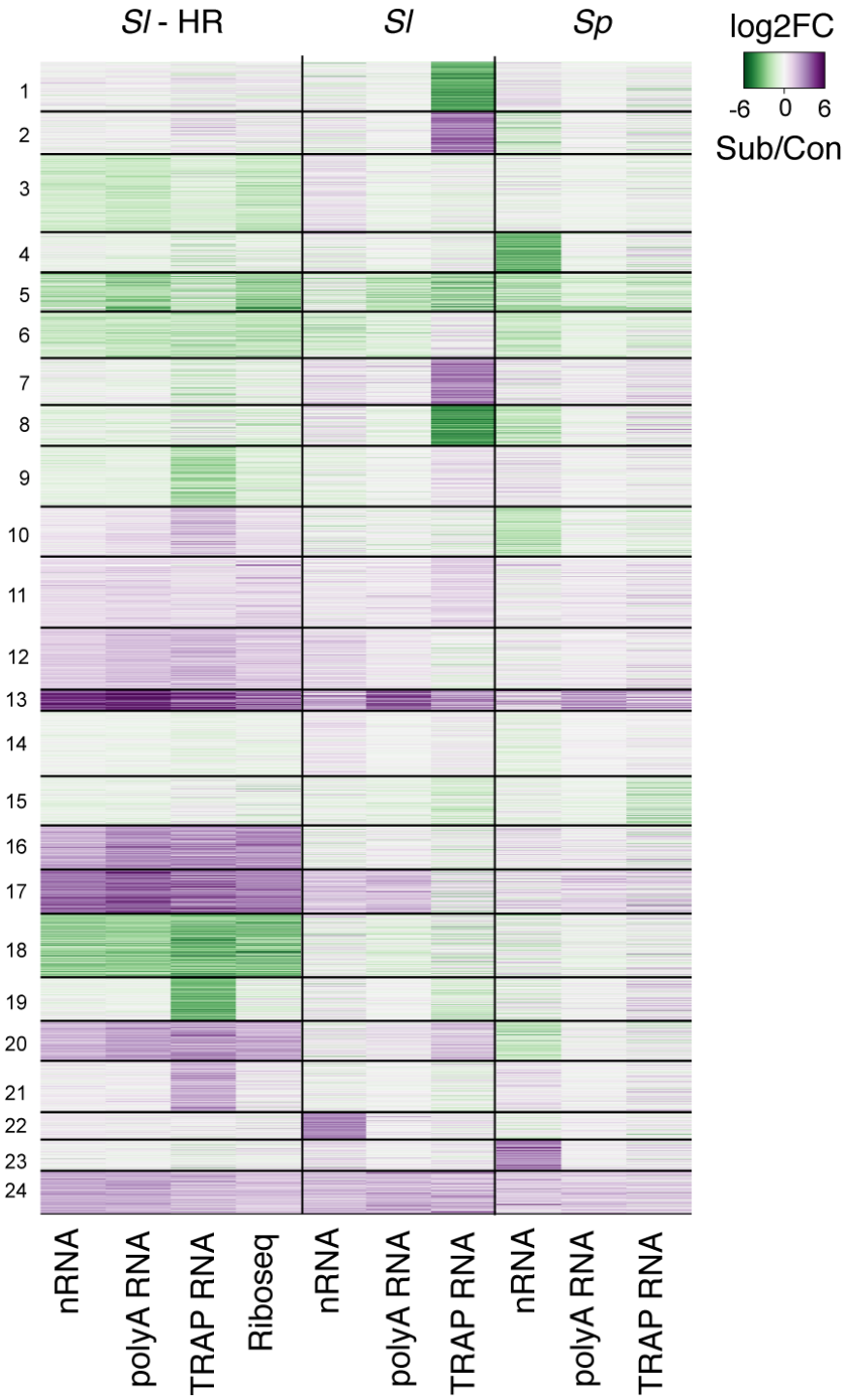

Fig. S21. Stress regulation of syntenic genes for two *Solanum* species. Figure related to Fig 3A**.** Heatmap representing the $\log_2$ FC of syntenic genes that are regulated in at least one RNA population across the *Solanum* species analyzed. Plotted as a line in fig. S22C. Data presented in data S11.

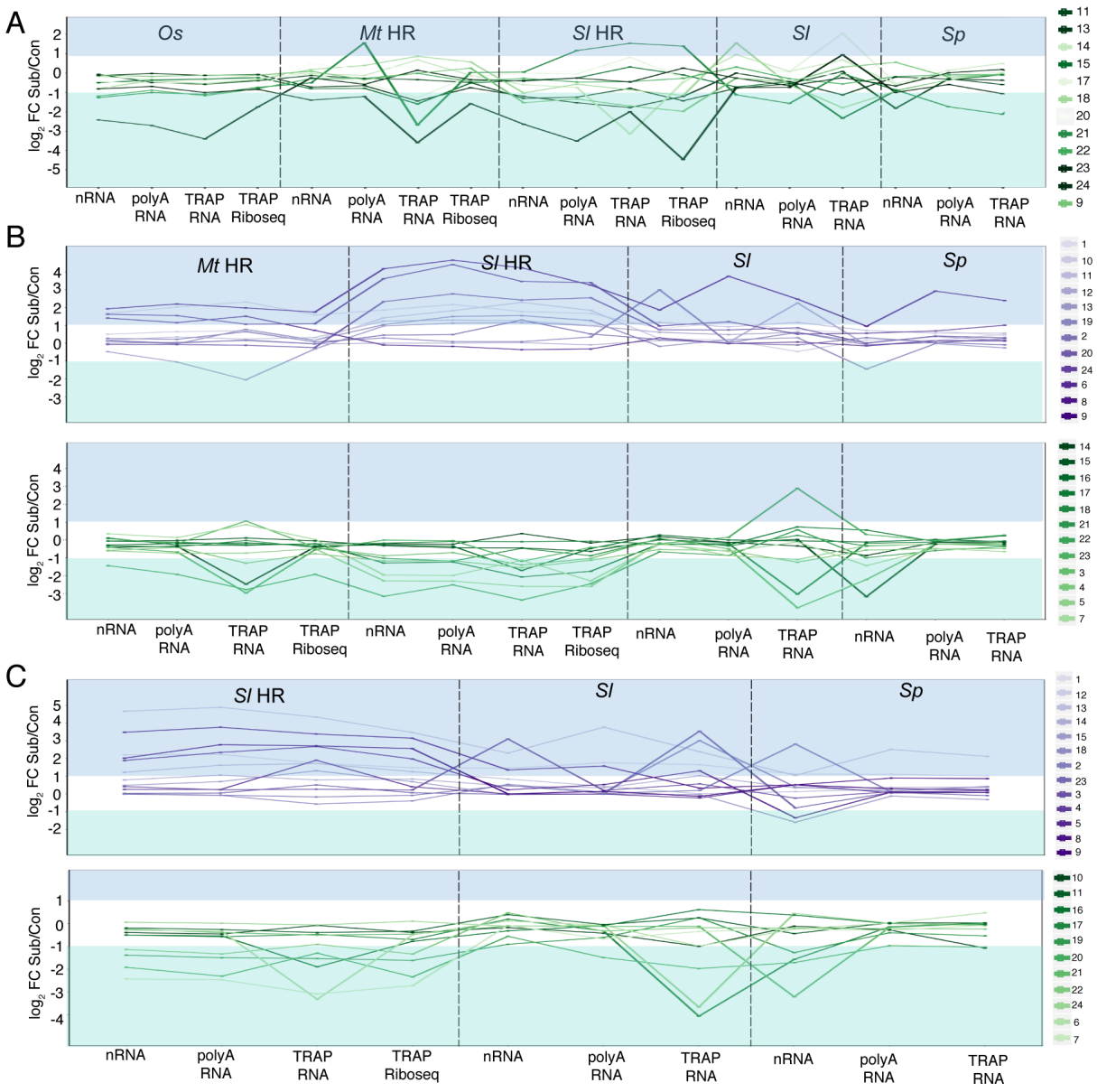

Fig. S22. Stress regulation of syntenic genes is not coordinated across species. (**A**) Line graphs representing the median of $\log_2$ FC of downregulated clusters of syntenic genes across all species analyzed. Upregulated genes shown in Fig. 3A. (**B**) Line graphs representing the median of $\log_2$ FC of clusters of syntenic genes across *Medicago* and the *Solanum* species analyzed. (**C**) Line graphs representing the median of $\log_2$FC of clusters of syntenic genes across the *Solanum* species analyzed. Data presented in data S11.

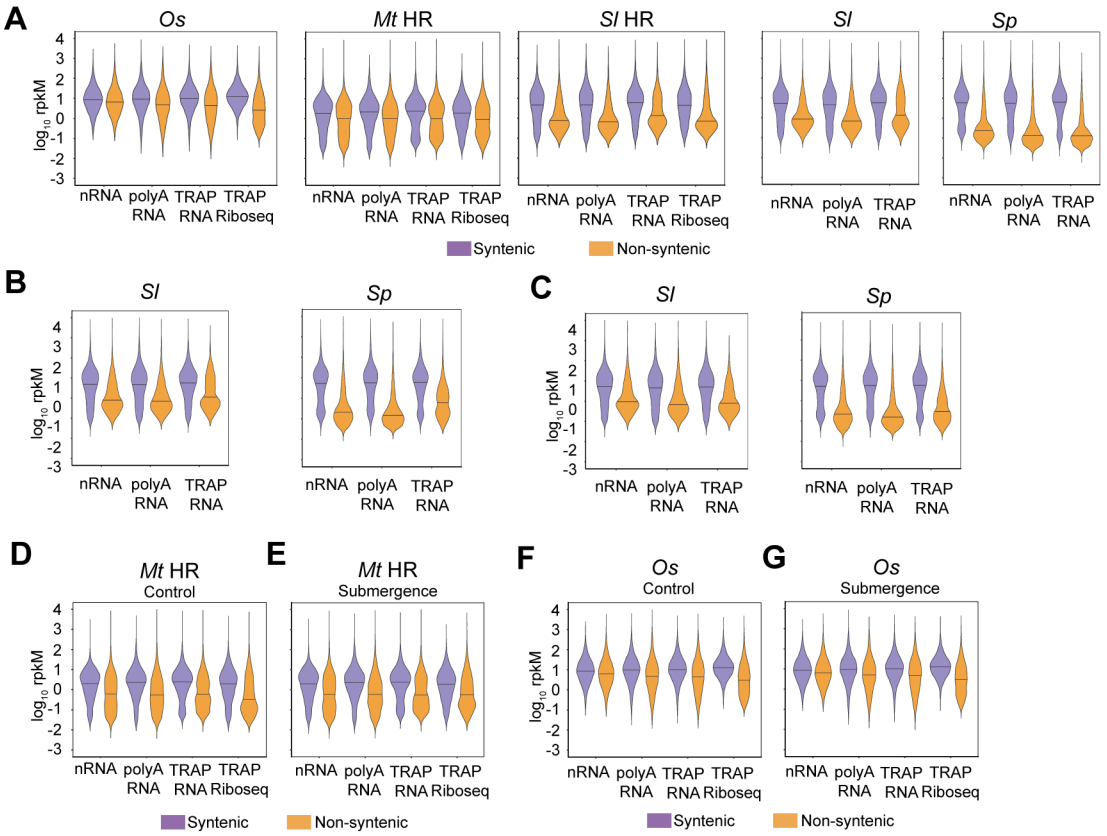

Fig. S23. Expression levels of syntenic genes are higher than non-syntenic genes under submergence in roots and shoot. Figure related to Fig 3B. (**A**) Violin plots represent $\log_{10}$ rpkM distribution for all detected genes classified as syntenic or non-syntenic under submergence condition in roots. Rice genes were evaluated for synteny to *Brachypodium distachyon* genes, *M. truncatula* genes to *Solanum lycopersicum* and *S. lycopersicum* to *S. pennellii* and *vice versa*. (**B-C**) Violin plots represent $\log_{10}$ rpkM distribution for all detected genes classified as syntenic and non-syntenic under control and submergence condition in shoot of two *Solanum* species, respectively. (**D-E**) To evaluate a species more closely related to *M. truncatula,* genes syntenic in the legume *Trifolium pratense* were identified and violin plots prepared for the $\log_{10}$ rpkM distribution for all detected genes classified as syntenic and non-syntenic genes in these legumes under control and submergence condition in roots.(**F-G**) To evaluate synteny to other crop species related to rice, all detected genes were classified as syntenic and non-syntenic in *Zea mays* and violin plots were prepared for the $\log_{10}$ rpKM distribution in control and submergence conditions in roots. Data presented in data S12-14.

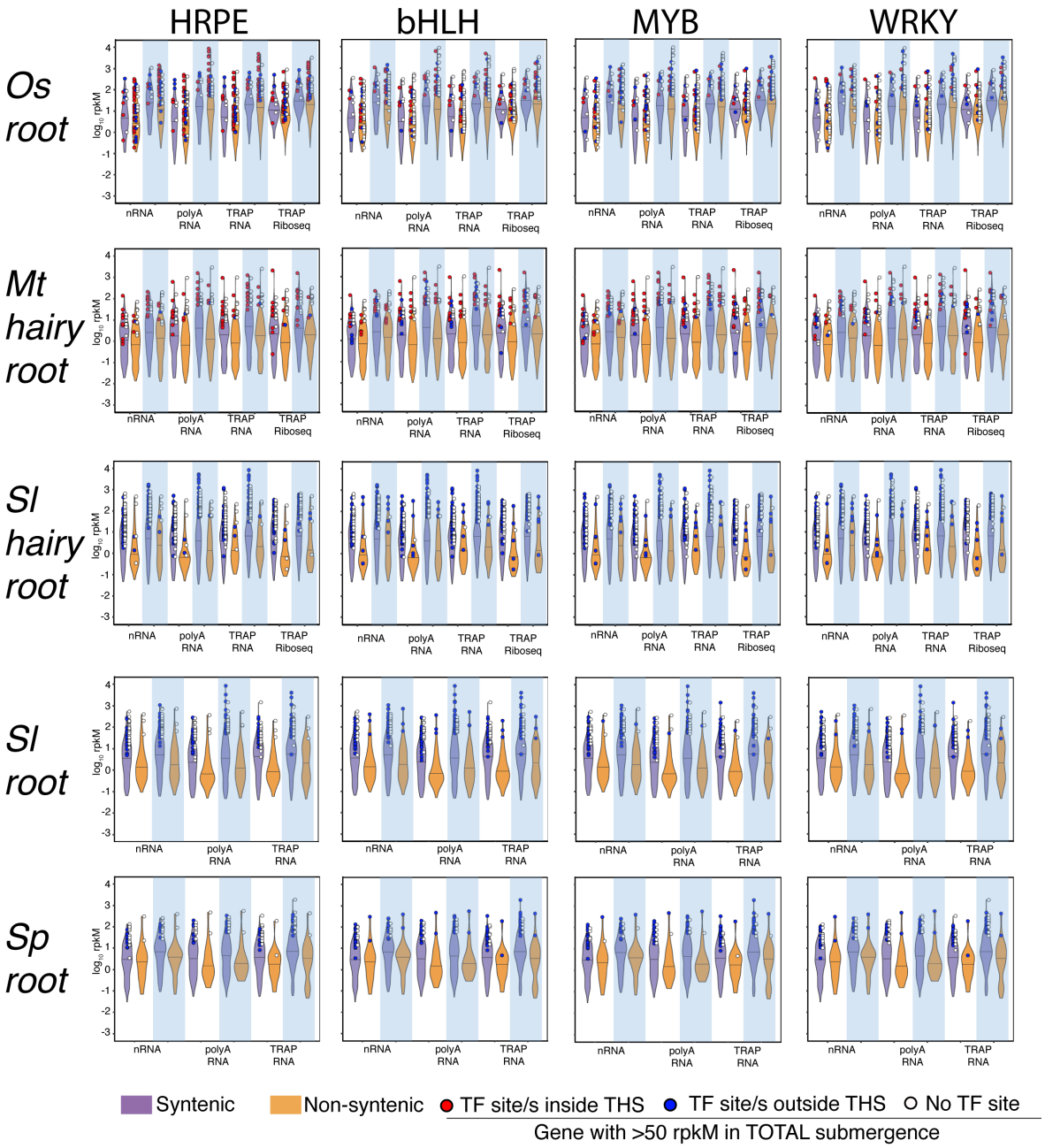

Fig. S24. Control and submergence violin plots for genes in conserved SURFs. Related to Figure 3C. For each RNA population and condition, genes are classified as syntenic (purple) or non-syntenic (orange). Rice genes were evaluated for synteny to *M. truncatula* genes, *M. truncatula* genes to *S. lycopersicum* and *S. lycopersicum* to *S. pennellii* and *vice versa*. Column color corresponds to treatment: Control (white columns) and submergence (blue columns). Highly expressed genes in submergence (>50 rpkM in total RNA under submergence) are indicated with a dot with color based on the presence of a TF motif in the promoter. White means no presence of motif, blue indicates the presence of at least one motif and red means that there is a TF motif inside a region of open chromatin (THS). Central horizontal lines indicate the median values. Data presented in data S15.

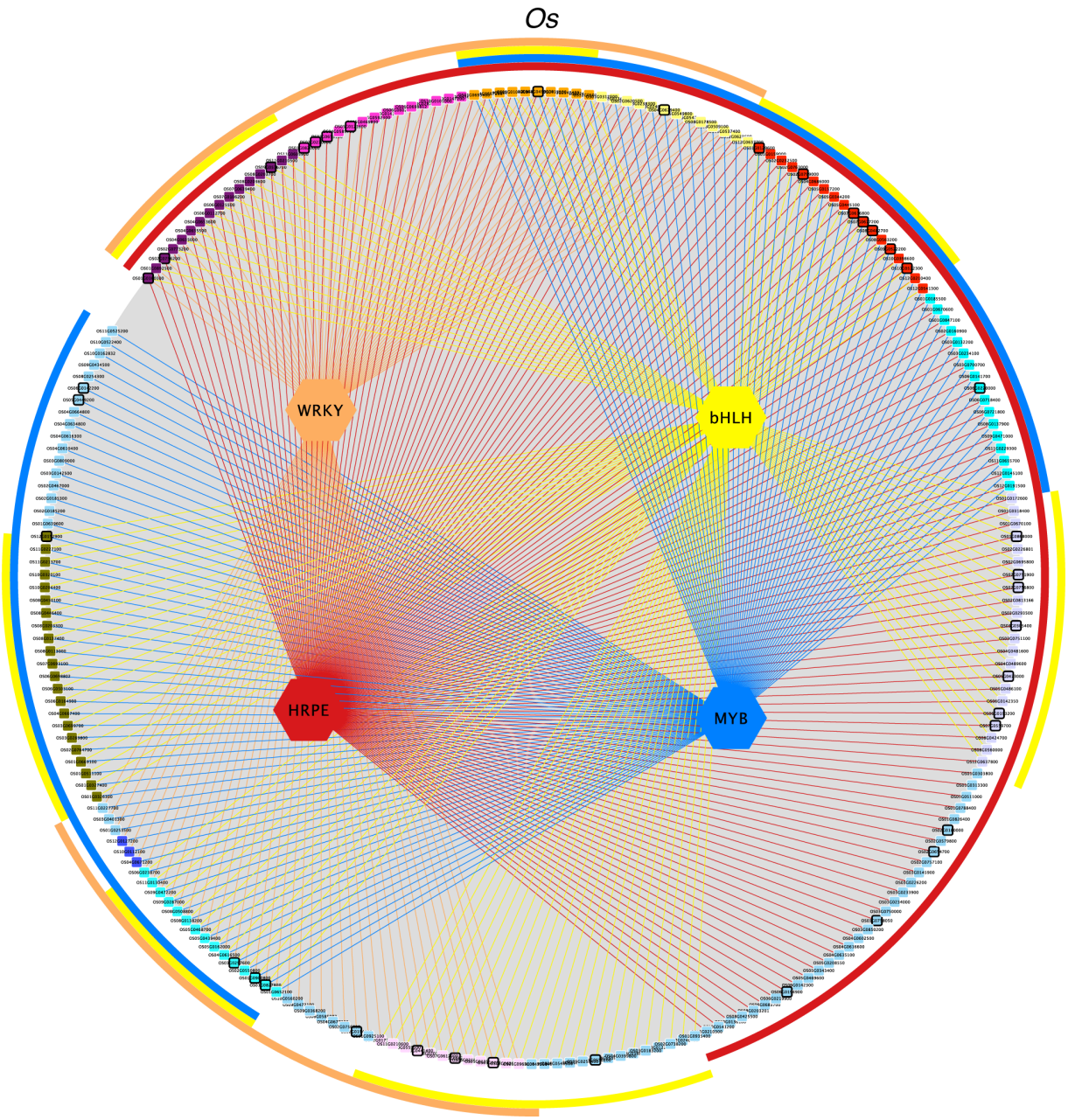

Fig. S25. Regulatory networks for conserved upregulated SURF genes in rice. Presented in Figure 4A. Colored hexagons indicate transcription factors (TFs) based on TF motif presence; Rectangles, genes; colored lines, interaction with TF. Outer circles use colors to indicate groups of genes with a TF type. Rice genes that have a syntenic ortholog in *M. truncatula* have borders in black. Of the upregulated *O. sativa* conserved SURF genes, 70.1% had more than one of the four TF sites. Data presented in data S16. The prevalence of the HRPE regulatory module in conjunction with increased chromatin accessibility associated with transcriptional activation in rice reflects its adaptation to an often inundated habitat. This characteristic of upregulated SURFs was less prevalent in the eudicots examined, especially the *Solanums* (fig. S16).

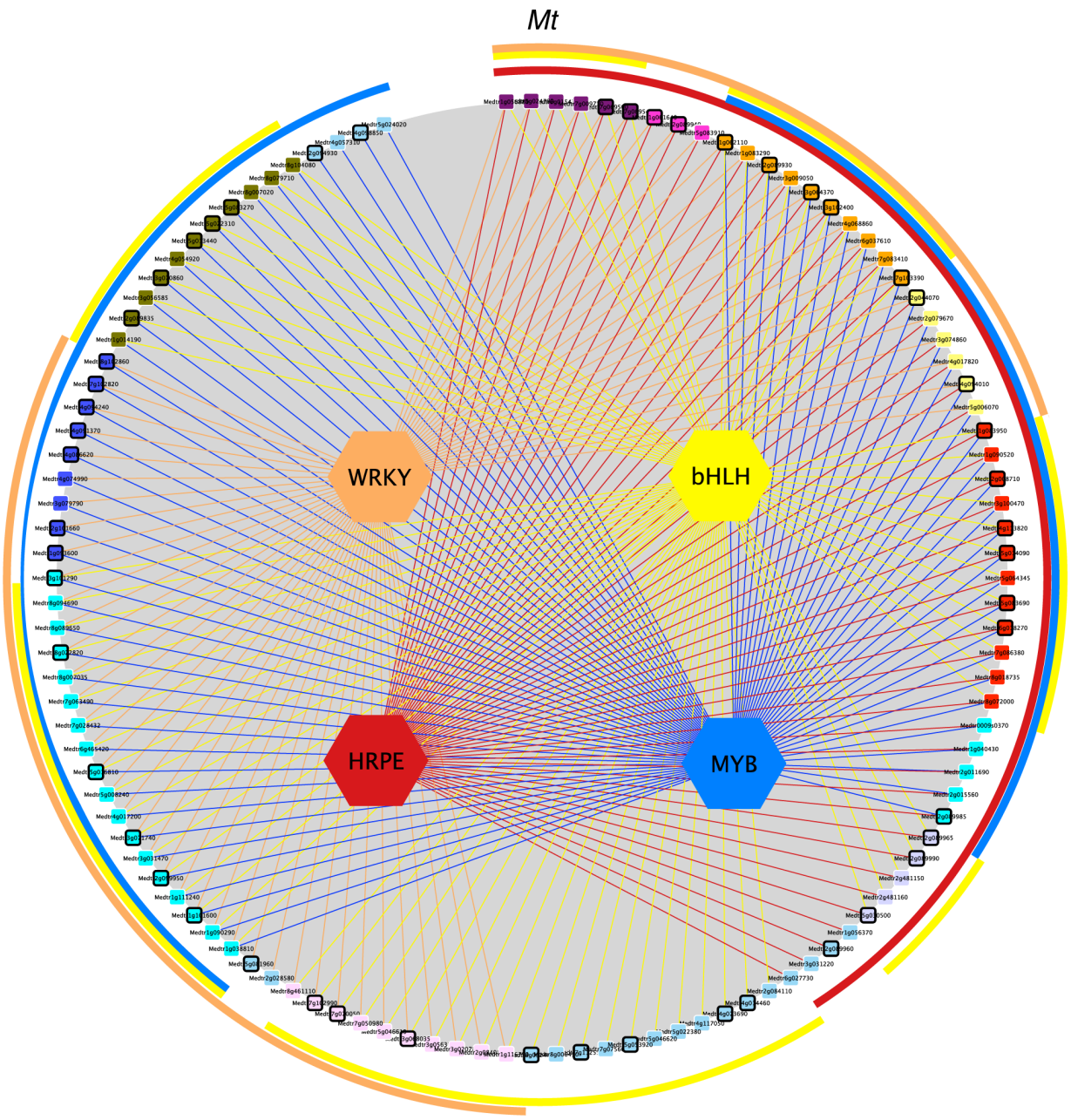

Fig. S26. Regulatory networks for conserved upregulated SURF genes in *M. truncatula*. Presented in Figure 4A. Colored hexagons indicate transcription factors (TFs); Rectangles, genes; colored line, interaction with TF. Outer circles use colors to indicate groups of genes with a TF type. *M. truncatula* genes that present a syntenic ortholog in *S.lycopersicum* have borders in black. Of the upregulated *M. truncatula* SURF genes, 81.8% had more than one of the four TF sites. Data presented in data S16. Flooding-sensitive *M. truncatula* showed less bias presence of the HRPE compared to rice. In this and the other species, the presence of multiple motifs per gene indicates these may be regulated in a combinatorial manner, and likely by multiple signals.

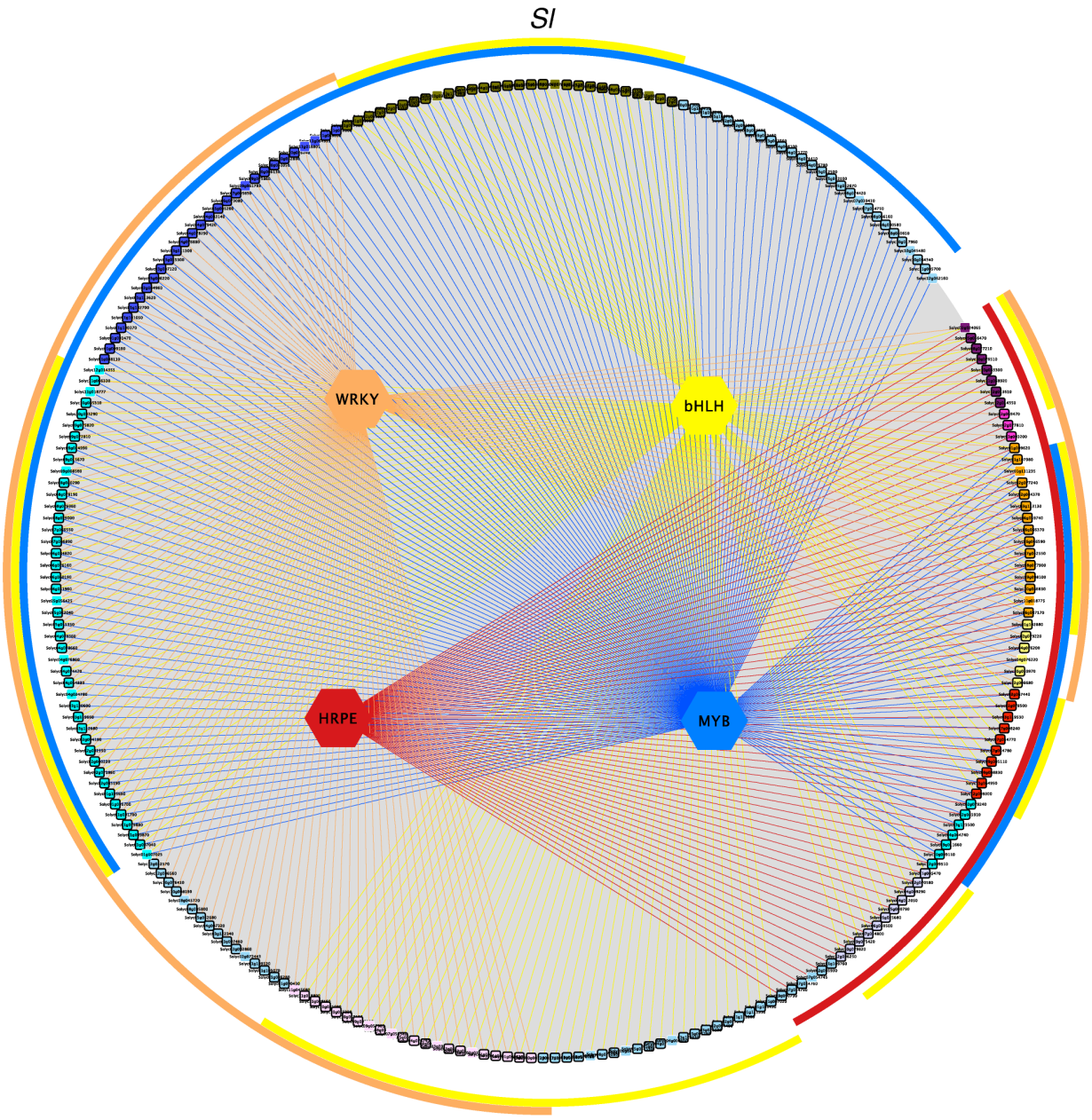

Fig. S27. Regulatory networks for conserved upregulated SURF genes in *S. lycopersicum*. Presented in Figure 4A. Colored hexagons indicate transcription factors (TFs); Rectangles, genes; colored line, interaction with TF. Outer circles use colors to indicate groups of genes with a TF type. *S. lycopersicum* genes that present a syntenic ortholog in *S. pennellii* have borders in black. Of the upregulated *S. lycopersicum* SURF genes, 72.4% had more than one of the four TF sites. Data presented in data S16. The upregulated SURFs in domesticated *S. lycopersicum* had greater frequency of bHLH, MYB and WRKY motifs than HRPEs, compared to rice. Most SURFs with HRPEs had one or more of the other motifs, indicating multiple modes of regulation. *S. lycopersicum* experiences periodic intense irrigation.

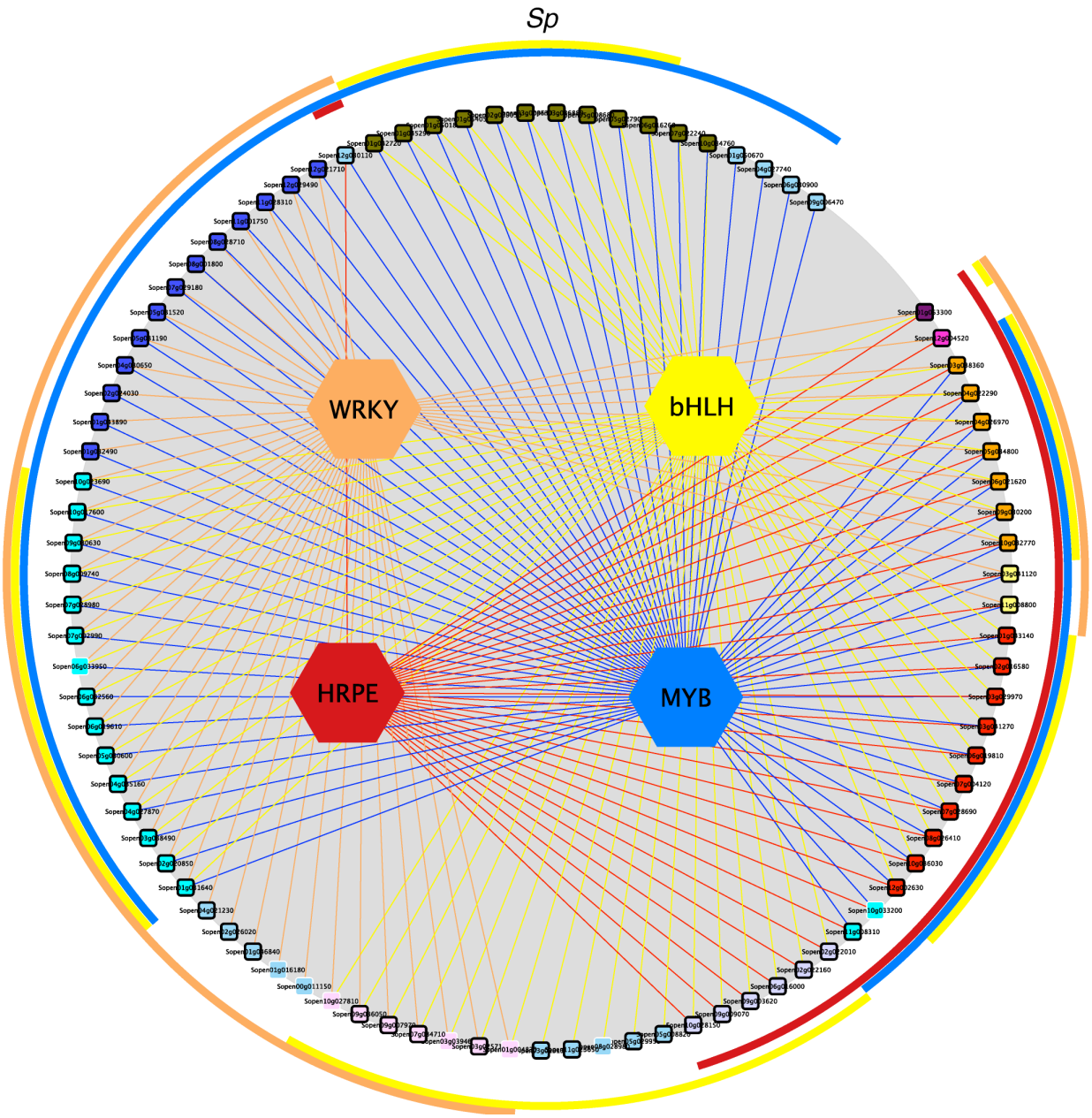

Fig. S28. Regulatory networks for conserved upregulated SURF genes in *S. pennellii*. Presented in Figure 4A. Colored hexagons indicate transcription factors (TFs); Rectangles, genes; colored line, interaction with TF. Outer circles use colors to indicate groups of genes with a TF type. *S. pennellii* genes that present a syntenic ortholog in *S. lycopersicum* have borders in black. Of the upregulated *S. pennellii* SURF genes 84.6% had more than one of the four TF sites. Data presented in data S16. Of the two *Solanum* species, the dryland-adapted wild species *S. pennelli* displayed the most limited number of upregulated SURFs and the most limited use of the HRPE.

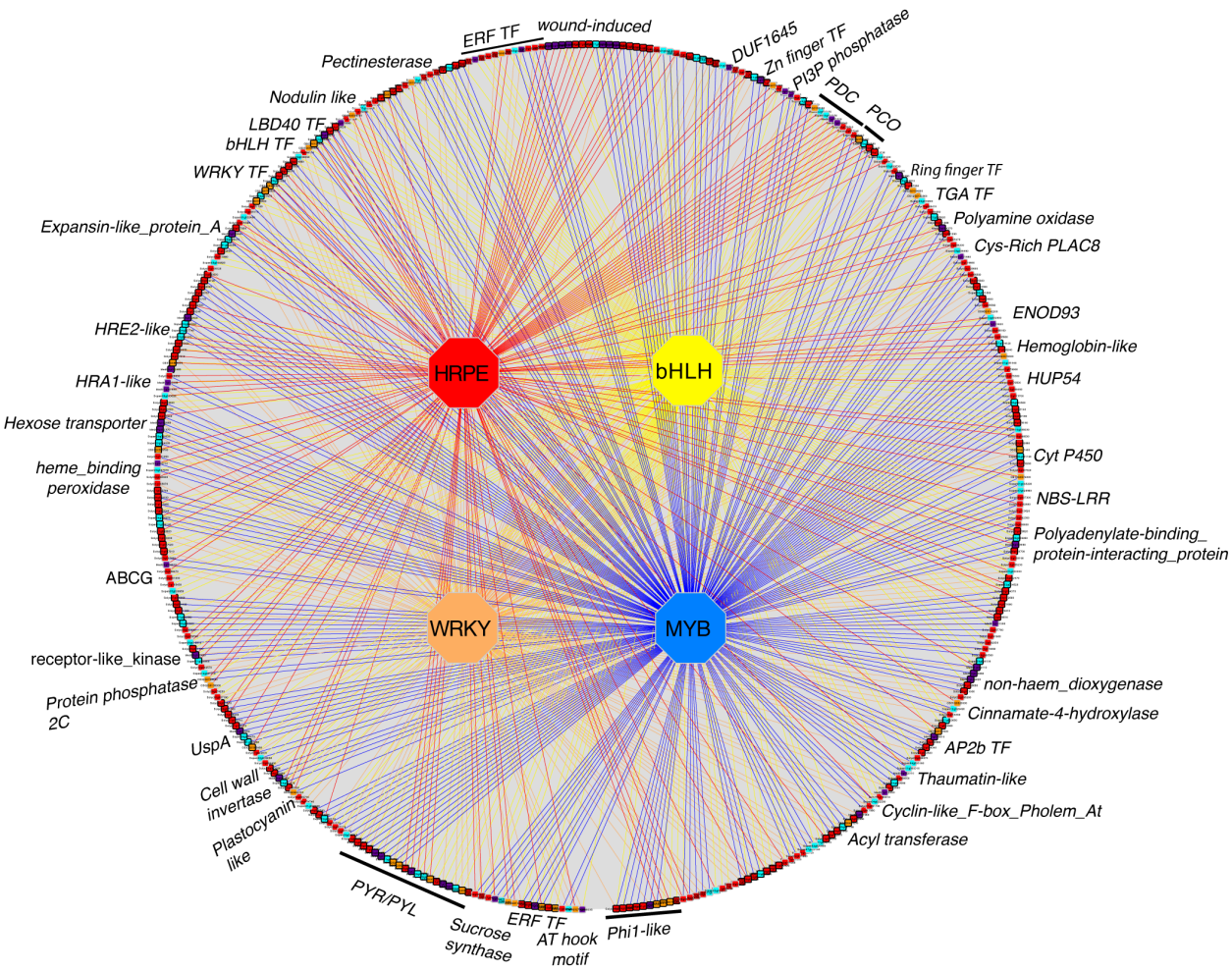

Fig. S29. **Regulatory network for syntenic conserved SURF genes across species.** Presented in Figure 4B. Rectangles indicate genes and octagons indicate TFs. A coloured line indicates an interaction between transcription factor and promoter, HRPE interactions are indicated in red, bHLH in yellow, MYB in blue and WRKY in orange. Genes of the same family have alternating borders in grey or black. Colored genes indicate different species, rice is indicated in orange, *M. truncatula* in purple, *S. lycopersicum* in red and *S. pennellii* in cyan. Location of families with syntelogs in three or more species represented are indicated. Data collated in data S16. ABCG, ATP-binding cassette G; AP2, Apetala 2; Cyt, cytochrome; DUF, domain of unknown function; ENOD, Early nodulin; ERF, ethylene response factor; HRA, hipoxia response attenuator; HRE, ERFVII hypoxia-responsive ERF; HUP, hypoxia unknown protein; LBD, Lateral organ boundaries domain containing; LRR, leucine-rich repeat; NBS, nucleotide-binding site; PCO, plant cysteine oxidase; PDC, pyruvate decarboxylase; Phi, phosphate-induced; PI3P, phosphatidylinositol 3-phosphate; PLAC8, placenta associated 8; PYR/PYL, PYRABACTIN RESISTANCE 1 / PYR1-LIKE; TGA, TGACG motif-binding; UspA, hypoxia-responsive universal stress protein. A number of these genes are involved in hypoxia or submergence survival: anaerobic metabolism (*SUCROSE SYNTHASE*; *PDC) (1),* survival [*USPA (61); HEMOGLOBIN1/PHYTOGLOBIN 1* (hemoglobin like) (*62*); *PHI-1-LIKE* (*63*); *HUP54* (*13*, *14*)] and transcription (*HRE2*) (*64*, *65*). The deeply conserved syntenic upregulated SURFs encode

two negative regulators of ERFVIIs: *HRA1* that limits transactivation of hypoxia-responsive genes by ERFVIIs (*66*) and *PCO* that catalyze the oxygen-promoted degradation of ERFVIIs (*18*, *67*, *68*). The upregulated SURFs included other proteins with known function in low oxygen survival but these were not syntenic across three or more species (*ADH1 (1)*, *RESPIRATORY BURST OXIDASE) (69, 70).*

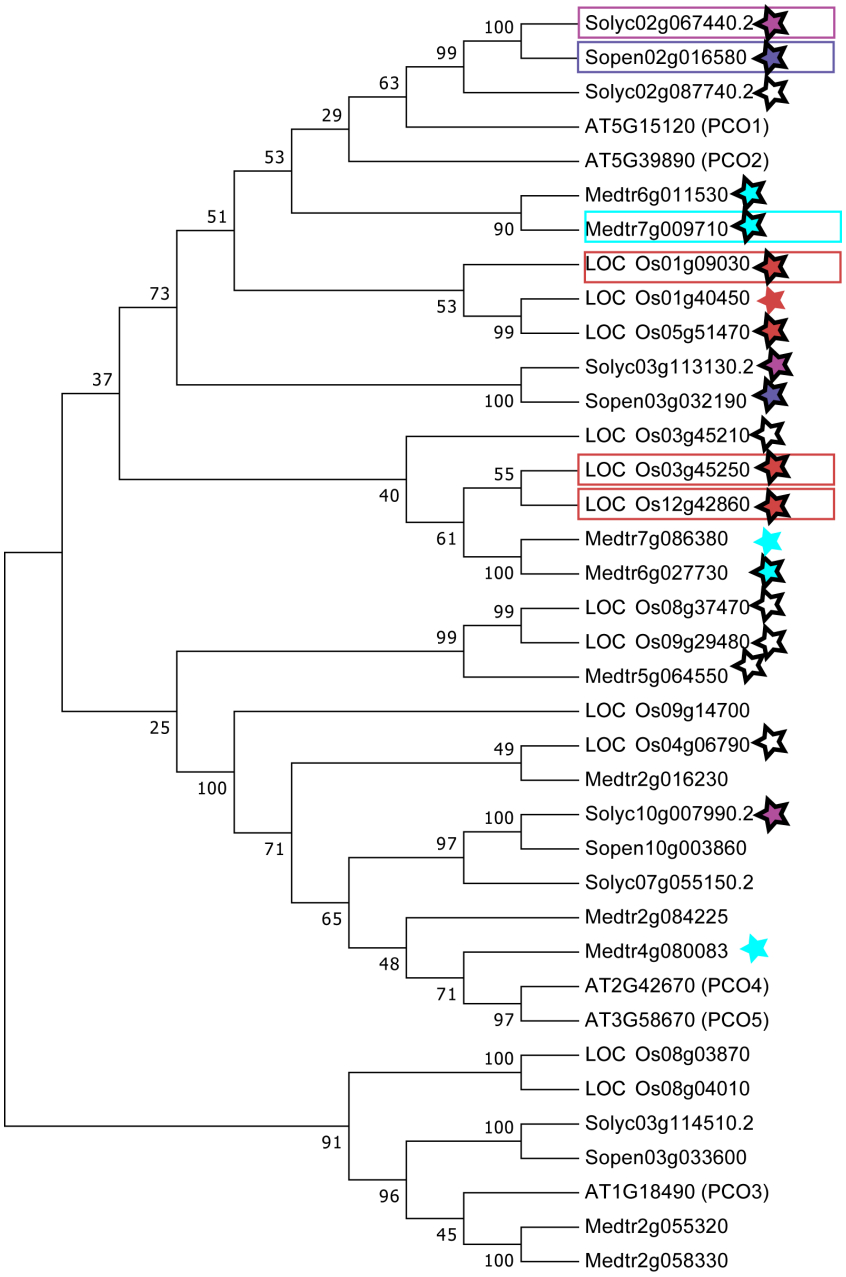

Fig. S30. Molecular phylogenetic analysis of the *PLANT CYSTEINE OXIDASE* (*PCO*) family (*18*, *67*)**.** MUSCLE alignment of maximum homology was based on a total of 177 amino acid positions of the 36 *PCO*s of the four species analyzed and Arabidopsis. All positions had >95% site coverage and <5% alignment gaps. The phylogenetic tree was generated by the Maximum Likelihood method based on the JTT matrix-based model with 1000 bootstrap replicates. The percentage of consensus is indicated next to each branch. Colored stars indicate genes upregulated to submergence in the four species, with a different color for each species; black border indicates presence of an HRPE element within 2 kb 5' and 0.5 kb 3' of the TSS. Boxes highlight genes with high expression levels. Arabidopsis *PCO1* and *PCO2* are upregulated by hypoxia (*6*, *18*). Data presented in data S17.

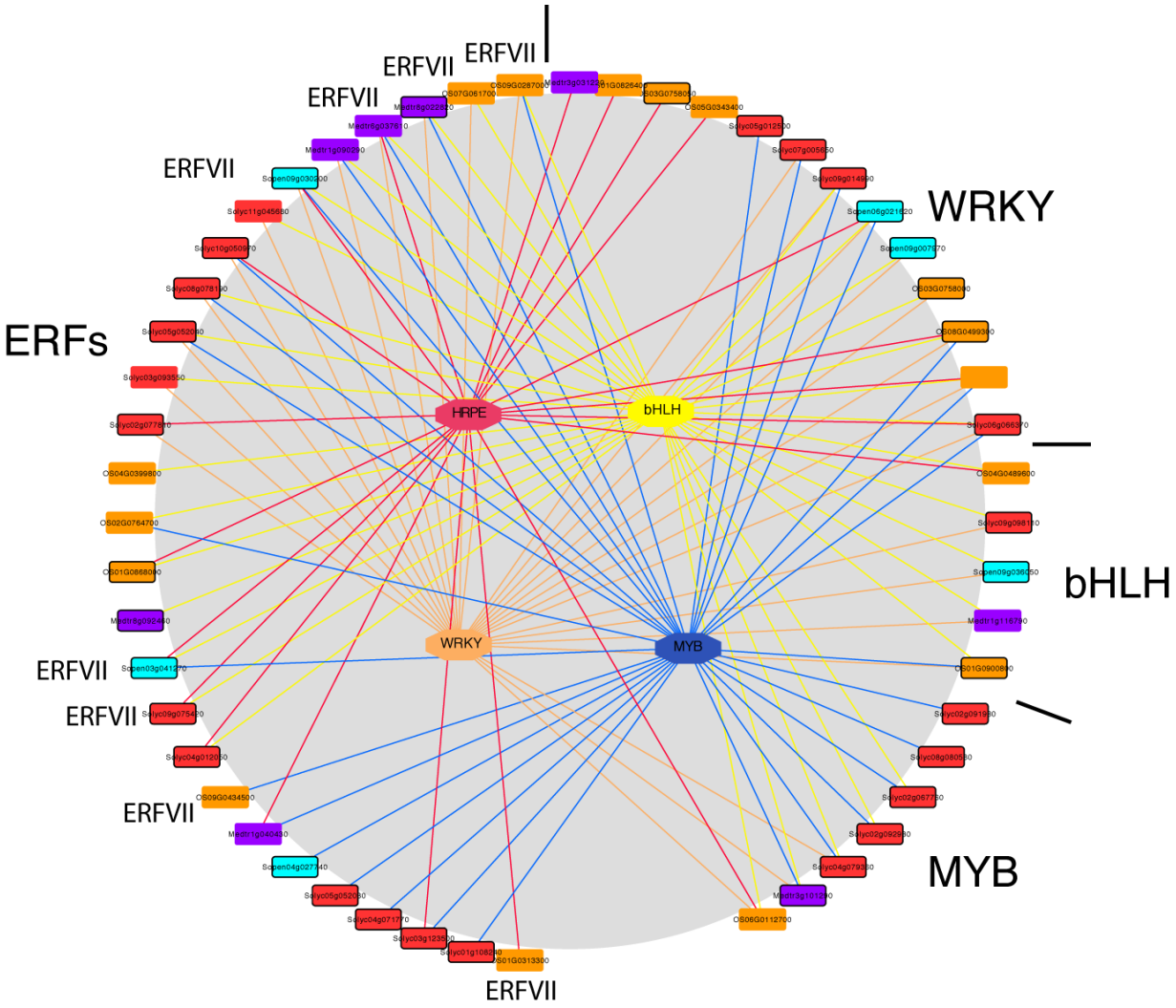

Fig. S31. **Regulatory network for upregulated members of *ERF, bHLH, MYB* and WRKY conserved SURF families across species.** Rectangles indicate upregulated genes and octagons indicate TFs. A colored line indicates an interaction between transcription factor and promoter, HRPE interactions are indicated in red, bHLH in yellow, MYB in blue and WRKY in orange. Colored genes indicate different species, rice is indicated in orange, *M. truncatula* in purple, *S. lycopersicum* in red and *S. pennellii* in cyan. Rice genes with a syntenic ortholog in *M. truncatula, M. truncatula* and *S. pennellii* genes that have a syntenic ortholog in *S. lycopersicum* and *S. lycopersicum* genes that have a syntenic ortholog in *S. pennellii* are indicated with black borders. *ERFVII* genes are indicated individually. Three of the five Arabidopsis ERFVIIs, not including the upregulated SURF *HRE2*, are known to directly transactivate the HRPE (*12*).

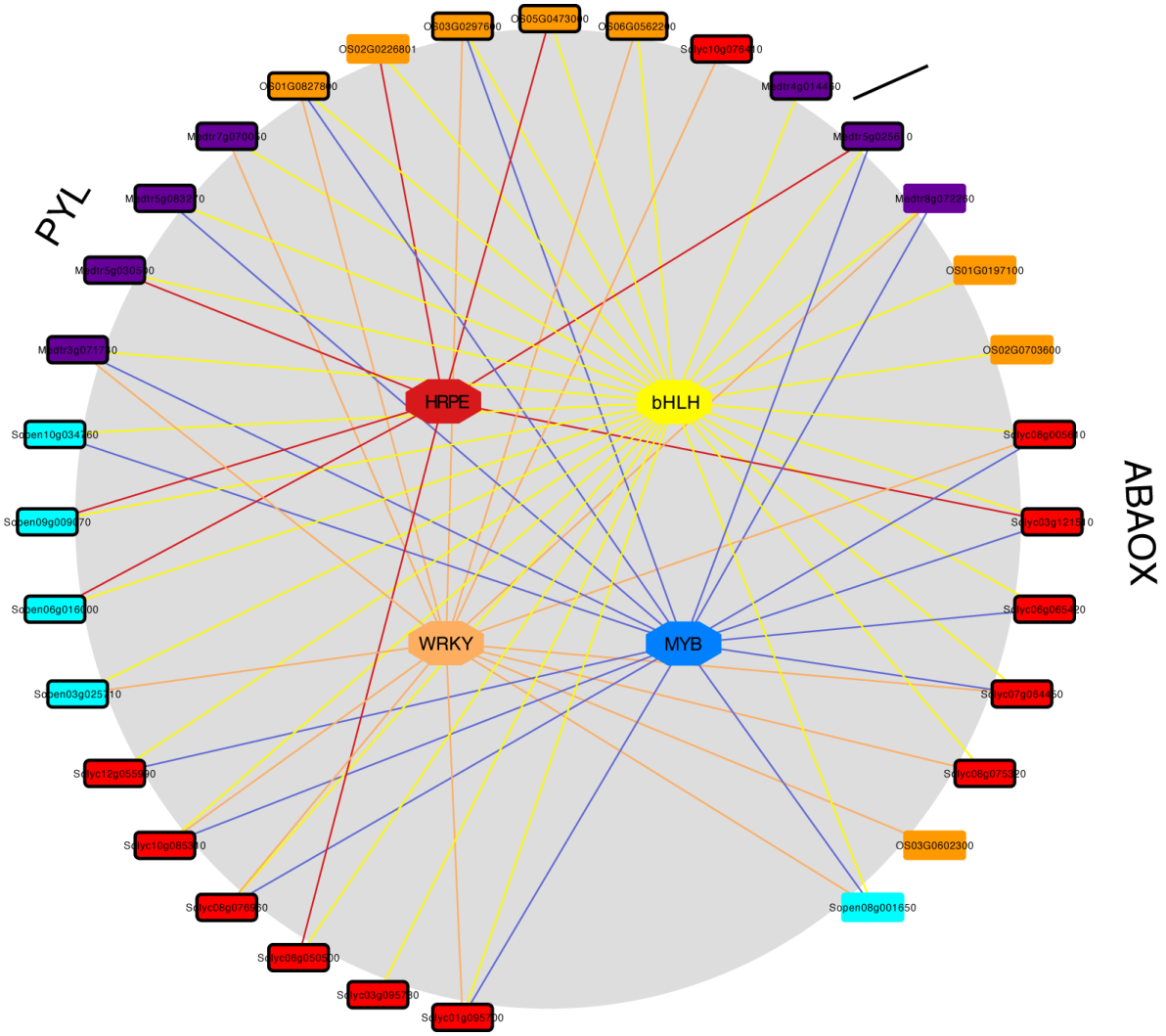

Fig. S32. **Regulatory network for upregulated members of *PYL/RCAR* conserved SURF and *ABAOX* family across species.** Analysis of the upregulated SURFs encoding receptors that perceive ABA intracellularly (PYRABACTIN RESISTANCE1 / PYR1-LIKE/ REGULATORY COMPONENTS OF ABA RECEPTORS (PYL/RCAR) (*71*, *72*)) and ABA 8'-HYDROXYLASE (ABAOX) catalyzing the first step of ABA catabolism (*1*). Rectangles indicate genes and octagons indicate TFs. A coloured line indicates an interaction between transcription factor and promoter, HRPE interactions are indicated in red, bHLH in yellow, MYB in blue and WRKY in orange. Colored genes indicate different species, rice is indicated in orange, *M. truncatula* in purple, *S. lycopersicum* in red and *S. pennellii* in cyan. Rice genes that have a syntenic ortholog in *M. truncatula, M. truncatula* and *S. pennellii* genes that have a syntenic ortholog in *S. lycopersicum* and *S. lycopersicum* that have a syntenic ortholog in *S. pennellii* are indicated with black borders. The *ABAOX* genes include a non-significantly upregulated member in *S. pennellii.*

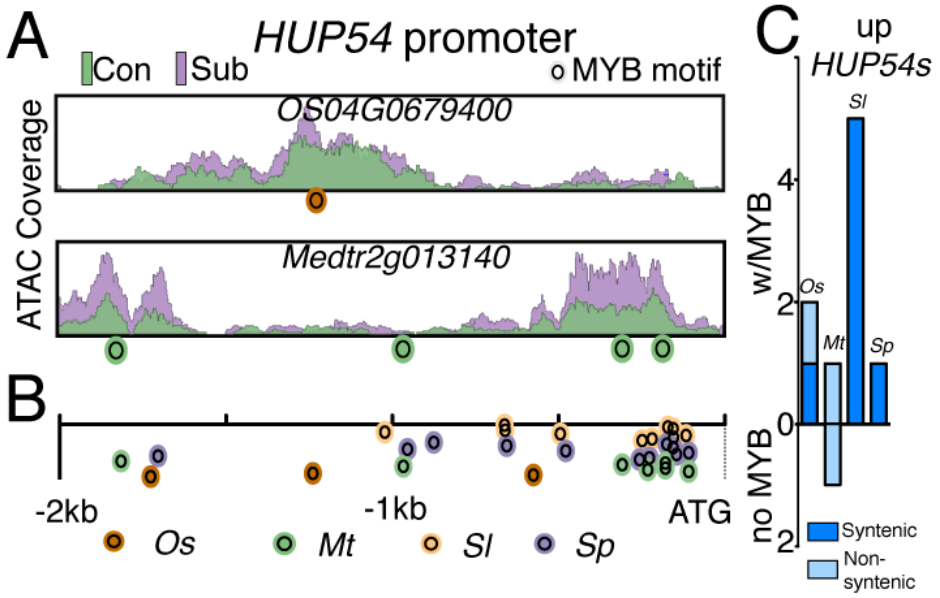

Fig. S33. Analysis of the *HYPOXIA UNKNOWN PROTEIN 54* (*HUP54*) upregulated family members (*14*)**. (A)** Chromatin accessibility in promoters of syntenic *HUP54* genes. For each species, ATAC coverage scale is the same for genes shown in each panel. MYB motif sites are marked below. (**B**) Promoter locations of MYB motifs for four species. (**C**) Number of upregulated genes containing motifs classified by syntenic and non-syntenic.

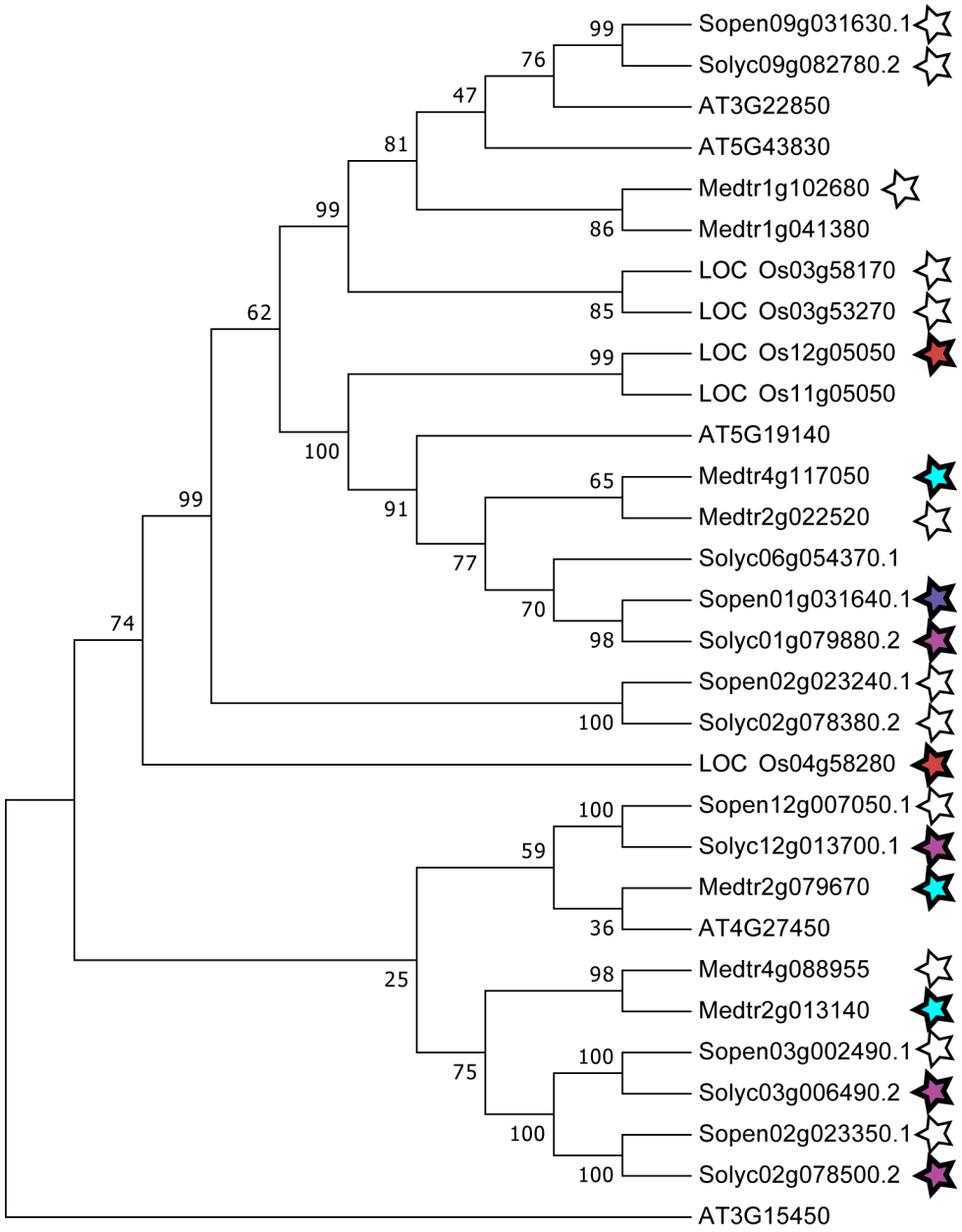

Fig. S34. Molecular Phylogenetic analysis of the *HYPOXIA UNKNOWN PROTEIN54 (HUP54)* family (*14*)**.** The phylogenetic tree was generated as described for fig. S30 with an alignment of 225 positions from 30 *HUP54* genes of the four species analyzed and Arabidopsis. Colored stars indicate genes upregulated to submergence, with a different color for each species; black border indicates presence of a MYB element within 2 kb 5' and 0.5 kb 3' of the TSS. Boxes highlight genes with high expression levels. Data presented in data S17.

Captions for Data S1 to S18

Data S1. ATAC and RNA-sequencing data statistics.

Data S2. Correlation values for RNA populations evaluated.

Data S3. Tabulation of differentially regulated genes and the cluster analysis.

Data S4. List of genes analyzed and assigned to a family.

Data S5. Overlap of submergence-regulated gene families.

Data S6. Submergence upregulated families in roots and *Solanum* shoots.

Data S7. *Solanum* and Arabidopsis shoot and root contrast analysis.

Data S8. Transposase Hypersensitive Site (THS) analysis.

Data S9. Enrichment of transcription factor motifs in conserved SURF gene promoters.

Data S10. Transposase Hypersensitive Site (THS) and Transcription factor (TF) motif co-occurrence analysis.

Data S11. Clustering of submergence-regulated syntenic genes.

Data S12. Syntenic genes used in the analysis.

Data S13. Analysis of gene activity of syntenic genes.

Data S14. Comparison of gene activity of syntenic and non-syntenic genes.

Data S15. Submergence upregulated family (SURF) genes with high activity under submergence.

Data S16. Gene and transcription factor motif network analysis.

Data S17. *PLANT CYSTEINE OXIDASE* and *HYPOXIA UNKNOWN PROTEIN 54* gene family members.

Data S18. List of qPCR primers.

References and Notes

1. L. A. C. J. Voesenek, J. Bailey-Serres, Flood adaptive traits and processes: An overview. *New Phytol.* **206**, 57–73 (2015). doi:10.1111/nph.13209 Medline

2. C. Branco-Price, K. A. Kaiser, C. J. H. Jang, C. K. Larive, J. Bailey-Serres, Selective mRNA translation coordinates energetic and metabolic adjustments to cellular oxygen deprivation and reoxygenation in *Arabidopsis thaliana*. *Plant J.* **56**, 743–755 (2008). doi:10.1111/j.1365-313X.2008.03642.x Medline

3. R. Sorenson, J. Bailey-Serres, Selective mRNA sequestration by OLIGOURIDYLATE-BINDING PROTEIN 1 contributes to translational control during hypoxia in Arabidopsis. *Proc. Natl. Acad. Sci. U.S.A.* **111**, 2373–2378 (2014). doi:10.1073/pnas.1314851111 Medline

4. P. Juntawong, T. Girke, J. Bazin, J. Bailey-Serres, Translational dynamics revealed by genome-wide profiling of ribosome footprints in Arabidopsis. *Proc. Natl. Acad. Sci. U.S.A.* **111**, E203–E212 (2014). doi:10.1073/pnas.1317811111 Medline

5. R. B. Deal, S. Henikoff, The INTACT method for cell type-specific gene expression and chromatin profiling in *Arabidopsis thaliana*. *Nat. Protoc.* **6**, 56–68 (2011). doi:10.1038/nprot.2010.175 Medline

6. A. Mustroph, M. E. Zanetti, C. J. H. Jang, H. E. Holtan, P. P. Repetti, D. W. Galbraith, T. Girke, J. Bailey-Serres, Profiling translatomes of discrete cell populations resolves altered cellular priorities during hypoxia in Arabidopsis. *Proc. Natl. Acad. Sci. U.S.A.* **106**, 18843–18848 (2009). doi:10.1073/pnas.0906131106 Medline

7. J. D. Buenrostro, P. G. Giresi, L. C. Zaba, H. Y. Chang, W. J. Greenleaf, Transposition of native chromatin for fast and sensitive epigenomic profiling of open chromatin, DNA-binding proteins and nucleosome position. *Nat. Methods* **10**, 1213–1218 (2013). doi:10.1038/nmeth.2688 Medline

8. N. T. Ingolia, S. Ghaemmaghami, J. R. S. Newman, J. S. Weissman, Genome-wide analysis in vivo of translation with nucleotide resolution using ribosome profiling. *Science* **324**, 218–223 (2009). doi:10.1126/science.1168978 Medline

9. D. M. Goodstein, S. Shu, R. Howson, R. Neupane, R. D. Hayes, J. Fazo, T. Mitros, W. Dirks, U. Hellsten, N. Putnam, D. S. Rokhsar, Phytozome: A comparative platform for green plant genomics. *Nucleic Acids Res.* **40**, D1178–D1186 (2012). doi:10.1093/nar/gkr944 Medline

10. M. Klecker, P. Gasch, H. Peisker, P. Dörmann, H. Schlicke, B. Grimm, A. Mustroph, A Shoot-Specific Hypoxic Response of Arabidopsis Sheds Light on the Role of the Phosphate-Responsive Transcription Factor PHOSPHATE STARVATION RESPONSE1. *Plant Physiol.* **165**, 774–790 (2014). doi:10.1104/pp.114.237990 Medline

11. K. A. Maher, M. Bajic, K. Kajala, M. Reynoso, G. Pauluzzi, D. A. West, K. Zumstein, M. Woodhouse, K. Bubb, M. W. Dorrity, C. Queitsch, J. Bailey-Serres, N. Sinha, S. M. Brady, R. B. Deal, Profiling of accessible chromatin regions across multiple plant species and cell types reveals common gene regulatory principles and new control modules. *Plant Cell* **30**, 15–36 (2018). doi:10.1105/tpc.17.00581 Medline

12. P. Gasch, M. Fundinger, J. T. Müller, T. Lee, J. Bailey-Serres, A. Mustroph, Redundant ERF-VII Transcription Factors Bind to an Evolutionarily Conserved cis-Motif to Regulate Hypoxia-Responsive Gene Expression in Arabidopsis. *Plant Cell* **28**, 160–180 (2016). doi:10.1105/tpc.15.00866 Medline

13. S. C. Lee, A. Mustroph, R. Sasidharan, D. Vashisht, O. Pedersen, T. Oosumi, L. A. C. J. Voesenek, J. Bailey-Serres, Molecular characterization of the submergence response of the *Arabidopsis thaliana* ecotype Columbia. *New Phytol.* **190**, 457–471 (2011). doi:10.1111/j.1469-8137.2010.03590.x Medline

14. A. Mustroph, S. C. Lee, T. Oosumi, M. E. Zanetti, H. Yang, K. Ma, A. Yaghoubi-Masihi, T. Fukao, J. Bailey-Serres, Cross-kingdom comparison of transcriptomic adjustments to low-oxygen stress highlights conserved and plant-specific responses. *Plant Physiol.* **152**, 1484–1500 (2010). doi:10.1104/pp.109.151845 Medline

15. B. O. R. Bargmann, A. Marshall-Colon, I. Efroni, S. Ruffel, K. D. Birnbaum, G. M. Coruzzi, G. Krouk, TARGET: A transient transformation system for genome-wide transcription factor target discovery. *Mol. Plant* **6**, 978–980 (2013). doi:10.1093/mp/sst010 Medline

16. A. Para, Y. Li, A. Marshall-Colón, K. Varala, N. J. Francoeur, T. M. Moran, M. B. Edwards, C. Hackley, B. O. R. Bargmann, K. D. Birnbaum, W. R. McCombie, G. Krouk, G. M. Coruzzi, Hit-and-run transcriptional control by bZIP1 mediates rapid nutrient signaling in Arabidopsis. *Proc. Natl. Acad. Sci. U.S.A.* **111**, 10371–10376 (2014). doi:10.1073/pnas.1404657111 Medline

17. J. W. Walley, R. C. Sartor, Z. Shen, R. J. Schmitz, K. J. Wu, M. A. Urich, J. R. Nery, L. G. Smith, J. C. Schnable, J. R. Ecker, S. P. Briggs, Integration of omic networks in a developmental atlas of maize. *Science* **353**, 814–818 (2016). doi:10.1126/science.aag1125 Medline

18. D. A. Weits, B. Giuntoli, M. Kosmacz, S. Parlanti, H.-M. Hubberten, H. Riegler, R. Hoefgen, P. Perata, J. T. van Dongen, F. Licausi, Plant cysteine oxidases control the oxygen-dependent branch of the N-end-rule pathway. *Nat. Commun.* **5**, 3425 (2014). doi:10.1038/ncomms4425 Medline

19. J. Barba-Montoya, M. Dos Reis, H. Schneider, P. C. J. Donoghue, Z. Yang, Constraining uncertainty in the timescale of angiosperm evolution and the veracity of a Cretaceous Terrestrial Revolution. *New Phytol.* **218**, 819–834 (2018). doi:10.1111/nph.15011 Medline

20. M. A. Reynoso, G. C. Pauluzzi, K. Kajala, S. Cabanlit, J. Velasco, J. Bazin, R. Deal, N. R. Sinha, S. M. Brady, J. Bailey-Serres, Nuclear transcriptomes at high resolution using retooled INTACT. *Plant Physiol.* **176**, 270–281 (2018). doi:10.1104/pp.17.00688 Medline

21. D. Zhao, J. P. Hamilton, M. Hardigan, D. Yin, T. He, B. Vaillancourt, M. Reynoso, G. Pauluzzi, S. Funkhouser, Y. Cui, J. Bailey-Serres, J. Jiang, C. R. Buell, N. Jiang, Analysis of ribosome-associated mRNAs in rice Reveals the importance of transcript size and GC content in translation. *G3* **7**, 203–219 (2017). doi:10.1534/g3.116.036020 Medline

22. M. Ron, K. Kajala, G. Pauluzzi, D. Wang, M. A. Reynoso, K. Zumstein, J. Garcha, S. Winte, H. Masson, S. Inagaki, F. Federici, N. Sinha, R. B. Deal, J. Bailey-Serres, S. M. Brady, Hairy root transformation using *Agrobacterium rhizogenes* as a tool for exploring cell type-specific gene expression and function using tomato as a model. *Plant Physiol.* **166**, 455–469 (2014). doi:10.1104/pp.114.239392 Medline

23. B. T. Townsley, M. F. Covington, Y. Ichihashi, K. Zumstein, N. R. Sinha, BrAD-seq: Breath Adapter Directional sequencing: a streamlined, ultra-simple and fast library preparation protocol for strand specific mRNA library construction. *Front. Plant Sci.* **6**, 366 (2015). Medline

24. J. S. Yuan, A. Reed, F. Chen, C. N. Stewart Jr., Statistical analysis of real-time PCR data. *BMC Bioinformatics* **7**, 85 (2006). doi:10.1186/1471-2105-7-85 Medline

25. R. B. Deal, S. Henikoff, A simple method for gene expression and chromatin profiling of individual cell types within a tissue. *Dev. Cell* **18**, 1030–1040 (2010). doi:10.1016/j.devcel.2010.05.013 Medline

26. M. Bajic, K. A. Maher, R. B. Deal, Identification of open chromatin regions in plant genomes using ATAC-seq. *Methods Mol. Biol.* **1675**, 183–201 (2018). doi:10.1007/978-1-4939-7318-7_12 Medline

27. M. Reynoso, G. Pauluzzi, S. Cabanlit, J. Velasco, J. Bazin, R. Deal, S. Brady, N. Sinha, J. Bailey-Serres, K. Kajala, Isolation of Nuclei in Tagged Cell Types (INTACT), RNA extraction and ribosomal RNA degradation to prepare material for RNA-seq. *Bio-protocol* **8**, e2458 (2018). doi:10.21769/BioProtoc.2458

28. A. Mustroph, P. Juntawong, J. Bailey-Serres, Isolation of plant polysomal mRNA by differential centrifugation and ribosome immunopurification methods. *Methods Mol. Biol.* **553**, 109–126 (2009). doi:10.1007/978-1-60327-563-7_6 Medline

29. M. A. Reynoso, P. Juntawong, M. Lancia, F. A. Blanco, J. Bailey-Serres, M. E. Zanetti, Translating Ribosome Affinity Purification (TRAP) followed by RNA sequencing technology (TRAP-SEQ) for quantitative assessment of plant translatomes. *Methods Mol. Biol.* **1284**, 185–207 (2015). doi:10.1007/978-1-4939-2444-8_9 Medline

30. P. Juntawong, M. Hummel, J. Bazin, J. Bailey-Serres, Ribosome profiling: A tool for quantitative evaluation of dynamics in mRNA translation. *Methods Mol. Biol.* **1284**, 139–173 (2015). doi:10.1007/978-1-4939-2444-8_7 Medline

31. J. Bazin, K. Baerenfaller, S. J. Gosai, B. D. Gregory, M. Crespi, J. Bailey-Serres, Global analysis of ribosome-associated noncoding RNAs unveils new modes of translational regulation. *Proc. Natl. Acad. Sci. U.S.A.* **114**, E10018–E10027 (2017). doi:10.1073/pnas.1708433114 Medline

32. N. T. Ingolia, G. A. Brar, S. Rouskin, A. M. McGeachy, J. S. Weissman, The ribosome profiling strategy for monitoring translation in vivo by deep sequencing of ribosome-protected mRNA fragments. *Nat. Protoc.* **7**, 1534–1550 (2012). doi:10.1038/nprot.2012.086 Medline

33. T. Girke, systemPipeR: NGS workflow and report generation environment. UC Riverside. https://github.com/tgirke/systemPipeR (2014); available at www.bioconductor.org/packages/release/bioc/html/systemPipeR.html.

34. L. Calviello, N. Mukherjee, E. Wyler, H. Zauber, A. Hirsekorn, M. Selbach, M. Landthaler, B. Obermayer, U. Ohler, Detecting actively translated open reading frames in ribosome profiling data. *Nat. Methods* **13**, 165–170 (2016). doi:10.1038/nmeth.3688 Medline

35. M. E. Ritchie, B. Phipson, D. Wu, Y. Hu, C. W. Law, W. Shi, G. K. Smyth, limma powers differential expression analyses for RNA-sequencing and microarray studies. *Nucleic Acids Res.* **43**, e47 (2015). doi:10.1093/nar/gkv007 Medline

36. S. Su, C. W. Law, C. Ah-Cann, M.-L. Asselin-Labat, M. E. Blewitt, M. E. Ritchie, Glimma: Interactive graphics for gene expression analysis. *Bioinformatics* **33**, 2050–2052 (2017). doi:10.1093/bioinformatics/btx094 Medline

37. M. D. Young, M. J. Wakefield, G. K. Smyth, A. Oshlack, Gene ontology analysis for RNA-seq: Accounting for selection bias. *Genome Biol.* **11**, R14 (2010). doi:10.1186/gb-2010-11-2-r14 Medline

38. D. Koenig, J. M. Jiménez-Gómez, S. Kimura, D. Fulop, D. H. Chitwood, L. R. Headland, R. Kumar, M. F. Covington, U. K. Devisetty, A. V. Tat, T. Tohge, A. Bolger, K. Schneeberger, S. Ossowski, C. Lanz, G. Xiong, M. Taylor-Teeples, S. M. Brady, M. Pauly, D. Weigel, B. Usadel, A. R. Fernie, J. Peng, N. R. Sinha, J. N. Maloof, Comparative transcriptomics reveals patterns of selection in domesticated and wild tomato. *Proc. Natl. Acad. Sci. U.S.A.* **110**, E2655–E2662 (2013). doi:10.1073/pnas.1309606110 Medline

39. E. L. L. Sonnhammer, G. Östlund, InParanoid 8: Orthology analysis between 273 proteomes, mostly eukaryotic. *Nucleic Acids Res.* **43**, D234–D239 (2015). doi:10.1093/nar/gku1203 Medline

40. E. Lyons, M. Freeling, How to usefully compare homologous plant genes and chromosomes as DNA sequences. *Plant J.* **53**, 661–673 (2008). doi:10.1111/j.1365-313X.2007.03326.x Medline

41. E. Lyons, B. Pedersen, J. Kane, M. Freeling, The value of nonmodel genomes and an example using SynMap within CoGe to dissect the hexaploidy that predates the Rosids. *Trop. Plant Biol.* **1**, 181–190 (2008). doi:10.1007/s12042-008-9017-y

42. B. Langmead, S. L. Salzberg, Fast gapped-read alignment with Bowtie 2. *Nat. Methods* **9**, 357–359 (2012). doi:10.1038/nmeth.1923 Medline

43. A. Bolger, F. Scossa, M. E. Bolger, C. Lanz, F. Maumus, T. Tohge, H. Quesneville, S. Alseekh, I. Sørensen, G. Lichtenstein, E. A. Fich, M. Conte, H. Keller, K. Schneeberger, R. Schwacke, I. Ofner, J. Vrebalov, Y. Xu, S. Osorio, S. A. Aflitos, E. Schijlen, J. M. Jiménez-Goméz, M. Ryngajllo, S. Kimura, R. Kumar, D. Koenig, L. R. Headland, J. N. Maloof, N. Sinha, R. C. H. J. van Ham, R. K. Lankhorst, L. Mao, A. Vogel, B. Arsova, R. Panstruga, Z. Fei, J. K. C. Rose, D. Zamir, F. Carrari, J. J. Giovannoni, D. Weigel, B. Usadel, A. R. Fernie, The genome of the stress-tolerant wild tomato species *Solanum pennellii*. *Nat. Genet.* **46**, 1034–1038 (2014). doi:10.1038/ng.3046 Medline

44. P. Sijacic, M. Bajic, E. C. McKinney, R. B. Meagher, R. B. Deal, Changes in chromatin accessibility between Arabidopsis stem cells and mesophyll cells illuminate cell type-specific transcription factor networks. *Plant J.* **94**, 215–231 (2018). doi:10.1111/tpj.13882 Medline

45. H. Li, B. Handsaker, A. Wysoker, T. Fennell, J. Ruan, N. Homer, G. Marth, G. Abecasis, R. Durbin; 1000 Genome Project Data Processing Subgroup, The Sequence Alignment/Map format and SAMtools. *Bioinformatics* **25**, 2078–2079 (2009). doi:10.1093/bioinformatics/btp352 Medline

46. S. Heinz, C. Benner, N. Spann, E. Bertolino, Y. C. Lin, P. Laslo, J. X. Cheng, C. Murre, H. Singh, C. K. Glass, Simple combinations of lineage-determining transcription factors prime cis-regulatory elements required for macrophage and B cell identities. *Mol. Cell* **38**, 576–589 (2010). doi:10.1016/j.molcel.2010.05.004 Medline

47. A. R. Quinlan, I. M. Hall, BEDTools: A flexible suite of utilities for comparing genomic features. *Bioinformatics* **26**, 841–842 (2010). doi:10.1093/bioinformatics/btq033 Medline

48. S. Anders, P. T. Pyl, W. Huber, HTSeq—A Python framework to work with high-throughput sequencing data. *Bioinformatics* **31**, 166–169 (2015). doi:10.1093/bioinformatics/btu638 Medline

49. M. I. Love, W. Huber, S. Anders, Moderated estimation of fold change and dispersion for RNA-seq data with DESeq2. *Genome Biol.* **15**, 550 (2014). doi:10.1186/s13059-014-0550-8 Medline

50. F. Ramírez, D. P. Ryan, B. Grüning, V. Bhardwaj, F. Kilpert, A. S. Richter, S. Heyne, F. Dündar, T. Manke, deepTools2: A next generation web server for deep-sequencing data analysis. *Nucleic Acids Res.* **44**, W160–W165 (2016). doi:10.1093/nar/gkw257 Medline

51. M. Salmon-Divon, H. Dvinge, K. Tammoja, P. Bertone, PeakAnalyzer: Genome-wide annotation of chromatin binding and modification loci. *BMC Bioinformatics* **11**, 415 (2010). doi:10.1186/1471-2105-11-415 Medline

52. T. L. Bailey, C. Elkan, Fitting a mixture model by expectation maximization to discover motifs in bipolymers (1994); available at www.cs.toronto.edu/~brudno/csc2417_15/10.1.1.121.7056.pdf.

53. R. C. O'Malley, S. C. Huang, L. Song, M. G. Lewsey, A. Bartlett, J. R. Nery, M. Galli, A. Gallavotti, J. R. Ecker, Cistrome and Epicistrome Features Shape the Regulatory DNA Landscape. *Cell* **165**, 1280–1292 (2016). doi:10.1016/j.cell.2016.04.038 Medline

54. M. T. Weirauch, A. Yang, M. Albu, A. G. Cote, A. Montenegro-Montero, P. Drewe, H. S. Najafabadi, S. A. Lambert, I. Mann, K. Cook, H. Zheng, A. Goity, H. van Bakel, J.-C. Lozano, M. Galli, M. G. Lewsey, E. Huang, T. Mukherjee, X. Chen, J. S. Reece-Hoyes, S. Govindarajan, G. Shaulsky, A. J. M. Walhout, F.-Y. Bouget, G. Ratsch, L. F. Larrondo, J. R. Ecker, T. R. Hughes, Determination and inference of eukaryotic transcription factor sequence specificity. *Cell* **158**, 1431–1443 (2014). doi:10.1016/j.cell.2014.08.009 Medline

55. S. Gupta, J. A. Stamatoyannopoulos, T. L. Bailey, W. S. Noble, Quantifying similarity between motifs. *Genome Biol.* **8**, R24 (2007). doi:10.1186/gb-2007-8-2-r24 Medline

56. R. C. McLeay, T. L. Bailey, Motif Enrichment Analysis: A unified framework and an evaluation on ChIP data. *BMC Bioinformatics* **11**, 165 (2010). doi:10.1186/1471-2105-11-165 Medline

57. C. E. Grant, T. L. Bailey, W. S. Noble, FIMO: Scanning for occurrences of a given motif. *Bioinformatics* **27**, 1017–1018 (2011). doi:10.1093/bioinformatics/btr064 Medline

58. P. Shannon, A. Markiel, O. Ozier, N. S. Baliga, J. T. Wang, D. Ramage, N. Amin, B. Schwikowski, T. Ideker, Cytoscape: A software environment for integrated models of biomolecular interaction networks. *Genome Res.* **13**, 2498–2504 (2003). doi:10.1101/gr.1239303 Medline

59. S. Kumar, G. Stecher, K. Tamura, MEGA7: Molecular Evolutionary Genetics Analysis Version 7.0 for Bigger Datasets. *Mol. Biol. Evol.* **33**, 1870–1874 (2016). doi:10.1093/molbev/msw054 Medline

60. M. A. Reynoso, F. A. Blanco, J. Bailey-Serres, M. Crespi, M. E. Zanetti, Selective recruitment of mRNAs and miRNAs to polyribosomes in response to rhizobia infection in *Medicago truncatula*. *Plant J.* **73**, 289–301 (2013). doi:10.1111/tpj.12033 Medline

61. S. Gonzali, E. Loreti, F. Cardarelli, G. Novi, S. Parlanti, C. Pucciariello, L. Bassolino, V. Banti, F. Licausi, P. Perata, Universal stress protein HRU1 mediates ROS homeostasis under anoxia. *Nat. Plants* **1**, 15151 (2015). doi:10.1038/nplants.2015.151 Medline

62. S. Hartman *et al*., Ethylene-mediated nitric oxide depletion pre-adapts plants to hypoxia stress. *Nat. Commun.* **10**, 4020 (2019). doi:10.1038/s41467-019-12045-4

63. F. Schröder, J. Lisso, C. Müssig, EXORDIUM-LIKE1 promotes growth during low carbon availability in Arabidopsis. *Plant Physiol.* **156**, 1620–1630 (2011). doi:10.1104/pp.111.177204 Medline

64. D. J. Gibbs, S. C. Lee, N. M. Isa, S. Gramuglia, T. Fukao, G. W. Bassel, C. S. Correia, F. Corbineau, F. L. Theodoulou, J. Bailey-Serres, M. J. Holdsworth, Homeostatic response to hypoxia is regulated by the N-end rule pathway in plants. *Nature* **479**, 415–418 (2011) . doi:10.1038/nature10534 Medline

65. F. Licausi, J. T. van Dongen, B. Giuntoli, G. Novi, A. Santaniello, P. Geigenberger, P. Perata, HRE1 and HRE2, two hypoxia-inducible ethylene response factors, affect anaerobic responses in Arabidopsis thaliana. *Plant J.* **62**, 302–315 (2010). doi:10.1111/j.1365-313X.2010.04149.x Medline

66. B. Giuntoli, S. C. Lee, F. Licausi, M. Kosmacz, T. Oosumi, J. T. van Dongen, J. Bailey-Serres, P. Perata, A trihelix DNA binding protein counterbalances hypoxia-responsive transcriptional activation in Arabidopsis. *PLOS Biol.* **12**, e1001950 (2014). doi:10.1371/journal.pbio.1001950 Medline

67. M. D. White, M. Klecker, R. J. Hopkinson, D. A. Weits, C. Mueller, C. Naumann, R. O'Neill, J. Wickens, J. Yang, J. C. Brooks-Bartlett, E. F. Garman, T. N. Grossmann, N. Dissmeyer, E. Flashman, Plant cysteine oxidases are dioxygenases that directly enable arginyl transferase-catalysed arginylation of N-end rule targets. *Nat. Commun.* **8**, 14690 (2017). doi:10.1038/ncomms14690 Medline

68. M. D. White, J. J. A. G. Kamps, S. East, L. J. Taylor Kearney, E. Flashman, The plant cysteine oxidases from *Arabidopsis thaliana* are kinetically tailored to act as oxygen sensors. *J. Biol. Chem.* **293**, 11786–11795 (2018). doi:10.1074/jbc.RA118.003496 Medline

69. C. Pucciariello, S. Parlanti, V. Banti, G. Novi, P. Perata, Reactive oxygen species-driven transcription in Arabidopsis under oxygen deprivation. *Plant Physiol.* **159**, 184–196 (2012). doi:10.1104/pp.111.191122 Medline

70. E. Yeung, H. van Veen, D. Vashisht, A. L. Sobral Paiva, M. Hummel, T. Rankenberg, B. Steffens, A. Steffen-Heins, M. Sauter, M. de Vries, R. C. Schuurink, J. Bazin, J. Bailey-Serres, L. A. C. J. Voesenek, R. Sasidharan, A stress recovery signaling network for enhanced flooding tolerance in *Arabidopsis thaliana*. *Proc. Natl. Acad. Sci. U.S.A.* **115**, E6085–E6094 (2018). doi:10.1073/pnas.1803841115 Medline

71. S. R. Cutler, P. L. Rodriguez, R. R. Finkelstein, S. R. Abrams, Abscisic acid: Emergence of a core signaling network. *Annu. Rev. Plant Biol.* **61**, 651–679 (2010). doi:10.1146/annurev-arplant-042809-112122 Medline

72. M. González-Guzmán, L. Rodríguez, L. Lorenzo-Orts, C. Pons, A. Sarrión-Perdigones, M. A. Fernández, M. Peirats-Llobet, J. Forment, M. Moreno-Alvero, S. R. Cutler, A. Albert, A. Granell, P. L. Rodríguez, Tomato PYR/PYL/RCAR abscisic acid receptors show high expression in root, differential sensitivity to the abscisic acid agonist quinabactin, and the capability to enhance plant drought resistance. *J. Exp. Bot.* **65**, 4451–4464 (2014). doi:10.1093/jxb/eru219 Medline

Evolutionary flexibility in flooding response circuitry in angiosperms

Mauricio A. Reynoso, Kaisa Kajala, Marko Bajic, Donnelly A. West, Germain Pauluzzi, Andrew I. Yao, Kathryn Hatch, Kristina Zumstein, Margaret Woodhouse, Joel Rodriguez-Medina, Neelima Sinha, Siobhan M. Brady, Roger B. Deal and Julia Bailey-Serres

Science **365** (6459), 1291-1295.
DOI: 10.1126/science.aax8862

Flood-resistance from gene regulation

Some plants tolerate flooding better than others. Reynoso *et al.* compared gene regulatory networks activated by flooding in rice, which is adapted to flooding, with those in species less adapted to flooding. Flood-related gene regulation was characterized according to chromatin accessibility as well as transcription. Although flood response circuitry is evident in dryland species as well, its activation is greater in wetland rice.

Science, this issue p. 1291